THE ECOLOGICAL IMPORTANCE OF DEEP CHLOROPHYLL MAXIMA IN THE LAURENTIAN GREAT LAKES

A Dissertation

Presented to the Faculty of the Graduate School

of Cornell University

In Partial Fulfillment of the Requirements for the Degree of

Doctor of Philosophy

by

Anne Scofield

August 2018

THE ECOLOGICAL IMPORTANCE OF DEEP CHLOROPHYLL MAXIMA IN THE LAURENTIAN GREAT LAKES

Anne Scofield, Ph. D.

Cornell University 2018

Deep chlorophyll maxima (DCM) are common in stratified lakes and oceans, and phytoplankton growth in DCM can contribute significantly to total ecosystem production. Understanding the drivers of DCM formation is important for interpreting their ecological importance. The overall objective of this research was to assess the food web implications of DCM across a productivity gradient, using the Laurentian Great Lakes as a case study. First, I investigated the driving mechanisms of DCM formation and dissipation in Lake Ontario during April–September 2013 using in situ profile data and phytoplankton community structure. Results indicate that in situ growth was important for DCM formation in early- to mid-summer but settling and photoadaptation contributed to maintenance of the DCM late in the stratified season. Second, I expanded my analysis to all five of the Great Lakes using a time series generated by the US Environmental Protection Agency (EPA) long-term monitoring program in August from 1996-2017. The cross-lake comparison showed that DCM were closely aligned with deep biomass maxima (DBM) and dissolved oxygen saturation maxima (DO_{max}) in meso-oligotrophic waters (eastern Lake Erie and Lake Ontario), suggesting that DCM are productive features. In oligotrophic to ultra-oligotrophic waters (Lakes Michigan, Huron, Superior), however, DCM were deeper than the DBM and DO_{max}, indicating that photoadaptation was of considerable importance. Across lakes, euphotic depth was a significant predictor

of both DCM depth and chlorophyll concentration, with greater water clarity associated with deeper and weaker DCM. Lastly, I investigated how DCM formation affects zooplankton diel vertical migration (DVM) by comparing the diel movements of different zooplankton size groups across three transects in southern Lake Michigan during summer 2015. Using taxonomy data from stratified net tows to inform our interpretation of laser optical plankton (LOPC) data, I concluded that phytoplankton distributions are an important determinant of zooplankton weighted mean depth. Trade-offs between optimal temperature, access to food resources, and predator avoidance contributed to differences in DVM among zooplankton size groups and regions of the lake. Overall, DCM production likely contributes significantly to phytoplankton biomass in oligotrophic lakes, causing selection pressure toward cold-adapted zooplankton that can effectively utilize DCM resources.

BIOGRAPHICAL SKETCH

Anne Scofield was born in Austin, TX and resided there until attending Stanford University. She completed her B.S. in Earth Systems with a concentration in Energy Sciences & Technology and a minor in Geological and Environmental Sciences. While at Stanford, she completed her first undergraduate research project through participation in the Stanford@SEA program – after which she decided to pursue marine science for her future studies. Her experience at Sea Education Association (SEA) inspired her to stay at Stanford University to complete a co-terminal M.S. degree in Earth Systems, during which she studied at Hopkins Marine Station in Monterey Bay, California.

After her time at Stanford University, Annie went to work for Sea Education Association (SEA), where she taught oceanography and marine biology to undergraduate students through hands-on science at sea. When she was ready to go back to graduate school, serendipity landed her at Cornell University where she had the opportunity to work in the Laurentian Great Lakes. She was skeptical (at first) about making the switch to fresh water, but the research was intriguing, so she made the leap. The Great Lakes proved to be an exciting system study, and she thoroughly enjoyed her time doing research aboard the R/V Lake Guardian, at the Cornell Biological Field Station, and at Cornell University in Ithaca, NY. Annie is looking forward to starting a post-doctoral research position at Purdue University in the fall, where she will continue working in the Great Lakes system.

I dedicate this dissertation to my parents and grandparents, who have always encouraged me to pursue my dreams, whatever they may be.

Thank you for your love and support.

Frank & Patricia Scofield

William & Dorothy Bonham

Frank & Alice Scofield

ACKNOWLEDGMENTS

This dissertation research was funded by the Great Lakes Fisheries Commission (2013_RUD_44029) and the Great Lakes Restoration Initiative, through grants from the USGS-Great Lakes Science Center (G13AC00064) and the U.S. Environmental Protection Agency (U.S. EPA) Cooperative Agreement to Cornell University (GL 00E01184-0). The research described in this dissertation has not been subjected to U.S. EPA review. Any opinions expressed in this publication are those of the authors and do not necessarily reflect the views or policies of the U.S. EPA. Any use of trade, product or firm names is for descriptive purposes only and does not imply endorsement by the U.S. EPA or USGS. I also acknowledge that Chapter 1 of this dissertation was previously published in the Journal of Great Lakes Research, published by Elsevier.

I am incredibly grateful to the mentors, staff, and other graduate students who have provided both technical and moral support throughout my years working on this dissertation research. I have truly enjoyed working with my committee chair Dr. Lars Rudstam, who has a contagious enthusiasm for the work that he does has provided endless feedback and support during my graduate studies. He has been a wonderful advisor and I am grateful for his advice, patience, and the freedom he gave me to explore my scientific interests. I also have enjoyed our travels for conferences and the community he fosters at the Cornell Biological Field Station. I also extend a thank you to my other special committee members, Drs. Patrick Sullivan, Nelson Hairston, and Brian Weidel, who have provided valuable insights, feedback, and encouragement over the past few years. I appreciate that you all made time to chat and brainstorm about my work even when you were incredibly busy with other obligations. I also thank Dr. Jim Watkins for his input and contributions.

I also grateful to the captains and crews of the R/V Lake Guardian and R/V Kaho, the technicians, graduate students, and staff at Cornell University, EPA GLNPO and

USGS that contributed to the data presented in this dissertation. This research would not have been possible without your efforts. Beyond the logical support, my friends at CBFS and my fellow Cornell graduate students have made my time here so much more meaningful through friendship and camaraderie – it has been a fantastic time!

A huge thank you to my parents and my extended family – all of whom have been amazingly supportive of me throughout this process in good times and bad. I am grateful to them all for believing in me, cheering me on, and taking such an interest in what I do. It means the world to me.

TABLE OF CONTENTS

PREFACE

Deep chlorophyll maxima (DCM) are common features in stratified lakes and oceans, and phytoplankton growth in DCM often contributes significantly to total system primary production. The primary mechanisms contributing to the formation of a DCM include growth of phytoplankton at depth due to increased nutrient availability, settling of phytoplankton cells at the thermocline, and photoadaptation (increased cell chlorophyll:carbon) of phytoplankton cells exposed to low-light environments (Camacho, 2006; Cullen, 1982). Understanding the drivers of DCM formation is needed to interpret its ecological importance as a food resource. The overall objective of this research was to improve our ability to assess the food web implications of various chlorophyll distributions observed across a productivity gradient, using the Laurentian Great Lakes as a case study.

Motivation for this dissertation was initially driven by the need to better understand the importance of DCM in Lake Ontario. Lake Ontario has undergone significant changes in nutrient concentrations, water clarity, and epilimnetic chlorophyll over the past several decades, due to the combined effects of reduced nutrient loading since the 1972 Great Lakes Water Quality Agreement (GLWQA) and impacts of invasive dreissenid mussels (Dove, 2009; Holeck et al., 2015; Mills et al., 2003; Rudstam et al., 2017). Spring total phosphorus has decreased from over 20 μg/L in the late 1960s to between 7 and 10 μg/L as of the mid-1990s (Dove and Chapra, 2015; Holeck et al., 2015), while lake-wide average euphotic depth has increased by over 50% during that time (Binding et al., 2015). Concerns about increasing oligotrophy and potential consequences for higher trophic levels in Lake Ontario prompted an interest in studying

whether the observed decreases in epilimnetic production might be offset by increased production in DCM. Although there was previous work describing the occurrence of the DCM during offshore Lake Ontario in summer (Watkins et al., 2015), the relative importance of various DCM-forming mechanisms had not thoroughly been assessed. To understand the potential bottom-up effects of the observed changes in Lake Ontario, we needed a more thorough understanding of DCM dynamics.

To address these concerns, I investigated the driving mechanisms of DCM formation and dissipation in Lake Ontario during April–September 2013 using in situ profile data and phytoplankton community structure (Chapter 1). Results indicate that in situ growth was important for DCM formation in early- to mid-summer but settling and photoadaptation contributed to maintenance of the DCM late in the stratified season. Supportive evidence includes: phytoplankton biovolume was 2.4× greater in the DCL than in the epilimnion during July, the DCL phytoplankton community of July was different from that of May and the July epilimnion ($p = 0.004$), and the DCM often coincided with maxima in fine particle concentration and dissolved oxygen saturation. Furthermore, the DCM phytoplankton community was largely comprised of diatoms including *Tabellaria*, *Fragilaria*, and *Diatoma* spp., which are known to be high-quality food for large zooplankton such as *Limnocalanus macrurus* and *Mysis diluviana*. The occurrence of a productive DCM feature during the stratified season suggests that Lake Ontario has undergone a state change since the 1970s, from a system in which summertime production was concentrated in the epilimnion, to a system where summer production is split between epilimnetic and metalimnetic phytoplankton growth.

There was also a need in the Great Lakes scientific community for a synthesis of

DCM properties across the lakes. While considerable work has been completed in recent years using datasets for one lake at a time, especially Lake Superior (Brooke, 2013; Oliver et al., 2014; White and Matsumoto, 2012), Lake Michigan (Fahnenstiel et al., 2010; Pothoven and Fahnenstiel, 2013), and more recently Lake Ontario (Twiss et al., 2012; Watkins et al., 2015), there was only one previously reported cross-lake comparison of DCM dynamics using standardized methods (Barbiero and Tuchman, 2001). In Chapter 2, I expanded my analysis of DCM in Lake Ontario to all five of the Great Lakes using a time series generated by the US EPA's long-term monitoring program from 1996-2017. My goal was not only to describe the features of DCM, in the context of different mechanisms, but also to put the patterns I observed in the context of general theory about DCM, which is largely based on examples from offshore marine environments. Our expectations based on previous theory (Camacho, 2006; Cullen, 2015; Moll and Stoermer, 1982) was that DCM depth and thickness would increase with increasing oligotrophy, while chlorophyll concentrations would decrease. Furthermore, we expected that in ultra-oligotrophic systems (Lake Superior and Lake Huron, for example), the DCM depth would be largely determined by photoadaptation rather than phytoplankton growth.

The Laurentian Great Lakes are particularly interesting lakes in which to study DCM because they are among the largest in the world, bridging the gap between marine systems and smaller lakes. In addition, these water bodies exhibit a trophic gradient, ranging from eutrophic (western Lake Erie) to ultra-oligotrophic (Lake Superior) and exhibit frequent DCM formation. In addition to the previously described changes in Lake Ontario, Lakes Michigan and Huron have undergone oligotrophication and increasing

water clarity since the GLWQA, due to the cumulative impacts of changing nutrient loads and the impacts of non-native dreissenid mussels (e.g. Dove and Chapra, 2015; Madenjian et al., 2002; Mills et al., 2003). As a result, the trophic states of Lakes Michigan and Huron have converged toward that of Lake Superior (Barbiero et al., 2012), while Lake Ontario has also become more oligotrophic (Dove, 2009; Rudstam et al., 2017).

The cross-lake comparison shows that both DCM depth and thickness did increase with decreasing productivity, while DCM chlorophyll generally decreased. In meso-oligotrophic waters (eastern Lake Erie and Lake Ontario), DCM were closely aligned with deep biomass maxima (DBM) and dissolved oxygen saturation maxima (DO_{max}), which agrees with previous evidence from Lake Ontario 2013 (Scofield et al., 2017, Ch.1) and suggests that DCM are productive biomass maxima. In more oligotrophic waters (Lakes Michigan, Huron, Superior), however, DCM were deeper than the DBM and DO_{max}, indicating that photoadaptation was of considerable importance. Across lakes, euphotic depth was a significant predictor of both DCM depth and chlorophyll concentration, with greater water clarity associated with deeper and weaker DCM. DCM depth has increased since 1996 only in Lake Michigan, coincident with increasing water clarity, while DCM chlorophyll concentrations have decreased significantly since 1996 in all lakes except Erie.

After investigating differences in DCM characteristics across a productivity gradient, I also wanted to explore how the distribution of zooplankton may be affected by the occurrence of DCM. In Lake Ontario, for example, we expect that the formation of a productive DCM with high abundance of large algae cells could contribute to the

zooplankton community shifts observed over the past decade: during that time, the biomass of *Leptodiaptomus sicilis* and *Limnocalanus macrurus* have increased while cyclopoid copepods and cladocerans have decreased (Barbiero et al., 2014). In Lakes Michigan and Huron, there have also been changes in community composition over the past two decades, with a convergence toward the zooplankton community of Lake Superior (Barbiero et al., 2012; Vanderploeg et al., 2015, GLNPO unpublished data).

The mechanism for changing zooplankton species along with oligotrophication may in part be due to shifting trade-offs associated with diel vertical migration (DVM). DVM is a common behavior in pelagic aquatic organisms, and the ultimate cause of DVM is thought to be trade-offs between favorable conditions for growth and predation risk. "Standard" DVM, in which organism move deeper in the water column during the day to reduce light-dependent predation risk and return to surface waters at night, is common across a wide range of taxa from zooplankton to fish (Hrabik et al., 2006; Ringelberg, 2009). Migrating animals may gain demographic benefits from inhabiting warm surface waters with high food density, but they migrate downward during the day to reduce light-dependent predation. In oligotrophic systems where phytoplankton are concentrated in deep chlorophyll maxima (DCMs), however, species which prefer warmer temperatures (such as *Daphnia*) experience a trade-off between food availability and optimal temperature (Kessler and Lampert, 2004; Lampert et al., 2003; Williamson et al., 1996). This trade-off can affect the magnitude of DVM and ultimately exert selection pressure against warm-adapted species in systems with a DCM. Furthermore, the high transparency of oligotrophic lakes requires zooplankton to migrate deeper to avoid light-dependent predation, and the negative effects of UV radiation may also drive migration

deeper during the day (Hairston, 1980; Williamson et al., 2011). Therefore, species which prefer cooler temperatures likely have a competitive advantage in deep oligotrophic lakes.

In Chapter 3, I investigated spatio-temporal patterns in zooplankton DVM in the offshore region of southern Lake Michigan – with the the goal of better understanding fine-scale migration patterns which may be affected by continued changes to water quality, especially chlorophyll. I used a combination of stratified net tows and fine-scale laser optical plankton counter (LOPC) data to study seasonal patterns in DVM, fine-scale spatial variability in DVM among zooplankton sizes, and potential drivers of DVM variation –including temperature, chlorophyll, and predator densities.

I found that during the summer, thermal structure and the mean weighted depth of beam attenuation coefficients (proxy for phytoplankton biomass) were important drivers of zooplankton depth distributions across taxa. However, we observed high variability in DVM patterns among size groups of zooplankton across seasons and sample locations. Copepodites, small diaptomids (*Leptodiaptomus ashlandi, Leptodiaptomus minutus*), and *Diacyclops thomasi* consistently migrated to surface waters at night, even when food resources were greater at depth. This pattern is likely driven by a combination of a preference for warm temperatures and avoidance of predation by *Limnocalanus* and *Mysis*, which typically migrate to the metalimnion at night. However, nauplii, veligers, and *L. sicilis* did not show clear DVM and thus sometimes had greater overlap with these predatory zooplankton than did copepodites and small diaptomid copepods. In general, the LOPC data provided insights into fine-scale migration patterns which were not discernable with more traditional methods such as stratified net tows but that could

significantly affect the fitness of zooplankton. LOPC technology have vastly improved our ability to observe fine-scale aspects of lower food dynamics such as phytoplankton and zooplankton communities, and continued monitoring efforts will improve our understanding of how the Great Lakes will respond to further changes in productivity, water clarity, invasive species, and a changing climate.

This research establishes that DCM are important features to monitor as part of lower food web evaluations in the Great Lakes. The mechanisms contributing to DCM formation vary across a productivity gradient, across seasons, and spatially within each lake. The results presented herein are also a step toward a more thorough understanding of how DCM dynamics are affected by long-term changes in lake nutrient status and transparency. In general, DCM production likely contributes significantly to phytoplankton biomass in oligotrophic lakes, which should ultimately favor cold-adapted zooplankton that can effectively utilize DCM resources. Such shifts have occurred in Lakes Michigan, Huron, and Ontario.

REFERENCES

Barbiero, R.P., Lesht, B.M., Warren, G.J., 2014. Recent changes in the offshore crustacean zooplankton community of Lake Ontario. J. Great Lakes Res. 40, 898–910. https://doi.org/10.1016/j.jglr.2014.08.007

Barbiero, R.P., Lesht, B.M., Warren, G.J., 2012. Convergence of trophic state and the lower food web in Lakes Huron, Michigan and Superior. J. Great Lakes Res. 38, 368–380. https://doi.org/10.1016/j.jglr.2012.03.009

Barbiero, R.P., Tuchman, M.L., 2001. Results from the U.S. EPA's biological open water surveillance program of the Laurentian Great Lakes: II. Deep chlorophyll maxima. J.

Great Lakes Res. 27, 155–166. https://doi.org/10.1016/S0380-1330(01)70629-6

Binding, C.E., Greenberg, T.A., Watson, S.B., Rastin, S., Gould, J., 2015. Long term water clarity changes in North America's Great Lakes from multi-sensor satellite observations. Limnol. Oceanogr. 60, 1976–1995. https://doi.org/10.1002/lno.10146

Brooke, W., 2013. PhD Thesis. A three-dimensional model of Lake Superior with ice and biogeochemistry: investigating interannual lake trends and the deep chlorophyll maximum. University of Minnesota.

Camacho, A., 2006. On the occurrence and ecological features of deep chlorophyll maxima (DCM) in Spanish stratified lakes. Limnetica 25, 453–478.

Cullen, J.J., 2015. Subsurface chlorophyll maximum layers: Enduring enigma or mystery solved? Ann. Rev. Mar. Sci. 7, 207–239. https://doi.org/10.1146/annurev-marine-010213-135111

Cullen, J.J., 1982. The deep chlorophyll maximum: comparing vertical profiles of chlorophyll a. Can. J. Fish. Aquat. Sci. 39, 791–803. https://doi.org/10.1139/f82-108

Dove, A., 2009. Long-term trends in major ions and nutrients in Lake Ontario. Aquat. Ecosyst. Health Manag. 12, 281–295. https://doi.org/10.1080/14634980903136388

Dove, A., Chapra, S.C., 2015. Long-term trends of nutrients and trophic response variables for the Great Lakes. Limnol. Oceanogr. 60, 696–721. https://doi.org/10.1002/lno.10055

Fahnenstiel, G., Pothoven, S., Vanderploeg, H., Klarer, D., Nalepa, T., Scavia, D., 2010. Recent changes in primary production and phytoplankton in the offshore region of southeastern Lake Michigan. J. Great Lakes Res. 36, 20–29. https://doi.org/10.1016/j.jglr.2010.03.009

Hairston, N.G.J., 1980. The vertical distribution of diaptomid copepods in relation to body pigmentation, in: Kerfoot, W.C. (Ed.), Evolution and Ecology of Zooplankton Communities. University Press of New England, Hanover, New Hampshire, pp. 98–110.

Holeck, K.T., Rudstam, L.G., Watkins, J.M., Luckey, F.J., Lantry, J.R., Lantry, B.F., Trometer, E.S., Koops, M.A., Johnson, T.B., 2015. Lake Ontario water quality during the 2003 and 2008 intensive field years and comparison with long-term trends. Aquat. Ecosyst. Health Manag. 18, 7–17. https://doi.org/10.1080/14634988.2015.1000787

Hrabik, T.R., Jensen, O.P., Martell, S.J.D., Walters, C.J., Kitchell, J.F., 2006. Diel vertical migration in the Lake Superior pelagic community. I. Changes in vertical migration of coregonids in response to varying predation risk. Can. J. Fish. Aquat. Sci. 63, 2286–2295. https://doi.org/10.1139/f06-124

Kessler, K., Lampert, W., 2004. Fitness optimization of *Daphnia* in a trade-off between food and temperature. Oecologia 140, 381–387. https://doi.org/10.1007/s00442-004-1592-5

Lampert, W., McCauley, E., Manly, B.F.J., 2003. Trade–offs in the vertical distribution of zooplankton: ideal free distribution with costs?. Proc. R. Soc. London B Biol. Sci. 270, 765–773. https://doi.org/10.1098/rspb.2002.2291

Madenjian, C.P., Fahnenstiel, G.L., Johengen, T.H., Nalepa, T.F., Vanderploeg, H.A., Fleischer, G.W., Schneeberger, P.J., Benjamin, D.M., Smith, E.B., Bence, J.R., Rutherford, E.S., Lavis, D.S., Robertson, D.M., Jude, D.J., Ebener, M.P., 2002. Dynamics of the Lake Michigan food web, 1970-2000. Can. J. Fish. Aquat. Sci. 59, 736–753. https://doi.org/10.1139/f02-044

Mills, E., Casselman, J., Dermott, R., Fitzsimons, J., Gal, G., Holeck, K., Hoyle, J., Johannsson, O., Lantry, B., Makarewicz, J., Millard, E., Munawar, I., Munawar, M., Owens, R., Rudstam, L., Schaner, T., Stewart, T., 2003. Lake Ontario: food web dynamics in a changing ecosystem (1970–2000). Can. J. Fish. Aquat. Sci. 60, 471–490. https://doi.org/10.1139/F03-033

Moll, R.A., Stoermer, E.F., 1982. A hypothesis relating trophic status and subsurface chlorophyll maxima of lakes. Arch. für Hydrobiol. 94, 425–440.

Oliver, S.K., Branstrator, D.K., Hrabik, T.R., Guildford, S.J., Hecky, R.E., Smith, R.,

2014. Nutrient excretion by crustacean zooplankton in the deep chlorophyll layer of Lake Superior. Can. J. Fish. Aquat. Sci. 72, 390–399.

Pothoven, S.A., Fahnenstiel, G.L., 2013. Recent change in summer chlorophyll a dynamics of southeastern Lake Michigan. J. Great Lakes Res. 39, 287–294. https://doi.org/10.1016/j.jglr.2013.02.005

Ringelberg, J., 2009. Diel vertical migration of zooplankton in lakes and oceans: causal explanations and adaptive significances. Springer Science & Business Media. doi:10.1007/978-90-481-3093-1

Rudstam, L.G., Holeck, K.T., Watkins, J.M., Hotaling, C., Lantry, J.R., Bowen, K.L., Munawar, M., Weidel, B.C., Barbiero, R., Luckey, F.J., Dove, A., Johnson, T.B., Biesinger, Z., 2017. Nutrients, phytoplankton, zooplankton, and macrobenthos, in: O'Gorman, R. (Ed.), GLFC Special Publication. pp. 10–32.

Scofield, A.E., Watkins, J.M., Weidel, B.C., Luckey, F.J., Rudstam, L.G., 2017. The deep chlorophyll layer in Lake Ontario: extent, mechanisms of formation, and abiotic predictors. J. Great Lakes Res. 43, 782–794. https://doi.org/10.1016/j.jglr.2017.04.003

Twiss, M.R., Ulrich, C., Zastepa, A., Pick, F.R., 2012. On phytoplankton growth and loss rates to microzooplankton in the epilimnion and metalimnion of Lake Ontario in mid-summer. J. Great Lakes Res. 38, 146–153. https://doi.org/10.1016/j.jglr.2012.05.002

Vanderploeg, H.A., Bunnell, D.B., Carrick, H.J., Höök, T.O., 2015. Complex interactions in Lake Michigan's rapidly changing ecosystem. J. Great Lakes Res. 41, 1–6. https://doi.org/10.1016/j.jglr.2015.11.001

Watkins, J.M., Weidel, B.C., Rudstam, L.G., Holeck, K.T., 2015. Spatial extent and dissipation of the deep chlorophyll layer in Lake Ontario during the Lake Ontario lower foodweb assessment, 2003 and 2008. Aquat. Ecosyst. Health Manag. 18, 18–27. https://doi.org/10.1080/14634988.2014.937316

White, B., Matsumoto, K., 2012. Causal mechanisms of the deep chlorophyll maximum

in Lake Superior: a numerical modeling investigation. J. Great Lakes Res. 38, 504–513. https://doi.org/10.1016/j.jglr.2012.05.001

Williamson, C.E., Fischer, J.M., Bollens, S.M., Overholt, E.P., Breckenridge, J.K., 2011. Toward a more comprehensive theory of zooplankton diel vertical migration: integrating ultraviolet radiation and water transparency into the biotic paradigm. Limnol. Oceanogr. 56, 1603–1623. https://doi.org/10.4319/lo.2011.56.5.1603

Williamson, C.E., Sanders, R.W., Moeller, R.E., Stutzman, P.L., 1996. Utilization of subsurface food resources for zooplankton reproduction: implications for diel vertical migration theory. Limnol. Oceanogr. 41, 224–233. https://doi.org/10.4319/lo.1996.41.2.0224

Journal of Great Lakes Research 43 (2017) 782–794

Contents lists available at ScienceDirect

Journal of Great Lakes Research

journal homepage: www.elsevier.com/locate/jglr

The deep chlorophyll layer in Lake Ontario: extent, mechanisms of formation, and abiotic predictors

Anne E. Scofield [a,*], James M. Watkins [a], Brian C. Weidel [b], Frederick J. Luckey [c], Lars G. Rudstam [a]

[a] Department of Natural Resources and the Cornell Biological Field Station, Cornell University, Ithaca, NY 14850, USA
[b] U.S. Geological Survey, Great Lakes Science Center, Lake Ontario Biological Station, 17 Lake Street, Oswego, NY 13126, USA
[c] United States Environmental Protection Agency, Region 2, New York, NY, USA

ARTICLE INFO

Article history:
Received 1 October 2016
Accepted 17 April 2017
Available online 12 May 2017

Keywords:
Deep chlorophyll maximum
Oligotrophication
Phytoplankton
Fluorescence

ABSTRACT

Epilimnetic production has declined in Lake Ontario, but increased production in metalimnetic deep chlorophyll layers (DCLs) may compensate for these losses. We investigated the spatial and temporal extent of DCLs, the mechanisms driving DCL formation, and the use of physical variables for predicting the depth and concentration of the deep chlorophyll maximum (DCM) during April–September 2013. A DCL with DCM concentrations 2 to 3 times greater than those in the epilimnion was present when the euphotic depth extended below the epilimnion, which occurred primarily from late June through mid-August. In situ growth was important for DCL formation in June and July, but settling and photoadaptation likely also contributed to the later-season DCL. Supporting evidence includes: phytoplankton biovolume was 2.4× greater in the DCL than in the epilimnion during July, the DCL phytoplankton community of July was different from that of May and the July epilimnion ($p = 0.004$), and there were concurrences of DCM with maxima in fine particle concentration and dissolved oxygen saturation. Higher nutrient levels in the metalimnion may also be a necessary condition for DCL formation because July metalimnetic concentrations were 1.5× (nitrate) and 3.5× (silica) greater than in the epilimnion. Thermal structure variables including epilimnion depth, thermocline depth, and thermocline steepness were useful for predicting DCM depth; the inclusion of euphotic depth only marginally improved these predictions. However, euphotic depth was critical for predicting DCM concentrations. The DCL is a productive and predictable feature of the Lake Ontario ecosystem during the stratified period.

Introduction

Peaks in chlorophyll concentration commonly occur below the surface mixed layer in nutrient-poor lakes and oceans, but the causes and ecological importance of these deep chlorophyll layers (DCLs) are highly variable among systems. There are a number of non-exclusive physical and biological processes that can cause a DCL to form, including in situ phytoplankton growth at depth, settling of algal cells along the pycnocline, photoadaptation by phytoplankton (increased cell chlorophyll:carbon), and high zooplankton grazing rates in the epilimnion (Camacho, 2006; Cullen, 1982). Whether the DCL contributes significantly to total lake primary production depends on the relative importance of these processes in each system; for example, phytoplankton photoadaptation would not affect food availability for zooplankton grazers in the metalimnion, while phytoplankton growth depth may impact food web dynamics.

Efforts to study the processes forming DCLs in the Laurentian Great Lakes began in the late 1970s to 1980s (e.g. Fahnenstiel and Glime, 1983; Fahnenstiel and Scavia, 1987; Moll and Stoermer, 1982), shortly after the presence of subsurface maxima in chlorophyll and phytoplankton biomass were documented in Lake Michigan and Lake Superior (Brooks and Torke, 1977; Watson et al., 1975). These early DCL studies in the upper Great Lakes showed that in situ production was an important mechanism causing DCL formation, and ^{14}C-based primary production estimates suggest that the DCL contributed from 30% to 60% of areal production in Lake Michigan at that time (Moll et al., 1984). There has been continued interest in studying DCLs in recent years (e.g. Pothoven and Fahnenstiel, 2013; Watkins et al., 2015; White and Matsumoto, 2012), partly because of growing concerns about declining primary production negatively affecting fish production, as observed in Lake Huron (Bunnell et al., 2014; Riley et al., 2008).

In Lake Ontario, increased summer production in deep chlorophyll layers (DCLs) may at least partly compensate for declines in epilimnetic production observed over the past several decades. Metalimnetic chlorophyll maxima were less common during the period of cultural eutrophication from the 1960s to 1980s, when average chlorophyll concentrations were much higher than present day. During that time, the DCLs that were observed in Lake Ontario occurred at a relatively shallow average depth of 10 m, and they had mean values of about 9 μg/L

* Corresponding author.
E-mail address: as2895@cornell.edu (A.E. Scofield).

http://dx.doi.org/10.1016/j.jglr.2017.04.003
0380-1330/

(maximum 17 μg/L) while surface values averaged 8 μg/L (maximum > 14 μg/L) (Dobson, 1984). Maximum phytoplankton biomass was also sometimes observed in the mid-thermocline region, where the community was dominated by phytoflagellates (Munawar et al., 1974). These DCL features were absent during surveys in the 1980s (Lean et al., 1987), however, and light limitation likely restricted net phytoplankton production to the epilimnion during the 1970s–1980s. Depth-stratified production estimates from the 1970s indicate that maximal production occurred in the epilimnion (Stadelmann et al., 1974), and observations of metalimnetic oxygen depletion suggest that there was net respiration below the thermocline (Boyd, 1980). However, Lake Ontario has become considerably more oligotrophic. Spring total phosphorus concentrations declined from over 20 μg/L in the late 1960s to between 7 and 10 μg/L by the mid-1990s (Holeck et al., 2015; Dove and Chapra, 2015). Furthermore, the lakewide average euphotic zone has increased by over 50%, from an ice-free season (March–October) average of 9.8 m (Secchi depth 4.9 m) for the years 1978–1985 to 15.4 m (Secchi depth 7.7 m) for 2004–2015 (Binding et al., 2015). Increased transparency can be attributed to a combination of decreased epilimnetic chlorophyll concentrations, likely a result of decreased nutrients and mussel filtering (Holeck et al., 2015; Rudstam et al., 2017), and fewer summertime whiting events due to reduced production (Binding et al., 2007; Watkins et al., 2013). A deeper euphotic zone can lead to the vertical redistribution of phytoplankton biomass to the metalimnion as the water column stratifies and epilimnetic nutrients become depleted, causing a productive DCL to form when the euphotic zone overlaps with the metalimnion. Therefore, we expect that the importance of the DCL has increased in Lake Ontario in response to oligotrophication.

Consistent with this expectation, DCLs have commonly been observed in Lake Ontario monitoring data since at least 1998 (Barbiero and Tuchman, 2001), and a DCL feature was ubiquitous in offshore waters during sampling efforts in 2003 and 2008 (Watkins et al., 2015). Furthermore, measurements of phytoplankton growth and loss rates to microzooplankton suggest that production in the DCL during midsummer is at least as high as in the epilimnion (Twiss et al., 2012), and the observation of metalimnetic peaks in dissolved oxygen saturation (DO) and beam attenuation (BAT, proxy for particle density) during sampling in July 2008 suggests a productive DCL (Watkins et al., 2015). In addition, a recent analysis of Lake Ontario phytoplankton data from April and August 2007–2012 suggests that in situ growth contributes to DCL formation. Although some relict taxa from spring were commonly observed in the DCL, the August metalimnetic community was distinct from April and August epilimnetic phytoplankton (Bramburger and Reavie, 2016), which indicates that some metalimnetic phytoplankton were produced in the DCL. The fact that the DCL in Lake Ontario appears productive has sparked continued interest in studying its dynamics, and this paper expands upon previous work by addressing two primary questions: 1) Which of the most common DCL-forming processes was dominant in Lake Ontario: photoadaptation, passive settling, or in situ growth? 2) Can we predict DCL characteristics from abiotic variables? We used data from whole lake surveys completed in 2013 to revisit the observations of DCL formation made in 2003 and 2008 (Watkins et al., 2015), expand on the seasonally-limited phytoplankton composition data in the DCL compared to the epilimnion from Bramburger and Reavie (2016), and predict the location and chlorophyll concentration of the deep chlorophyll maximum (DCM).

To investigate the conditions under which DCLs form, we used discrete-depth chlorophyll and nutrient concentrations, depth-stratified phytoplankton biomass and taxonomy data, and in situ profiles of temperature, photosynthetically active radiation (PAR), and proxies for phytoplankton biomass and production (BAT and DO, respectively). We hypothesize that the DCL in Lake Ontario is a productive feature with elevated phytoplankton biomass for most of the summer but that the DCL will no longer be productive and will dissipate if the epilimnion extends below the euphotic depth. Because nutrient limitation in the surface is the primary explanation for the vertical redistribution of phytoplankton production, we expect to observe differences in the availability of limiting nutrients between the epilimnion and metalimnion. If in situ growth of phytoplankton in the metalimnion is important to DCL formation, we expect to observe not only greater phytoplankton biomass within the DCL compared to the epilimnion but also a DCL phytoplankton community that is distinct from both integrated spring and summer epilimnetic communities. Furthermore, a productive DCL would cause supersaturation of dissolved oxygen at depth, whereas oxygen depletion would suggest that the passive settling of senescent cells is causing the biomass peak (if present). If, however, we fail to observe greater phytoplankton biomass within the DCL, then photoadaptation is likely an important factor. It is also possible that we will observe both greater biomass and oxygen supersaturation at depth but that the maxima will be offset from the DCM. In this case, there may be several factors contributing to DCL formation and maintenance that change in relative importance with depth. Our expectation is that if the peaks are asynchronous, the productivity peak will likely be shallower than the DCM because greater production per unit chlorophyll could occur near the top of the DCL where light levels are higher than at the peak, and photoadaptation may contribute to elevated chlorophyll near the bottom of the DCL. Furthermore, we expect that the processes contributing to DCL maintenance may change over the course of the stratified season as the thermocline deepens and there is less overlap of the euphotic zone and metalimnion.

Methods

Sampling plan

The offshore waters of Lake Ontario were sampled from aboard the US EPA's R/V Lake Guardian during the months of April, May, July, August, and September 2013 (Fig. 1). All sites included in the present analysis had a bottom depth >40 m. Ten sites designated by the US EPA Great Lakes National Program Office (GLNPO) long-term monitoring program were visited on both April 4–5 and August 12–14. Through the Cooperative Science and Monitoring Initiative (CSMI) program for Lake Ontario, efforts to sample three south to north transects were coordinated by the US EPA GLNPO and Cornell University during May 20–23, July 19–22, and September 10–13. Profile data from three additional programs aboard the R/V Lake Guardian during the summer of 2013 were included in our analysis: the Clarkson University cruise on June 18–19, the Center for Ocean Sciences Education Excellence (COSEE) cruise on July 8–12, and the An Li Sediment Survey on July 23–25. Profile data from the R/V Lake Guardian surveys were grouped into six time periods: April (GNPO), May (CSMI), Late June–Early July (Clarkson and COSEE), Late July (CSMI and An Li Sediment Survey), August (GLNPO), and September (CSMI). Discrete-depth fractionated chlorophyll data from three sites offshore from Oswego, NY (with bottom depths of 50, 100, and 200 m) and additional samples for taxonomic analysis of phytoplankton from the deepest site (200-m) were provided by the United States Geological Survey Lake Ontario Biological Field Station (USGS-LOBS), which completed sampling on the following dates: April 10, May 15–17, June 11–14, July 9, August 8, August 27–29, and September 24.

Field and lab methods

All R/V Lake Guardian sites were sampled with a rosette assembly consisting of a 12 Niskin bottle array and the following instrumentation: SBE-911 Conductivity Temperature Depth (CTD) profile; Seapoint chlorophyll *a* fluorometer (Seapoint Sensors, Inc., Exeter, NH); dissolved oxygen sensor (SBE 43); Biospherical/Licor sensor to measure Photosynthetically Available Radiation (PAR); and transmissometer (WETlab C-Star) to measure beam attenuation at 660 nm wavelengths. The rosette was deployed at a constant speed of 0.5 m per second for the

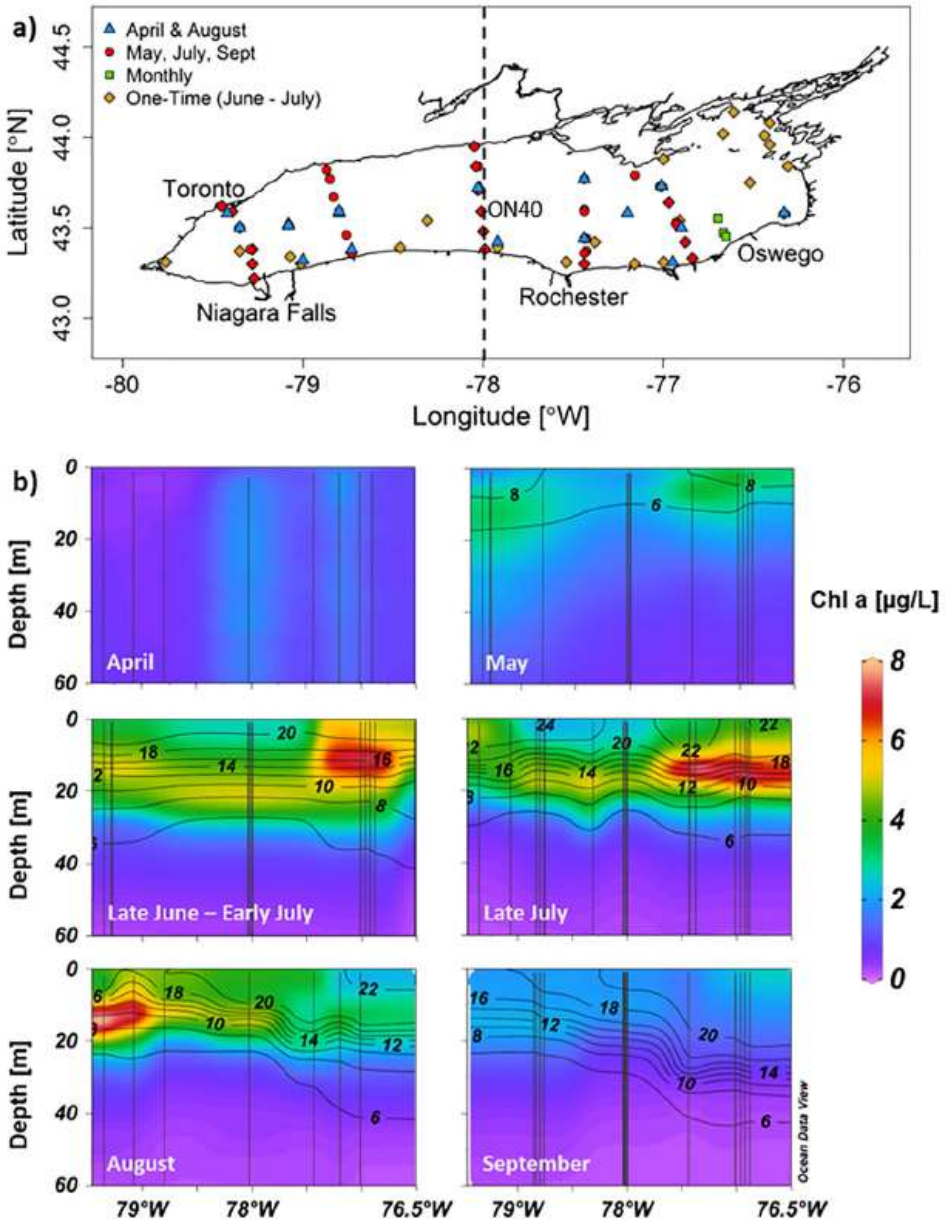

Fig. 1. a) Map of sites sampled during the 2013 intensive survey effort. Triangles are sites visited during the Great Lakes National Program Office (GLNPO) long-term monitoring program spring and summer surveys (April, August). Circles indicate sites sampled during the Cooperative Monitoring Initiative (CSMI) cruises on the Lake Guardian (May, Late July, Sept). Diamonds indicate sites that were sampled only once through auxiliary programs aboard the RV Lake Guardian (Late June–July), and squares designate sites sampled monthly through the Great Lakes Restoration Initiative (GLRI) sampling effort offshore from Oswego, NY. GLRI stations have bottom depths of 50, 100, and 200 m, from nearshore to offshore. The dashed line indicates the longitude break for designating the "west" or "east" regions of the lake. b) Seasonal patterns in spatial distribution of chlorophyll *a* concentration and thermal structure for offshore sites (bottom depth > 40 m). Vertical lines show the location of profile data for the given time point, between which data are interpolated using inverse distance weighting for pattern visualization. The color scale is corrected in situ chlorophyll *a* concentration [µg/L] and the contour lines with labels show isotherms [°C].

downcast, and water samples were collected at discrete depths during the upcast.

Water samples for measurements of chlorophyll *a* (hereafter referred to as chlorophyll) and nutrients were collected during the GLNPO and CSMI cruises. Integrated epilimnetic water samples were generated by equally mixing water from three depths within the epilimnion. During isothermal conditions, water samples were collected at standard depth intervals. When the water column was stratified, discrete depth samples from each depth layer (epilimnion, metalimnion, hypolimnion) and the DCM, if present, were chosen by the chief scientist based on real-time rosette sensor displays of the temperature and chlorophyll fluorescence profiles. Chlorophyll samples were filtered using EPA Standard Operating Procedure (SOP) LG404 (Revision 7, 2013) and analyzed within three weeks of collection using a calibrated Turner Designs 10-AU bench-top fluorometer following EPA SOP LG405 (Revision 9, 2013) using the non-acidification method (Welschmeyer, 1994). In addition to these whole extracted chlorophyll measurements, discrete-depth water samples were size fractionated (<2 μm, 2–20 μm and >20 μm) before analysis for samples collected at the Oswego transect sites. Water was also analyzed for concentrations of nitrite + nitrate, soluble reactive phosphorus (SRP), and dissolved reactive silica (Si) following EPA SOPs LG203, LG204, and LG205, respectively.

Phytoplankton samples were collected at all CSMI sites in May and July and from the deepest USGS LOBS site (200-m bottom depth) offshore from Oswego, NY in April through September. At the CSMI stations, samples were taken from integrated epilimnetic water and integrated metalimnetic water collected at three depths between 15 and 35 m (isothermal conditions) or three depths within the DCL (stratified conditions). At the USGS LOBS 200-m site, four (isothermal) to six (stratified) discrete depth water samples were collected for phytoplankton community analysis. All samples were preserved in 1% Lugol's iodine solution and counted by Phycotech, Inc. (Dr. Ann St. Amand). Phycotech counted and measured 400 natural units including all algal cells alive at the time of sampling (cells with content) using 500× magnification, with the additional use of 250× and 1250× magnifications when required. The algae were mounted on slides, and the amount of water mounted varied with the density of algal cells (0.1 to 100 mL/slide). Algal taxa were identified to genus level and measured to provide genus-specific biovolumes by cell and by natural units (colonies, paired or other multiples of cells). The wet-weight biomass [mg/L] was calculated from biovolume [μ^3/mL] assuming a specific weight of 1.0 g biomass per μ^3.

Profile processing & definitions

Rosette sensor water column profiles were first aligned to account for differences in data acquisition time among instruments, after which only downcast data were used. The profile data were then binned into 0.25-m depth intervals and a smoothing algorithm was applied to minimize noise. Percent oxygen saturation was calculated using ambient temperature and the equation from Baca and Arnett (1976). To account for quenching effects on in situ fluorescence, as well as instrument bias, we corrected in situ chlorophyll measurements based on a model optimized with matching samples for extracted chlorophyll *a*, PAR, and temperature values. The model structure corrected for the quenching effects of temperature and light with an optimized cut-off value for the light level that produced a quenching effect:

$$Extracted\ \ Chl = (in\ \ situ\ \ Chl) \times (\boldsymbol{a} \times Temp + \boldsymbol{b}) \times \frac{\max(PAR, \boldsymbol{P})^{\boldsymbol{c}}}{\boldsymbol{P}^{\boldsymbol{c}}} \qquad (1)$$

where $\boldsymbol{a}$ and $\boldsymbol{b}$ are linear model parameters for the temperature effect, $\boldsymbol{P}$ is a cut-off value for PAR, below which there is no impact of PAR on the correction, and $\boldsymbol{c}$ is an exponential term applied to either the in situ PAR measurement, or the parameter $\boldsymbol{P}$, whichever is greater. The optimized parameters values were a = 0.0468 (SE = 0.006), b = 0.885 (SE = 0.058), c = 0.240 (SE = 0.025), and P = 18.5 (SE = 4.83). We used this equation to calculate corrected chlorophyll profiles from in situ chlorophyll data.

Applying the optimized model to correct in situ chlorophyll measurements improved the overall linear regression R^2 value for extracted vs. in situ chlorophyll concentrations; the R^2 values increased from 0.78 for the original data to 0.87 for the corrected in situ chlorophyll values. Applying the above correction also accounted for fluorescence quenching in surface waters and resolved the difference in the correlations for measurements taken near the surface (<10 m) and at depth (>10 m). After the correction, none of the relationships were significantly different from a one-to-one relationship (Fig. 2). We then visualized corrected chlorophyll profiles in Ocean Data View (Schlitzer, 2015) and performed further data analyses in R software packages (R Core Team, 2016).

We defined several terms for specific water depths and layers for profile data in this paper, which are described here. The thermocline was defined as the region of the water column for which the negative temperature gradient was at least 0.5 °C/m, and the presence of a thermocline was used to define "stratification" of the water column. The bottom depths of the "epilimnion" and the "metalimnion" were designated by the shallowest and deepest depths of the thermocline, respectively. We defined "thermocline depth" as the depth at which the greatest absolute temperature slope occurs and "thermocline steepness" as the absolute value of the temperature slope at the thermocline depth. "Euphotic depth" was determined from the depth at which the PAR values were 1% of the surface values and was only calculated for daytime profile data. We defined the DCL as the region below the epilimnion for which chlorophyll concentrations were at least 2 μg/L, following the definition of Fahnenstiel and Scavia (1987). In some cases, the DCL started at the epilimnion-metalimnion boundary, but at other times it began deeper within the metalimnion. The bottom of the DCL was defined as the deepest depth at which the threshold concentration of 2 μg/L occurred. At sites where a DCL was present, the term "deep chlorophyll maximum" (DCM) was used for the point within the DCL at which the chlorophyll concentration was greatest, the value of which we refer to as "DCM magnitude". The "beam attenuation (BAT) maximum" was defined as the depth below the epilimnion at which the beam attenuation coefficient was highest. If dissolved oxygen supersaturation (>100%) occurred below the epilimnion, the "dissolved oxygen (DO) maximum" was defined as the depth at which the maximum saturation value occurred. We only included a DO maximum when the DCM occurred at a depth >9 m because when the DCM occurred shallower in the water column, stratification was typically weak and thus there would have been considerable gas exchange with the surface.

Data analysis

First, we used the profile and water quality data to describe the spatio-temporal patterns of the DCL during 2013 using the metrics of DCL presence/absence, DCM depth, DCM chlorophyll relative to epilimnetic chlorophyll, and seasonal patterns in size-fractionated chlorophyll data. To assess the general conditions under which a DCL occurred, we considered the epilimnion depth, euphotic depth, and discrete-depth nutrient concentrations for nitrate + nitrite, DRP, and Si. Since the full extent of the DCL, when present, always fell within the upper 30 m of the water column, we used the percentage of water column chlorophyll from 0 to 30 m contributed by the metalimnion as a metric for DCL importance from April through September. We then framed much of our data analysis to address which of the three most common DCL-forming processes is likely dominant in Lake Ontario: photoadaptation, settling of senescent cells, or in situ phytoplankton growth. Finally, we considered seasonal patterns in physical conditions as drivers for DCL formation and used multiple linear regression to test whether we could use thermal structure variables and euphotic depth to predict DCM depth and magnitude.

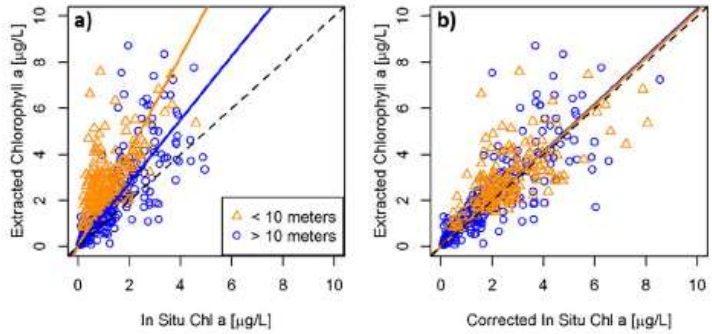

Fig. 2. Correlation of extracted chlorophyll *a* concentration [µg/L] versus in situ chlorophyll *a* measurement [µg/L] a) before corrections and b) after corrections were applied. Triangles indicate samples taken at shallow depths in the water column (< 10 m), and circles designate samples collected deeper than 10 m in the water column; solid lines show depth-specific linear regressions; the dotted line indicates the 1:1 relationship.

To address whether photoadaptation was the primary factor in DCL formation, we used the available data in three different ways. First, we tested the hypotheses that phytoplankton biomass [mg/m^3] and cell concentration [cells/mL] were higher in the metalimnion than the epilimnion at sites with a DCL using one-tailed paired *t*-tests on depth-stratified phytoplankton data from the July CSMI cruise. If there were no significant differences in biomass and cell concentration, then photoadaptation likely caused the high chlorophyll in the metalimnion. We also used phytoplankton biomass data from the Oswego 200 m site to examine temporal patterns in epilimnetic vs. metalimnetic phytoplankton biomass, although there were not replicate samples for statistical analysis at that site. Second, we compared phytoplankton biomass with chlorophyll concentrations for epilimnetic and metalimnetic samples where a DCL was present; if photoadaptation was important, we expect that the linear regression of chlorophyll vs. phytoplankton biomass would be different for epilimnion and DCL samples since DCL phytoplankton would exhibit elevated chlorophyll content. Finally, we considered whether the depth of the BAT maximum within the metalimnion was correlated with the DCM depth. All significance tests were performed at the alpha = 0.05 level.

It is possible, however, that high phytoplankton biomass in the DCL could have been caused by the settling of senescence phytoplankton cells at the pycnocline rather than by in situ growth. To evaluate the relative importance of these two processes, we considered two additional types of data: the presence/absence of DO supersaturation within the metalimnion and the depth-stratified phytoplankton community data from May and July CSMI cruises. We used linear regression to assess the relative depths of the DO maximum and the DCM when DO supersaturation occurred within the metalimnion. To quantify the similarity between the epilimnetic and metalimnetic phytoplankton communities in spring and summer, we analyzed all samples collected in May and July using non-metric multidimensional scaling (NMDS) and analysis of similarity (ANOSIM) (Clarke, 1993) within the program Primer 7 (Clarke and Gorley, 2015). Genus-level contributions to assemblages were evaluated using similarity percentages (SIMPER) (Clarke, 1993). Lastly, qualitative patterns in the phytoplankton community at the 200-m site offshore from Oswego were evaluated on the division level for samples collected in the epilimnion and the metalimnion in April through September.

Table 1
Summary of variables related to deep chlorophyll layer (DCL) occurrence in Lake Ontario from April through September 2013 by lake region (west or east of latitude 78°E). a) The number of sites visited during each sampling period, the proportion of those sites at which a DCL was present, and the means and standard errors for epilimnion depth, DCM depth, and DCM height. b) The means (± 1 SE) for surface chlorophyll (from extracted values where available), average chlorophyll in the epilimnion (from corrected profile data for the epilimnion depth range), DCM chlorophyll (from corrected chlorophyll profile data), and average chlorophyll for the full depth range of the DCL (from corrected chlorophyll profile data). All chlorophyll data are shown in µg/L.

a)

Time period	Number samples		Proportion with DCL		Epilimnion depth (m)		DCM depth (m)		DCM height (m)	
	West	East	West	East	West	East	West	East	West	East
April	5	5	–	–	–	–	–	–	–	–
May	8	7	0.38	–	2.96 ± 0.65	–	9.11 ± 1.46	–	27.39 ± 1.27	–
June–July	5	5	1	1	3.63 ± 0.90	7.2 ± 1.19	13.97 ± 2.49	12.09 ± 2.22	23.87 ± 1.33	19.39 ± 3.45
Late July	7	8	1	1	6.94 ± 1.02	11.69 ± 1.38	15.50 ± 0.90	17.04 ± 1.56	17.71 ± 1.33	16.74 ± 1.01
August	15	12	1	1	8.94 ± 2.15	16.88 ± 2.09	15.43 ± 2.31	19.13 ± 1.91	15.61 ± 2.48	7.68 ± 1.93
September	14	10	0.64	0	10.9 ± 1.13	22.96 ± 1.38	13.10 ± 1.03	–	7.65 ± 1.40	–

b)

Time period	Surface chlorophyll		Average epilimnion chlorophyll		DCM chlorophyll		Average DCL chlorophyll	
	West	East	West	East	West	East	West	East
April	2.30 ± 1.16	1.51 ± 0.51	–	–	–	–	–	–
May	2.36 ± 0.23	3.72 ± 0.58	3.57	–	4.06 ± 0.43	–	3.13 ± 0.18	–
June–July	–	–	2.87 ± 0.23	5.29 ± 0.46	5.22 ± 0.33	6.87 ± 0.66	3.94 ± 0.20	4.66 ± 0.32
Late July	2.30 ± 0.34	2.96 ± 0.26	2.69 ± 0.26	4.26 ± 0.33	5.31 ± 0.22	7.41 ± 0.73	3.92 ± 0.20	4.88 ± 0.36
August	3.25 ± 0.40	2.43 ± 0.11	3.64 ± 0.29	2.94 ± 0.15	6.17 ± 0.90	3.58 ± 0.46	4.37 ± 0.33	2.90 ± 0.16
September	2.62 ± 0.14	2.48 ± 0.15	2.03 ± 0.04	–	2.65 ± 0.16	–	2.40 ± 0.11	–

To assess the dependence of DCL characteristics on physical variables, we used multiple linear regression to predict DCM depth and DCM chlorophyll from mean-centered abiotic variables derived from profile data. For all stations where a DCL occurred ($n = 63$), the full model included epilimnion depth, thermocline depth, thermocline steepness, and all second-order interaction terms. We also tested the subset of stations sampled during the day ($n = 24$) with euphotic depth and interaction terms added to the full model. We selected the best fit model for each dependent variable (DCM depth and DCM chlorophyll) using forward and backward stepwise regression with Akaike's Information Criterion (AIC) to determine significance at the 2-AIC unit level.

Results

Spatio-temporal patterns of DCL formation

The DCL developed with the onset of water column stratification and occurred throughout the summer, although there were differences from west to east in the timing of DCL onset and dissipation (Table 1). There were differences in nutrient concentrations between the epilimnion and metalimnion throughout the stratified season, which likely affected the formation of a DCL. While there were no differences in SRP concentrations with depth, both the nitrate + nitrite and Si concentrations were higher in the metalimnion than the epilimnion during July (1.4× and 3.5×, respectively), and these differences intensified through September (Fig. 3). Weak stratification occurred as early as May at 3 of 15 sites, all on the western end of the lake, and thus had the criteria for a DCL (DCM 3.0–5.4 μg/L). During late June through July, the DCL developed lakewide (DCM 3.9–9.7 μg/L). While the western side of the lake developed a DCL earlier and maintained it longer, the eastern side of the lake had greater DCM chlorophyll (DCM consistently >7 μg/L) during July (Fig. 1). All sites still exhibited a DCL in August (DCM 2.3–8.5 μg/L), but it was of considerably lower magnitude on the eastern side of the lake, where the concentrations within the DCL were near the 2 μg/L threshold and generally below the average epilimnetic concentrations. By September, a weak DCL (DCM 2.1–3.6 μg/L) occurred only at sites on the western end of the lake and was absent elsewhere (Table 1).

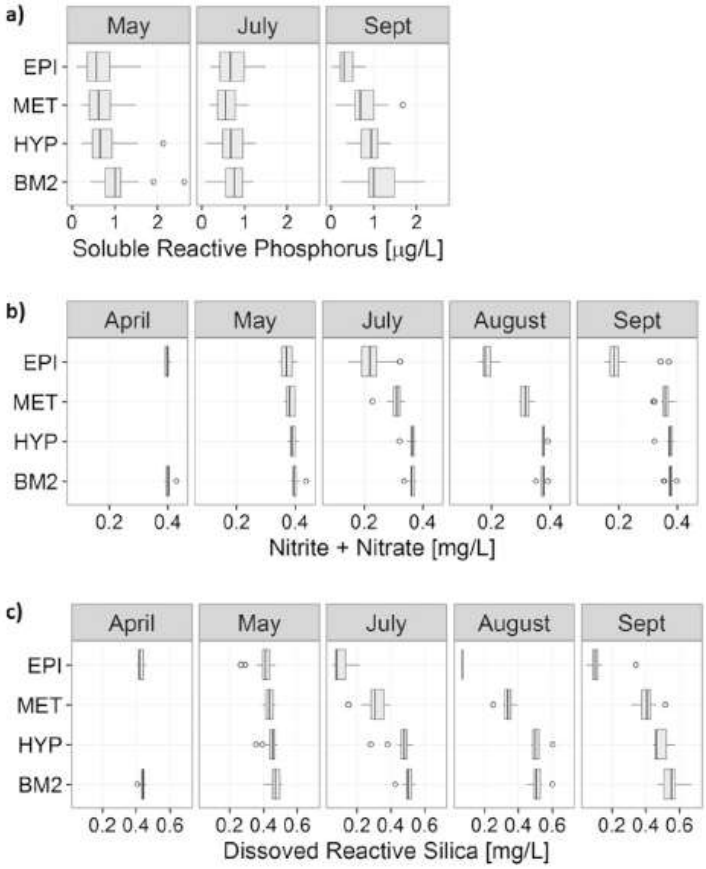

Fig. 3. Lake Ontario nutrient concentrations for a) soluble reactive phosphorus [μg/L], b) dissolved nitrite + nitrate [mg/L] and c) dissolved silica [mg/L] measured from discrete depth water samples at offshore sites (>45 m bottom depth) from April through September 2013. Depth layers shown are: integrated epilimnetic (EPI) and discrete depth samples from the metalimnion (MET), middle hypolimnion (HYP), and bottom depth minus 2 m (BM2). Boxes represent first and third quartiles with the median marked; whiskers extend to most extreme data point within 1.5 times the interquartile range from the box, and open circles show outliers.

On average, DCL chlorophyll made up more than half of the total water column chlorophyll during the stratified season. Throughout the sampling period, the full extent of the DCL, where present, was within the top 30 m of the water column, and mean chlorophyll concentration for 0–30 m increased from April (1.0 μg/L) and May (2.3 μg/L) through July (4.0 μg/L), and then decreased in August (3.2 μg/L) and September (1.8 μg/L). Lakewide mean surface extracted chlorophyll concentrations (upper 3 m) were lowest in April (1.8 μg/L), highest in May (3.1 μg/L), and lower during July through September (2.6 to 2.8 μg/L). During late June to early July sampling, metalimnetic chlorophyll made up 77% of total integrated chlorophyll to 30 m, but this percentage decreased from 71% in late July to 57% in August and approximately 50% in September (Fig. 4).

Size fractionated chlorophyll data from sites offshore of Oswego, NY showed clear seasonal shifts in phytoplankton size structure, but differences between depth layers were only obvious during the month of July (Fig. 5). Throughout the water column, the proportion of chlorophyll contributed by picoplankton (<2 μm) decreased and the importance of microplankton (>20 μm) increased from spring to fall. During the month of July, when the DCL was at its peak, there were notable differences with depth: microplankton made up a smaller proportion of total chlorophyll in the epilimnion (9%) than in the metalimnion (28%); picoplankton, however, contributed more to epilimnetic than metalimnetic chlorophyll (42% and 28%, respectively); nanoplankton (2–20 μm) proportions were more similar between the epilimnion and metalimnion (50% and 44%, respectively). As the DCL dissipated, the phytoplankton size structure within the DCL stayed consistent even as total chlorophyll decreased.

Characteristics of the DCL

The DCL was generally associated with elevated phytoplankton concentrations, metalimnetic DO supersaturation, and a unique phytoplankton community. In the metalimnion, phytoplankton biomass [mg/m^3] was 2.4 times higher ($p = 0.01$) and algal cell concentration [cells/mL] was 1.6 times higher ($p = 0.04$) than in the epilimnion at sites with a DCL during the July CSMI cruise. Depth-stratified phytoplankton data from the Oswego 200 m station indicated that phytoplankton biomass was greater in the metalimnion than the epilimnion for the months of June through August (Fig. 6). There was a significant positive correlation ($R^2 = 0.40$) of phytoplankton biomass with chlorophyll concentration, and there was no apparent difference in this relationship between depth strata (Fig. 7). Furthermore, metalimnetic BAT maxima occurred when a DCL was present, and the BAT maximum depth was highly correlated with the DCM depth (slope = 0.81, $R^2 = 0.60$) (Fig. 8). Oxygen supersaturation in the metalimnion occurred consistently when a DCL was present in July and August but was mostly absent in September, when metalimnetic oxygen depletion to approximately 70% saturation occurred on the eastern side of the lake. The DO maximum was generally shallower than the BAT maximum and the DCM, and the depth discrepancy increased with DCM depth (slope = 0.55, $R^2 = 0.45$) (Fig. 8).

The epilimnetic and metalimnetic phytoplankton communities were significantly different in July ($p = 0.002$), but not in May ($p = 0.236$). All other comparisons (crossing depth layers and months) were significant at the 0.001 level (Fig. 9). Differences between the overall May and

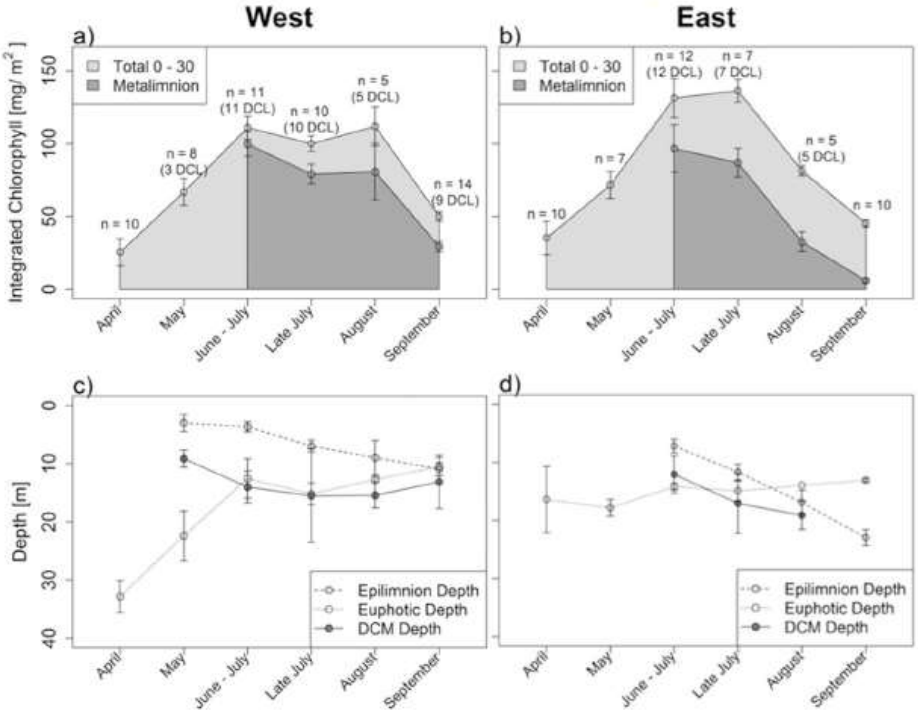

Fig. 4. Mean integrated total chlorophyll [mg/m^2] from 0 to 30 m and integrated metalimnetic chlorophyll [mg/m^2] down to 30 m for all sites by sampling period and region: a) west or b) east of longitude 78° W. The mean depths with standard errors are shown for the epilimnion depth, euphotic depth, and deep chlorophyll maximum (DCM) depth for c) west and d) east regions.

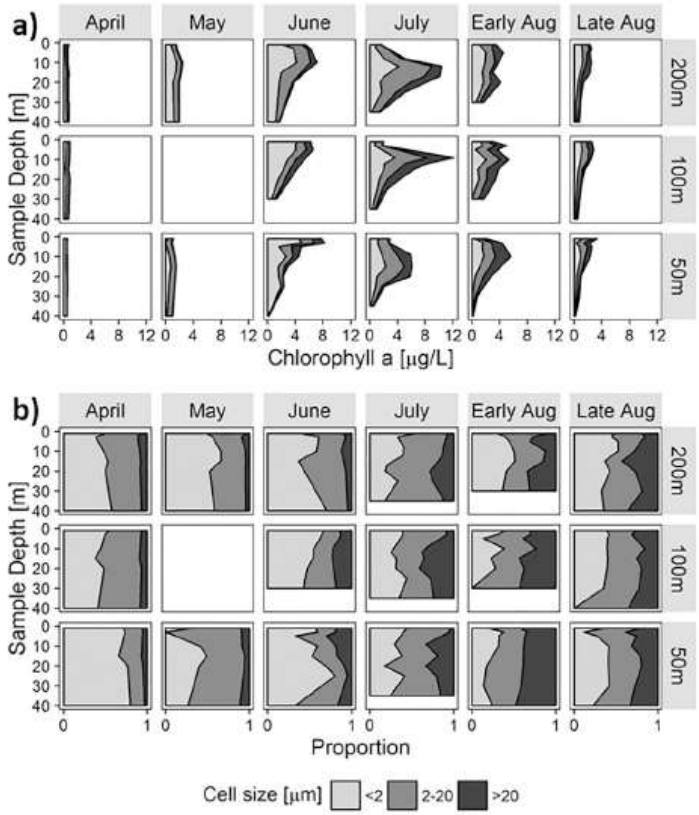

Fig. 5. Seasonal and depth trends for fractionated chlorophyll in a) absolute concentration [µg/L] and b) proportion of total chlorophyll at offshore sites along the Oswego transect (200 m, 100 m, 50 m sites. The 100 m site was not sampled in May (empty square).

July DCL communities were largely driven by inconsistencies in diatom assemblages (Bacillariophyta), and dinoflagellates (Pyrrhophyta) made up a larger proportion of average spring-time biomass. Over 25% of the dissimilarity between May and July communities was explained by *Fragilaria* (6.1%), *Synedra* (5.1%), *Diatoma* (4.8%), *Stephanodiscus* (4.2%), *Peridinium* (4.2%), and *Tabellaria* (4.2%) combined. In July, the vertical structure in the phytoplankton community was largely driven by differences in the abundances of large colonial diatom taxa (*Tabellaria*, 4.9%, *Fragilaria*, 4.5%, *Diatoma* 4.2%) and some cyanophytes (*Pseudanabaena*, 4.1%, *Synechocystis*, 3.9%), all of which were more abundant in the metalimnion. Dinoflagellates were more abundant in the epilimnion and contributed notably to observed community differences between the two depth regions (*Peridinium*, 4.1%, *Ceratium*, 2.8%).

It was also apparent from the more frequent samples collected at the Oswego 200 m site that there was considerable seasonal variation in phytoplankton community assemblage within the DCL (Fig. 6) The newly-formed DCL in June consisted of a mixed community with diatoms, chrysophytes, cryptophytes, and dinoflagellates contributing significant proportions to the total DCL biomass. The community was less diverse in July, when colonial diatom taxa dominated the DCL biomass; above and below the DCM, however, cryptophytes also contributed notably to total biomass. As the DCL weakened in August, green algae (*Chlorophyta*) and dinoflagellates increased in abundance throughout the water column – a trend which continued into early fall.

Abiotic predictors of the DCM

A DCL formed when the euphotic depth was near or below the epilimnion depth, and thermal structure variables were useful for predicting the DCM depth but not magnitude. Once the water column stratified, the DCL formed and was maintained until the epilimnion deepened beyond the euphotic zone, which occurred earlier on the eastern half of the lake in August to September (Fig. 4). The DCM depth was correlated with the epilimnion depth (slope = 0.62, intercept = 9.5, $R^2 = 0.38$) and thermocline depth (intercept = 6.8, slope = 0.64, $R^2 = 0.34$) independently, while thermocline steepness and euphotic depth were weak predictors on their own ($R^2 = 0.09$ and $R^2 = 0.10$, respectively) but improved the multiple linear regression model fit. The best-fit linear multiple regression model for DCM depth using only thermal structure variables included epilimnion depth, thermocline depth, thermocline steepness, and interaction terms for epilimnion depth with both thermocline depth and thermocline steepness ($R^2 = 0.47$, Table 2a). When the epilimnion depth was

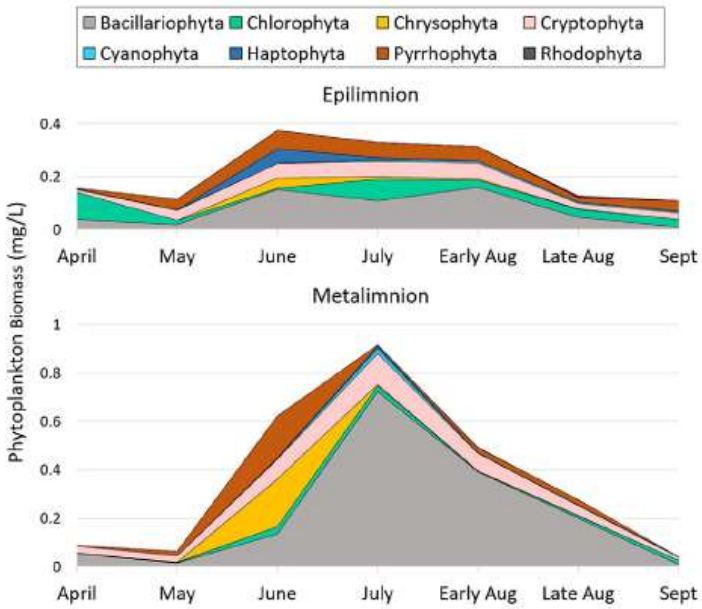

Fig. 6. Phytoplankton biomass and community composition by depth layer at the site offshore from Oswego, NY with a bottom depth of 200 m. When more than one sample was collected from a depth stratum, the biomass data for all available samples were averaged.

shallow (0–6 m), DCM depth was positively correlated with thermocline steepness; when the epilimnion was deep (>11 m), the DCM depth exhibited a strong positive correlation with thermocline depth. Including the euphotic depth in model selection produced a slightly better regression fit for the subset of stations sampled during the day ($R^2 = 0.52$). When euphotic depth was included, the only differences in the best-fit model were the addition of euphotic depth and the exchange of the interaction term between epilimnion depth and thermocline steepness for an interaction term between thermocline steepness and euphotic depth (Table 2b).

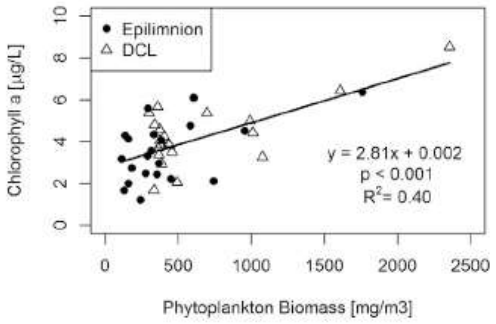

Fig. 7. Correlation of chlorophyll *a* concentration [µg/L] versus total phytoplankton biomass [mg/m^3] for samples collected when a DCL was present. The included samples were collected through the Cooperative Science and Monitoring Initiative sampling in July and the Great Lakes Restoration Initiative sampling offshore from Oswego, NY (200-m site only) from June through August.

While thermal structure variables appeared useful for predicting DCM depth, they did not predict DCM chlorophyll concentration well. The stepwise regression results only included epilimnion depth in the best-fit model, which was extremely weak ($R^2 = 0.10$, Table 2c). However, the addition of euphotic depth into the model produced a better fit on the subset of daytime data ($R^2 = 0.42$), suggesting that euphotic depth is critically important for determining the maximum chlorophyll concentration within the DCL. The model interpretation is challenging, however, because all interaction terms except thermocline depth with euphotic depth were included in the best-fit model (Table 2d).

Discussion

Previous work has reported conflicting information about the importance of likely drivers of DCL formation in Lake Ontario, including photoadaptation, in situ growth, or a combination of processes (e.g. Barbiero and Tuchman, 2001; Munawar et al., 1974; Twiss et al., 2012; Watkins et al., 2015). Our results indicate that in situ phytoplankton growth drives DCL formation in Lake Ontario during midsummer but that maximal production likely occurs shallower than the biomass and chlorophyll maxima. Later in the stratified season, settling and photoadaptation likely contribute to the maintenance of a DCL. Overlap of the euphotic zone with the metalimnion was a necessary condition for DCL formation in all cases, which provides a simple metric for assessing when a DCL will occur. The occurrence of greater nutrient concentrations in the metalimnion than the epilimnion (nitrate and silica) may also be a precondition for DCL formation and was observed throughout the stratified season in 2013. Furthermore, the DCM depth and chlorophyll concentration could be predicted reasonably well (adjusted $R^2 = 0.47$ and adjusted $R^2 = 0.42$, respectively) using multiple linear regression models with abiotic input variables, which offers promise for the development of empirical models to predict DCL characteristics in Lake Ontario.

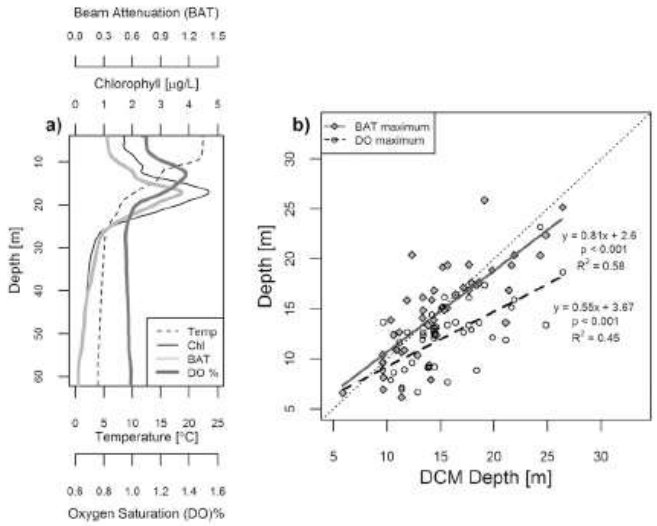

Fig. 8. a) Example profile data from station ON41 on July 20, 2013 showing temperature, chlorophyll, beam attenuation (BAT) and dissolved oxygen (DO) saturation %. b) Linear regressions for the depth of maxima in beam attenuation coefficient (BAT, gray diamonds) and dissolved oxygen saturation (DO, open circles) versus the depth of the deep chlorophyll maximum (DCM). The dotted line shows the 1:1 relationship for reference.

We based our conclusion that in situ growth is an important mechanism driving DCL formation on several lines of evidence: 1) phytoplankton biomass was significantly higher in the DCL than in the epilimnion during July ($p = 0.01$), phytoplankton biomass was correlated with chlorophyll concentration when a DCL was present in July (Fig. 7), and metalimnetic BAT maxima were observed within the DCL (Fig. 8), all of which suggest that photoadaptation was not the dominant cause of the DCL; 2) supersaturation of DO occurred within the metalimnion when a DCL was present (Fig. 8), suggesting that there was net production in the metalimnion; 3) the July DCL phytoplankton community was significantly different from the May and July epilimnetic communities (Fig. 9), indicating that a unique community developed within the DCL and thus settling cannot be the only cause of the DCL. Our results generally agree with and extend recent observations from Lake Ontario (Bramburger and Reavie, 2016; Twiss et al., 2012; Watkins et al., 2015), providing further evidence that it will be important to include the DCL in future total productivity estimates and projections about the possible bottom-up effects of oligotrophication.

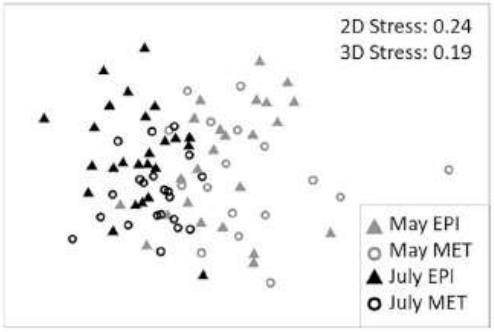

Fig. 9. Non-metric multidimensional scaling (NMDS) plot for the log-transformed Bray-Curtis similarity resemblance matrix by month and depth category. Epilimnetic (EPI) and metalimnetic (MET) communities were significantly different in July ($p = 0.002$), but not in May ($p = 0.236$). All other comparisons (crossing depth layers and months) were significant at the 0.1% level.

Spatio-temporal patterns of DCL formation

Our conclusions suggest that the Lake Ontario DCL shares characteristics with the upper Great Lakes, where the DCL historically contributed significantly to production, especially early in the stratified season (Fahnenstiel and Glime, 1983; Fahnenstiel and Scavia, 1987). Since oligotrophication has occurred in Lake Ontario, it is closer to the trophic status of the upper lakes than the more productive Lake Ontario of the 1970s (Dove and Chapra, 2015). However, Lake Ontario is still more productive than the upper lakes, and the DCL generally forms shallower in the water column. In Lake Ontario, the full extent of the DCL is typically within the metalimnion, whereas it often develops in the hypolimnion in Lake Michigan and Lake Superior. These differences are likely due to lower water transparency and higher overall productivity in Lake Ontario. During June through July of 2013, Lake Ontario DCLs formed considerably shallower and had greater magnitude (DCM 15 ± 1 m, 6.19 ± 0.29 µg/L) than recent observations from Lake Michigan (33 ± 2 m, 2.26 ± 0.13 µg/L) (Pothoven and Fahnenstiel, 2013). Data from the August 2013 GLNPO monitoring survey indicate that Lake Ontario DCMs were shallower and of greater magnitude than those in all the upper Great Lakes (Ontario 18 ± 1 m, 3.07 ± 0.64 µg/L; Michigan 40 ± 2 m, 1.58 ± 0.15 µg/L; Huron 36 ± 5 m, 1.03 ± 0.14 µg/L; Superior 35 ± 4 m, 1.51 ± 0.14 µg/L). The contribution of the DCL to total phytoplankton production may be greater for lakes closer to a mesotrophic than oligotrophic state (Moll and Stoermer, 1982). Because Lake Ontario is somewhat more productive, the DCL in Lake Ontario is likely to be as, if not more, important to total production than it currently is in the upper Great Lakes. Further study of the DCL's contribution to total lake productivity is warranted. High depth-resolution productivity measurements extending through the metalimnion have not been reported in

Table 2
Multiple linear regression parameter estimates for the best fit model for predicting a) DCM depth using thermal structure variables with all stations ($n = 63$, $p < 0.001$, adjusted $R^2 = 0.47$) b) DCM depth using thermal structure variables and euphotic depth for daytime stations only ($n = 24$, $p = 0.004$, adjusted $R^2 = 0.52$) c) DCM chlorophyll using thermal structure variables with all stations ($n = 63$, $p = 0.006$, adjusted $R^2 = 0.10$) and d) DCM chlorophyll using thermal structure variables and euphotic depth for daytime stations only ($n = 24$, $p = 0.039$, adjusted $R^2 = 0.42$). Significant p values in bold font.

Parameter	Estimate	p-Value
a) DCM depth vs. thermal structure variables		
$n = 63$; $p < 0.001$; $R^2 = 0.47$		
(Intercept)	14.6	**<2e−16**
Epilimnion depth	0.06	0.746
Thermocline depth	0.46	**0.009**
Thermocline steepness	1.54	**0.010**
Epilimnion depth × thermocline depth	0.04	**0.031**
Epilimnion depth × thermocline steepness	−0.21	**0.009**
b) DCM depth vs. thermal structure variables & euphotic depth		
$n = 24$; $p = 0.004$; $R^2 = 0.52$		
(Intercept)	13.6	**5.48e−11**
Epilimnion depth	0.08	0.787
Thermocline depth	0.60	0.071
Thermocline steepness	2.31	**0.033**
Euphotic depth	0.51	0.216
Epilimnion depth × thermocline depth	0.08	0.061
Thermocline steepness × euphotic depth	0.64	0.092
c) DCM chlorophyll vs. thermal structure variables		
$n = 63$; $p = 0.006$; $R^2 = 0.10$		
(Intercept)	5.28195	**<2e−16**
Epilimnion depth	−0.13078	**0.00622**
d) DCM chlorophyll vs. thermal structure variables & euphotic depth		
$n = 24$; $p = 0.039$; $R^2 = 0.42$		
(Intercept)	6.71985	**8.84e−09**
Epilimnion depth	−0.28175	0.08152
Thermocline depth	0.14848	0.38755
Thermocline steepness	−0.42987	0.34532
Euphotic depth	0.30578	0.18002
Epilimnion depth × thermocline depth	−0.03826	0.08871
Epilimnion depth × thermocline steepness	−0.27309	0.07083
Epilimnion depth × euphotic depth	0.17656	**0.00431**
Thermocline depth × thermocline steepness	0.30388	0.15179
Thermocline steepness × euphotic depth	−0.28735	0.21822

recent decades, although initial efforts toward providing these for Lake Ontario began during the CSMI year 2013 (Weidel, unpublished data).

Mechanisms of DCL formation

Photoadaptation of phytoplankton under low light has been suggested as a mechanism contributing to DCL formation in each of the Great Lakes, including Lake Ontario (Barbiero and Tuchman, 2001), but its relative importance is likely to vary among lakes and seasons. Of course, photoadaptation and in situ growth are not mutually exclusive processes. For example, there is evidence that they operate together to form the DCL in Lake Superior (Barbiero and Tuchman, 2004; White and Matsumoto, 2012). Fahnenstiel and Scavia (1987) suggested that the DCL in Lake Michigan is due primarily to in situ growth early in the season, but as the DCL deepens during mid- to late-stratification the importance of photoadaptation increases. Similarly, our results indicate that photoadaptation is not the primary mechanism of DCL formation during the summer in Lake Ontario. Primary evidence for this conclusions includes the occurrence of metalimnetic BAT maxima as consistent features of profile data when a DCL was present, indicating that the DCL is associated with an increase in particle concentrations. In addition, the phytoplankton biomass to chlorophyll ratio did not vary greatly with depth (Fig. 7). Note, however, that picoplankton was not included in our phytoplankton count data, and thus is excluded from phytoplankton biomass estimates. Picoplankton contributes significantly to total production in Lake Ontario (Munawar et al., 2015) and accounted for 28% (DCL) to 42% (epilimnion) of the total chlorophyll measured in July. Therefore, the total phytoplankton biomass used for comparison with chlorophyll was underestimated in our study, especially in the metalimnion. The importance of picoplankton could cause us to underestimate the role of photoadaptation based on this dataset, and we expect that photoadaptation may be important toward the bottom of the DCL (our samples are a composite from three depths within the DCL) and during late summer and fall.

Our data suggest that there was net production in the metalimnion during summer stratification because we found that a metalimnetic supersaturation of DO occurred when a DCL was present. However, the DO max was often shallower than the BAT max and the DCM, especially when the DCM occurred relatively deep (Fig. 8). Our findings agree with general observations from Lake Ontario in 2008, which suggested that the DO peak sometimes occurs above the DCM (Watkins et al., 2015). Thus, maximal production may occur at shallower depths where light levels are higher, or the DCM may consist of less active phytoplankton that are concentrated in the pycnocline. Depth-stratified primary production measurements in Lake Superior exhibit a similar discrepancy between the production, biomass, and chlorophyll maxima (Sterner, 2010), and this difference may be caused by photoadaptation below the productivity and biomass peaks. A similar process may occur in Lake Ontario. As the DCL deepens through late summer and fall, the productivity maxima (DO maxima) diverge from the DCM and BAT maxima. However, the interpretation of the metalimnetic DO maximum as a productivity peak should be done with caution. Recently, Wilkinson et al. (2015) challenged this generally accepted connection because physical processes, namely warming of gases trapped below the thermocline, could contribute to the development of a metalimnetic oxygen peak. Such physical mechanisms may contribute to the observed discrepancies in the depths of the DO saturation maximum, BAT maximum and DCM in Lake Ontario. Furthermore, the DCM occurs below the euphotic depth in August to September (Fig. 4), which suggests that the late season DCL is likely less productive and may be maintained by the settling of phytoplankton along the pycnocline or photoadaptation. The few samples available from the Oswego 200-m site in August and September do not show differences in the ratio of chlorophyll to phytoplankton biomass with depth, however, suggesting that settling may be a greater factor than is photoadaptation.

Additional support for our conclusion that in situ growth is a major contributor to DCL formation in Lake Ontario is provided by the phytoplankton taxonomy data from May and July. Since the July DCL phytoplankton community was distinct from both the springtime and the overlying summer epilimnetic communities, phytoplankton growth within the metalimnion likely affected DCL community structure. Bramburger and Reavie (2016) also reported significant differences between springtime integrated, summer epilimnetic, and summer DCL phytoplankton communities, which were driven largely by differences in diatom assemblage and were attributed to in situ growth. Our analysis confirms their findings using samples from late spring (May) to midsummer (July) rather than their longer period from early spring (April) and late summer (August), which fills in the temporal gap and demonstrates that the DCL hosts a distinct phytoplankton community as early as July. However, the July phytoplankton community did have considerable overlap with both the spring and summer epilimnetic communities, even though it was statistically different (Fig. 9). This overlap indicates that sinking and settling of phytoplankton along the pycnocline probably contributed to the DCL as well. This agrees with Bramburger and Reavie (2016) who concluded that sinking of heavier individuals contributed to the DCL community in August because conspecific individuals from the two depth layers exhibited higher average cell size in the metalimnion. Our data support the conclusion that the DCL may be seeded by the sinking of phytoplankton from overlying waters throughout the season, but the dominant DCL diatom taxa (*Tabellaria*, *Fragilaria*, *Diatoma*) and cyanophytes (*Pseudanabaena*, *Synechocystis*) are better able to persist and grow in the metalimnion, driving the development of a unique community at depth.

Nutrient limitation in the epilimnion likely drives the redistribution of phytoplankton production during stratification and thus influences DCL formation. Depletion of epilimnetic nutrients is known to contribute to DCL formation, as limiting nutrients are often more available below the thermocline. For example, the DCM in Lake Tahoe is commonly associated with a nitracline (Coon et al., 1987), nitrate and dissolved silica are higher in the DCL than the epilimnion in Lake Michigan (Moll et al., 1984) and DCL phytoplankton in Lake Superior are phosphorus-enriched (Barbiero and Tuchman, 2004). In Lake Ontario during 2013, SRP did not exhibit major changes with depth, but nitrate + nitrite and dissolved reactive silica concentration gradients developed during July. In July through September, epilimnetic Si concentrations were low enough to limit diatom growth, but they were above limiting concentrations in the DCL (Fig. 3) (Sommer, 1988). These data suggest that increased nutrient availability of silica, and possibly nitrate, may be a major factor in determining the depth of diatom-dominated DCLs in Lake Ontario. The lack of a peak in SRP in the DCL suggests that this nutrient is taken up quickly by the phytoplankton in both the epilimnion and the DCL. The contribution of SRP by zooplankton residing in the DCL may therefore also be important (Oliver et al., 2015).

Significant zooplankton grazing pressure in the epilimnion can also cause the development of a DCM feature when grazing pressure in the metalimnion is relatively low (Pilati and Wurtsbaugh, 2003), and DCLs formed in this way are essentially artifacts of zooplankton activity. However, the zooplankton community structure of Lake Ontario gives us reason to expect that high zooplankton grazing in the epilimnion is not a primary contributor to DCL formation. Daytime grazing rates are likely relatively low in the epilimnion because zooplankton density is typically highest in the metalimnion during the day in summer. Although much of the zooplankton, especially the dominant cyclopoid copepod *Diacyclops thomasi*, do exhibit diel vertical migration (DVM) to the epilimnion at night (Watkins et al., this issue), DVM may be motivated by factors such as a preference for warmer temperatures combined with predation evasion, rather than food density or food quality (Williamson et al., 1996). Predation risk from *Mysis diluviana* and *Limnocalanus macrurus*, which migrate from the hypolimnion to the metalimnion at night, may drive smaller zooplankton to migrate into the epilimnion even when food resources are highest in the DCL. While it would be useful to explicitly study the effect that variable zooplankton grazing may have on DCL dynamics, there is considerable evidence presented here that in situ growth is likely more important than grazing pressure as a driver of DCL formation in Lake Ontario.

Abiotic predictors of the DCM

Our analysis shows that DCL presence/absence, depth, and chlorophyll concentrations can be predicted reasonably well using simple thermal structure variables and euphotic depth. The results from our multiple linear regression analyses indicate that the depth of the DCM is positively correlated with epilimnion depth, thermocline depth, and thermocline steepness, and the interactions of epilimnion depth with both thermocline depth and thermocline steepness were significant ($p = 0.031$ and $p = 0.009$, respectively). Graphical exploration of the interaction terms suggests that water column stability strongly affects the depth at which a DCM occurs when the epilimnion is shallow, such as during early-season stratification. This dependence on thermocline steepness is likely due to the impact of water column stability on the diffusivity of nutrients. If the water column is only weakly stratified, we would expect the DCM to remain somewhat shallower because higher nutrient diffusion would allow for phytoplankton growth shallower in the water column. When the epilimnion extended beyond 11 m, however, the water column was typically strongly stratified and there was greater nutrient depletion within the epilimnion.

Previous DCL modeling efforts have generally taken mechanistic approaches, employing ecological models coupled with physical or hydrodynamic models (Hodges and Rudnick, 2004; Varela et al., 1992; White and Matsumoto, 2012). For example, White and Matsumoto (2012) used a three-dimensional hydrodynamic model coupled with an ecological model to investigate the causal mechanisms of DCLs in Lake Superior and found that photoadaptation was a primary mechanism contributing to the DCM depth, while other factors such as zooplankton grazing and phytoplankton settling were important for determining the DCM magnitude. While our empirical regression model approach does not directly address mechanisms of DCL formation, it may prove useful for scaling up our observations of spatio-temporal patterns in DCL formation. For example, an empirical model predicting DCL depth and magnitude from thermal structure could be directly applied to the output of hydrodynamic models to better predict lakewide DCL characteristics.

Such spatially and temporally comprehensive estimates of DCL characteristics will be critical to predicting the long-term effects of ecosystem change on zooplankton and fish. For example, the observed high abundance of large diatoms in the DCL could contribute to a zooplankton community shift toward dominance by large metalimnetic and hypolimnetic zooplankton species such as *Limnocalanus macrurus* and *Leptodiaptomus sicilis*, which has been observed in Lake Ontario over the past decade (Barbiero et al., 2014; Rudstam et al., 2015). A productive DCL may provide a competitive advantage to these species as well as to mysids, which are physiologically better adapted to grazing at colder temperatures and typically migrate from the hypolimnion to the metalimnion at night. Such changes in zooplankton biomass distribution may also affect fish communities, for example, by improving conditions for the restoration of coregonid populations.

The current prominence of a biologically active DCL during summer suggests that Lake Ontario has undergone a state change since the 1970s – from a system where most summertime primary production occurred within the epilimnion and there was net respiration in the metalimnion (Boyd, 1980), to a system where summer production is also occurring within the metalimnion. The major drivers of this change were likely reduced phosphorus loading and the impacts of *Dreissena* mussels introduced in the early 1990s, both of which have contributed to decreased surface chlorophyll and increased water clarity (Mills et al., 2003). Therefore, future estimates of whole water column production for Lake Ontario need to include quantifying DCL production throughout the season.

Acknowledgements

This study was supported by the Great Lakes Fisheries Commission (2013_RUD_44029) and the Great Lakes Restoration Initiative, through grants from the USGS-Great Lakes Science Center (G13AC00064) and the U.S. Environmental Protection Agency (U.S. EPA) Cooperative Agreement to Cornell University (GL 00E01184-0). The research described in this article has not been subjected to U.S. EPA review. Any opinions expressed in this publication are those of the authors and do not necessarily reflect the views or policies of the U.S. EPA. Any use of trade, product or firm names is for descriptive purposes only and does not imply endorsement by the U.S. EPA or USGS. We are grateful to the captains and crews of the R/V Lake Guardian and R/V Kaho, and the technicians and graduate students at Cornell University and USGS that contributed to the data presented in this paper.

References

Baca, R.G., Arnett, R.C., 1976. A Limnological Model for Eutrophic Lakes and Impoundments. Batelle, Pacific Northwest Laboratories.

Barbiero, R.P., Lesht, B.M., Warren, G.J., 2014. Recent changes in the offshore crustacean zooplankton community of Lake Ontario. J. Great Lakes Res. 40:898–910. http://dx.doi.org/10.1016/j.jglr.2014.08.007.

Barbiero, R.P., Tuchman, M.L., 2001. Results from the U.S. EPA's biological open water surveillance program of the Laurentian Great Lakes: II. Deep chlorophyll maxima. J. Great Lakes Res. 27:155–166. http://dx.doi.org/10.1016/S0380-1330(01)70629-6.

Barbiero, R.P., Tuchman, M.L., 2004. The deep chlorophyll maximum in Lake Superior. J. Great Lakes Res. 30, 256–268.

Binding, C.E., Greenberg, T.A., Watson, S.B., Rastin, S., Gould, J., 2015. Long term water clarity changes in North America's Great Lakes from multi-sensor satellite observations. Limnol. Oceanogr. 60: 1976–1995. http://dx.doi.org/10.1002/lno.10146.
Binding, C.E., Jerome, J.H., Bukara, R.P., Booty, W.G., 2007. Trends in water clarity of the lower Great Lakes from remotely sensed color. J. Great Lakes Res. 33, 828–841.
Boyd, J.D., 1980. Metalimnetic oxygen minima in Lake Ontario, 1972. J. Great Lakes Res. 6: 95–100. http://dx.doi.org/10.1016/S0380-1330(80)72087-7.
Bramburger, A.J., Reavie, E.D., 2016. A comparison of phytoplankton communities of the deep chlorophyll layers and epilimnia of the Laurentian Great Lakes. J. Great Lakes Res. 42, 1016–1025.
Brooks, A.S., Torke, B.G., 1977. Vertical and seasonal distribution of chlorophyll a in Lake Michigan. J. Fish. Res. Board Can. 34:2280–2287. http://dx.doi.org/10.1139/f77-306.
Bunnell, D.B., Barbiero, R.P., Ludsin, S.A., Madenjian, C.P., Warren, G.J., Dolan, D.M., Brenden, T.O., Briland, R., Gorman, O.T., He, J.X., Johengen, T.H., Lantry, B.F., Lesht, B.M., Nalepa, T.F., Riley, S.C., Riseng, C.M., Treska, T.J., Tsehaye, I., Walsh, M.G., Warner, D.M., Weidel, B.C., 2014. Changing ecosystem dynamics in the Laurentian Great Lakes: bottom-up and top-down regulation. Bioscience 64:26–39. http://dx.doi.org/10.1093/biosci/bit001.
Camacho, A., 2006. On the occurrence and ecological features of deep chlorophyll maxima (DCM) in Spanish stratified lakes. Limnetica 25, 453–478.
Clarke, K.R., 1993. Non-parametric multivariate analyses of changes in community structure. Aust. J. Ecol. 18, 117–143.
Clarke, K.R., Gorley, R.N., 2015. PRIMER v7: User Manual/Tutorial. PRIMER-E, Plymouth (296 pp.).
Coon, T.G., Lopez, M.M., Richerson, P.J., Powell, T.M., Goldman, C.R., 1987. Summer dynamics of the deep chlorophyll maximum in Lake Tahoe. J. Plankton Res. 9: 327–344. http://dx.doi.org/10.1093/plankt/9.2.327.
Cullen, J.J., 1982. The deep chlorophyll maximum: comparing vertical profiles of chlorophyll a. Can. J. Fish. Aquat. Sci. 39:791–803. http://dx.doi.org/10.1139/f82-108.
Dobson, H.F.H., 1984. Lake Ontario Water Chemistry Atlas. Environ. Can. Sci. Series No. 139.
Dove, A., Chapra, S.C., 2015. Long-term trends of nutrients and trophic response variables for the Great Lakes. Limnol. Oceanogr. 60:696–721. http://dx.doi.org/10.1002/lno.10055.
Fahnenstiel, G.L., Glime, J., 1983. Subsurface chlorophyll maximum and associated Cyclotella pulse in Lake Superior. Int. Rev. Gesamten Hydrobiol. Hydrogr. 68, 605–616.
Fahnenstiel, G.L., Scavia, D., 1987. Dynamics of Lake Michigan phytoplankton: the deep chlorophyll layer. J. Great Lakes Res. 13:285–295. http://dx.doi.org/10.1016/S0380-1330(87)71652-9.
Hodges, B.A., Rudnick, D.L., 2004. Simple models of steady deep maxima in chlorophyll and biomass. Deep Sea Res. Part I Oceanogr. Res. Pap. 51:999–1015. http://dx.doi.org/10.1016/j.dsr.2004.02.009.
Holeck, K.T., Rudstam, L.G., Watkins, J.M., Luckey, F., Lantry, J.R., Lantry, B.F., Trometer, B., Koops, M., Johnson, T., 2015. Lake Ontario water quality during the 2003 and 2008 intensive field years and comparison with long-term trends. Aquat. Ecosyst. Health Manag. 18, 7–17.
Lean, D.R.S., Fricker, H.J., Charlton, M.N., Cuhel, R.L., Pick, F.R., 1987. The Lake Ontario life support system. Can. J. Fish. Aquat. Sci. 44, 2230–2240.
Mills, E., Casselman, J., Dermott, R., Fitzsimons, J., Gal, G., Holeck, K., Hoyle, J., Johannsson, O., Lantry, B., Makarewicz, J., Millard, E., Munawar, I., Munawar, M., Owens, R., Rudstam, L., Schaner, T., Stewart, T., 2003. Lake Ontario: food web dynamics in a changing ecosystem (1970–2000). J. Fish. Aquat. Sci. 60:471–490. http://dx.doi.org/10.1139/F03-033.
Moll, R.A., Brache, M.Z., Peterson, T.P., 1984. Phytoplankton dynamics within the subsurface chlorophyll maximum of Lake Michigan. J. Plankton Res. 6:751–766. http://dx.doi.org/10.1093/plankt/6.5.751.
Moll, R.A., Stoermer, E.F., 1982. A hypothesis relating trophic status and subsurface chlorophyll maxima of lakes. Arch. Hydrobiol. 94, 425–440.
Munawar, M., Munawar, I.F., Fitzpatrick, M., Niblock, H., Lorimer, A.J., 2015. The phytoplankton community of Lake Ontario in 2008: structure, biodiversity and long term changes. Aquat. Ecosyst. Health Manag. 18 (1), 28–42.
Munawar, M., Stadelmann, P., Munawar, I.F., 1974. Phytoplankton biomass, species composition and primary production at a nearshore and a midlake station of Lake Ontario during IFYGL (IFYGL) International Field Year for the Great Lakes. Proc Conf Great Lakes Res.
Oliver, S.K., Branstrator, D.K., Hrabik, T.R., Guildford, S.J., Hecky, R.E., 2015. Nutrient excretion by crustacean zooplankton in the deep chlorophyll layer of Lake Superior. Can. J. Fish. Aquat. Sci. 72, 390–399.
Pilati, A., Wurtsbaugh, W.A., 2003. Importance of zooplankton for the persistence of a deep chlorophyll layer: a limnocorral experiment. Limnol. Oceanogr. 48, 249–260.
Pothoven, S.A., Fahnenstiel, G.L., 2013. Recent change in summer chlorophyll a dynamics of southeastern Lake Michigan. J. Great Lakes Res. 39, 287–294.
R Core Team, 2016. R: A Language and Environment for Statistical Computing. R Foundation for Statistical Computing, Vienna, Austria (URL https://www.R-project.org/).
Riley, S.C., Roseman, E.F., Nichols, S.J., O'Brien, T.P., Kiley, C.S., Schaeffer, J.S., 2008. Deepwater demersal fish community collapse in Lake Huron. Trans. Am. Fish. Soc. 137: 1879–1890. http://dx.doi.org/10.1577/T07-141.1.
Rudstam, L.G., Holeck, K.T., Bowen, K.L., Watkins, J.M., Weidel, B.C., Luckey, F.J., 2015. Lake Ontario zooplankton in 2003 and 2008: community changes and vertical redistribution. Aquat. Ecosyst. Health Manag. 18, 43–62.
Rudstam, L.G., Holeck, K.T., Watkins, J.M., Hotaling, C., Lantry, J.R., Bowen, K.L., Munawar, M., Weidel, B.C., Barbiero, R.P., Luckey, F.J., Dove, A., Johnson, T.B., Biesinger, Z., 2017. Nutrients, Phytoplankton, Zooplankton, and Macrobenthos. Great Lakes Fisheries Commission Special Publications 2013. State of Lake Ontario.
Schlitzer, R., 2015. Ocean Data View. http://odv.awi.de.
Sommer, U., 1988. Growth and Survival Strategies of Planktonic Diatoms. Growth Reprod. Strateg. Freshw. Phytoplankton Camb.Univ. Press Camb., pp. 227–260.
Stadelmann, P., Moore, J.E., Pickett, E., 1974. Primary production in relation to temperature structure, biomass concentration, and light conditions at an inshore and offshore station in Lake Ontario. J. Fish. Res. Board Can. 31:1215–1232. http://dx.doi.org/10.1139/f74-145.
Sterner, R.W., 2010. In situ-measured primary production in Lake Superior. J. Great Lakes Res. 36:139–149. http://dx.doi.org/10.1016/j.jglr.2009.12.007.
Twiss, M.R., Ulrich, C., Zastepa, A., Pick, F.R., 2012. On phytoplankton growth and loss rates to microzooplankton in the epilimnion and metalimnion of Lake Ontario in mid-summer. J. Great Lakes Res. 38 (Supplement 4):146–153. http://dx.doi.org/10.1016/j.jglr.2012.05.002.
Varela, R.A., Cruzado, A., Tintore, J., Garda Ladona, E., 1992. Modelling the deep-chlorophyll maximum: a coupled physical-biological approach. J. Mar. Res. 50:441–463. http://dx.doi.org/10.1357/0022240927847976 38.
Watkins, J.M., Rudstam, L.G., Crabtree, D.L., Walsh, M.G., 2013. Is reduced benthic flux related to the Diporeia decline? Analysis of spring blooms and whiting events in Lake Ontario. J. Great Lakes Res. 39:395–403. http://dx.doi.org/10.1016/j.jglr.2013.05.007.
Watkins, J.M., Weidel, B.C., Rudstam, L.G., Holeck, K.T., 2015. Spatial extent and dissipation of the deep chlorophyll layer in Lake Ontario during the Lake Ontario lower foodweb assessment, 2003 and 2008. Aquat. Ecosyst. Health Manag. 18, 18–27.
Watson, N.H.F., Thomson, K.P.B., Elder, F.C., 1975. Sub-thermocline biomass concentration detected by transmissometer in Lake Superior. Verh. Int. Ver. Limnol. 19, 682–688.
Welschmeyer, N.A., 1994. Fluorometric analysis of chlorophyll a in the presence of chlorophyll b and pheopigments. Limnol. Oceanogr. 39, 1985–1992.
White, B., Matsumoto, K., 2012. Causal mechanisms of the deep chlorophyll maximum in Lake Superior: a numerical modeling investigation. J. Great Lakes Res. 38:504–513. http://dx.doi.org/10.1016/j.jglr.2012.05.001.
Wilkinson, G.M., Cole, J.J., Pace, M.L., Johnson, R.A., Kleinhans, M.J., 2015. Physical and biological contributions to metalimnetic oxygen maxima in lakes. Limnol. Oceanogr. 60:242–251. http://dx.doi.org/10.1002/lno.10022.
Williamson, C.E., Sanders, R.W., Moeller, R.E., Stutzman, P.L., 1996. Utilization of subsurface food resources for zooplankton reproduction: Implications for diel vertical migration theory. Limnol. Oceanogr. 41:224–233. http://dx.doi.org/10.4319/lo.1996.41.2.0224.

CHAPTER 2
TESTING THEORY OF DEEP CHLOROPHYLL MAXIMA FORMATION ACROSS A PRODUCTIVITY GRADIENT: A CASE STUDY IN THE LAURENTIAN GREAT LAKES

ABSTRACT

Deep chlorophyll maxima (DCM) are common features in stratified lakes and oceans, and phytoplankton growth in DCM often contributes significantly to total system primary production. Theory suggests that the mechanisms contributing to DCM formation should be predictable across a productivity gradient. DCM typically do not occur in eutrophic bodies of water due to high production in the epilimnion and low water clarity. We expect DCM to be near the thermocline, narrow, and highly productive in mesotrophic to meso-oligotrophic systems and become deeper, broader, and less productive with increasing oligotrophy. This study investigates the applicability of this theory to the Laurentian Great Lakes using data generated by the US Environmental Protection Agency's Great Lakes National Program Office (GLNPO) from 1996 through 2017. We found that DCM characteristics were generally consistent with theory, as both DCM depth and thickness increased while DCM chlorophyll decreased with oligotrophy. DCM in meso-oligotrophic waters were closely aligned with deep biomass maxima (DBM) and dissolved oxygen saturation maxima (DO_{max}), suggesting they are productive, while the depths at which the DCM/DBM/DO_{max} occurred diverged in ultra-oligotrophic waters. Euphotic depth was a significant predictor of both DCM depth and chlorophyll concentration across lakes, with greater water clarity associated with deeper and weaker

DCM. DCM depth has increased since 1996 only in Lake Michigan, while DCM chlorophyll concentrations have decreased significantly in all lakes except Lake Erie.

INTRODUCTION

Deep chlorophyll maxima (DCM) are common features in mesotrophic to oligotrophic lakes and oceans with stratified water columns, but the mechanisms driving their magnitude and depth can vary widely across systems. Processes contributing to DCM formation may include phytoplankton growth at depth, slower phytoplankton sinking rates at the pycnocline, high zooplankton grazing on epilimnetic phytoplankton, photoinhibition of phytoplankton growth near the surface, and phytoplankton photoadaptation to different light environments (Camacho, 2006; Cullen, 1982). While all of these processes can affect chlorophyll distributions, primary production below the mixed layer is often high in water bodies with stable stratification and nutrient depletion within the mixed layer. Limited surface production and high water clarity allow for phytoplankton growth at greater depths the water column, where there is greater nutrient availability (Cullen 2015). Thus, phytoplankton production often occurs near the top of the nutricline in oligotrophic waters, leading to the development of deep biomass maxima (DBM) associated with DCM (Banse, 1987; Jamart et al., 1977). Production in DCM can contribute over 60% to areal primary production in oligotrophic water bodies (e.g. Moll et al. 1984; Weston et al. 2005; Giling et al. 2017), making it important to include DCM in estimates of system productivity (Hemsley et al., 2015).

Another important process which can cause DCM formation is the physiological adaptation of phytoplankton to their light environment (photoadaptation). Chlorophyll is a commonly-used proxy for phytoplankton biomass, and thus DCM features are often

assumed to be associated with DBM. However, chlorophyll is not always a good measure of phytoplankton biomass across depths due to the variable chlorophyll content of phytoplankton, caused by both differences among taxa (Geider, 1993) and photoadaptation, whereby algal cells decrease the C:Chl in their cells in low light and increase C:Chl in high light. In ultra-oligotrophic systems with high water clarity, DCM may be largely attributed to differences in C:Chl across depth strata due to photoadaptation (e.g. Steele 1964; Fennel and Boss 2003a; White and Matsumoto 2012) rather than high phytoplankton biomass or production at depth. In such cases, DCM are not necessarily associated with DBM and thus could be misinterpreted if the role photoadaptation is not appropriately considered.

DCM are well-studied in offshore marine tropical systems with stable stratification and long-term nutrient depletion in the mixed layer (Cullen, 1982; Herbland and Voituriez, 1979; Yentsch, 1980). Of course, other marine and freshwater systems that maintain stable stratification long enough to develop a nutricline during the summer often exhibit seasonal DCM which can contribute significantly to summer production (Barbiero and Tuchman, 2001a; e.g. Coon et al., 1987; Estrada et al., 1993). Cullen (2015), in a review of DCM formation (primarily based on marine studies), summarized common features of systems with DCM and demonstrated that the depth of the nutricline/DCM is typically inversely related to chlorophyll concentration at the DCM, water column integrated chlorophyll, and integrated primary productivity (e.g. Yentsch 1974, 1980; Herbland and Voituriez 1979; Beckmann and Hense 2007). It can thus be inferred that as total system productivity decreases with oligotrophication, DCM should form deeper in the water column, decrease in magnitude, and become less productive as well. In ultra-

oligotrophic systems, nutrient conditions may be so poor that production is low throughout the water column and photoadaptation is primarily responsible for observed DCM. Previous observations from freshwater systems generally with these expectations (Barbiero et al., 2001; Camacho, 2006; Moll and Stoermer, 1982), although extensive studies of DCM dynamics for lakes are fewer than for offshore marine environments.

Basic hypotheses about DCM in lakes across a productivity gradient were proposed by Moll and Stoermer (1982), the fundamentals of which are consistent with the principles established by Cullen (2015). Using data from Lakes Michigan and Superior, Moll and Stoermer (1982) emphasized that DCM in large oligotrophic lakes generally form deeper and are broader than those described in more productive lakes (Fee, 1976). Furthermore, DCM chlorophyll concentrations were lower in the more oligotrophic Lake Superior than in Lake Michigan, suggesting that continued oligotrophication may lead to declines in DCM biomass (and likely production). In addition, multiple studies have shown that water clarity is an important factor determining DCM depth across lakes of varying types (e.g. Hamilton et al. 2010; Leach et al. 2017), while lake size (surface area and maximum depth) may be important for determining DCM thickness (Leach et al., 2018). Furthermore, the depth range at which phytoplankton growth can occur increases as lake transparency increases, which may lead to broader DCM in more oligotrophic waters with high transparency (Beckmann and Hense, 2007). There has been less attention given, however, to studying the relative distributions of production, biomass, and chlorophyll within the water column, and assessing how these distributions change across a productivity gradient is an important step toward improving our ability to assess the role of DCM.

The Laurentian Great Lakes are particularly interesting systems in which to study DCM because they are among the largest lakes in the world, bridging the gap between marine systems and smaller lakes. In addition, these lakes exhibit a productivity gradient, ranging from eutrophic (western Lake Erie) to ultra-oligotrophic (Lake Superior) and DCM formation is common in all except Lake Erie. Several of the Great Lakes have experienced oligotrophication over the past two decades due to lower nutrient loads, and the rapid spread of non-native dreissenid mussels may also have affected nutrient cycling and contributed to increased water clarity (Dove and Chapra, 2015; e.g. Madenjian et al., 2002; Mills et al., 2003). As a result, the trophic state of Lakes Michigan and Huron have converged toward that of Lake Superior (Barbiero et al., 2012), while Lake Ontario has also become more oligotrophic (Dove, 2009; Rudstam et al., 2017). In addition to changes in spring total phosphorus and water clarity, summer phytoplankton (Reavie et al., 2014) and zooplankton communities have shifted toward dominance by more oligotrophic species in Lakes Huron, Michigan, and Ontario (Barbiero et al., 2014, 2012), suggesting bottom-up changes to the food web (Bunnell et al., 2014) and driving increased interest in studying DCM in the Great Lakes (Koops et al., 2015; Oliver et al., 2014; Pothoven and Fahnenstiel, 2013; Watkins et al., 2015).

Previous research on DCM in the Great Lakes system includes multiple studies of Lakes Superior, Michigan, and Ontario, as well as a single cross-lake comparison based on summer data from 1998 (Barbiero and Tuchman, 2001b). Photoacclimation and phytoplankton sinking appear to be the most important drivers of DCM depth and magnitude in Lake Superior (Barbiero and Tuchman, 2004; White and Matsumoto, 2012), while the DCM in Lake Michigan has historically contributed up to 30-60% of

summertime production (Brooks and Torke, 1977; Fahnenstiel and Scavia, 1987; Moll et al., 1984). However, chlorophyll concentrations of DCM in Lake Michigan have decreased significantly since the 1970s as oligotrophication has occurred (Fahnenstiel et al., 2010), again suggesting convergence toward Lake Superior. There are fewer studies from Lake Ontario prior to the 2000s, but the available data suggest that in previous decades, maximum primary production occurred in the epilimnion and there was net respiration below the thermocline – consistent with light limitation rather than nutrient limitation (Boyd, 1980; Stadelmann et al., 1974). When DCM did form, they occurred at relatively shallow depths near the top of the thermocline and had chlorophyll concentrations only slightly higher than those found in the epilimnion. In recent years, however, DCM have become nearly ubiquitous during summer stratification, are associated with DBM, and are likely productive (Scofield et al., 2017; Twiss et al., 2012; Watkins et al., 2015). Although these studies suggest that the Great Lakes are consistent with patterns observed in marine systems, a comprehensive cross-lake comparison using standardized methods will provide more robust insights about DCM formation in the Great Lakes and allow us to test theory of DCM dynamics in a large freshwater system.

This study tests if hypotheses derived from DCM theory (Cullen 2015) can be applied to the Great Lakes using data collected through the US Environmental Protection Agency's Great Lakes National Program Office (GLNPO) monitoring program from 1996 to 2017. Specifically, we ask whether the patterns observed in cross-lake comparisons and over time align with expectations derived from previous observations by addressing the following research questions: (**1)** Are differences in DCM depth, thickness, and chlorophyll concentration consistent with expectations based on lake

trophic state? We hypothesize that DCM will become deeper, broader, and have lower chlorophyll concentrations in more oligotrophic lakes. (**2)** What abiotic factors are correlated with differences in DCM characteristics, both across lakes and over time? We consider water clarity, thermal structure, and nutrient concentrations as potential drivers of trends in the DCM. (**3)** Are indicators of DCM-forming mechanisms consistent with expectations based on lake productivity status? We examine potential mechanisms using beam attenuation coefficient and dissolved O_2 saturation profiles as proxies for phytoplankton biomass and productivity distributions, respectively. We hypothesize that biomass and production within the DCM will decline with oligotrophication, and that photoadaptation will become a more important driver of DCM in oligotrophic systems. Taken together, these research questions allow us to investigate whether Cullen's (2015) general framework for understanding DCM mechanisms across a trophic gradient derived using oceanographic data can be applied to these large lakes and perhaps lakes in general.

METHODS

Study system

The Laurentian Great Lakes are a chain of deep glacial freshwater lakes that contain one of the largest surface freshwater resource on Earth, representing approximately 20% of the world's supply. Water generally flows through the Great Lakes system from west to east, draining from Lake Superior and Lake Michigan to Lake Huron, through the St. Clair River and Detroit River to Lake Erie, and over Niagara Falls (or through the Welland Canal) to Lake Ontario (Fig. 1), and the Great Lakes watershed eventually drains to the Atlantic Ocean through the St. Lawrence (NOAA and

Laboratory, 2016). Lake Superior is the largest of the Great Lakes in terms of surface area (82,097 km^2), and it also has the greatest volume to due to its depth (mean 149 m, max 406 m). Lake Ontario is the second deepest (mean 86 m, max 244 m), although it has the smallest surface area (19,009 km^2), followed by Lake Michigan (mean 85 m, max 281 m, surface area 57,753 km^2) and Lake Huron (mean 59 m, max 229 m, surface area 59,565 km^2). Lake Erie is the shallowest (mean depth 19 m, max 64 m, surface area 25,655 km^2), although its 3 basins vary greatly in depth. The western basin of Lake Erie is shallowest (mean 10 m), followed by the central basin (mean 22 m) and eastern basin (mean 45 m).

The Great Lakes represent a trophic gradient, ranging from eutrophic in western Lake Erie to ultra-oligotrophic in Lakes Superior and Huron, based on both spring and summer metrics for productivity (Table 1). In recent decades, springtime secchi disk measurements range from 1.2 m in western Erie to 15.0 meters in Lake Superior; during summer, secchi measurements were comparable, with the lowest mean depth in western Erie (2.1 m) and the deepest in Lake Huron (15.0 m) rather than Lake Superior (12.1 m). Spring integrated chlorophyll (chl) and total phosphorus (TP) are highest in Lake Erie (4.54 µg/L chl and 6.39 µg/L TP), followed by Lake Ontario (1.55 µg/L chl and 2.97 µg/L TP) and Lake Michigan (1.01 µg/L chl and 2.06 µg/L TP). Lakes Huron and Superior are most similar in terms of chlorophyll and TP (0.76 µg/L and 0.70 µg/L chl; 1.56 µg/L and 1.60 µg/L TP, respectively). During summer, DCM occur in the offshore regions of all five of the lakes (note that western Erie does not form DCM and they are uncommon in central Erie).

Long-term monitoring summary

The US Environmental Protection Agency's Great Lakes National Program Office (GLPNO) began collecting in situ profile data in 1996 as part of their long-term monitoring program for the Laurentian Great Lakes. The GLNPO surveys samples standard sites across each of the Great Lakes (Fig. 1) during April and August each year. All samples were collected aboard the US EPA's R/V Lake Guardian. At each site, a rosette assembly equipped with 12 Niskin bottles and the following instrumentation was deployed: Seabird CTD, Seapoint Fluorometer (Seapoint Sensors, Inc., Exeter, NH), Biospherical/Licor sensor to measure photosynthetically available radiation (PAR); transmissometer (WETlab C-Star) with 660 nm wavelengths, and dissolved oxygen (O_2) probe (SBE 43). The rosette was deployed at a constant speed of 0.5 m/second during down-casts, and discrete-depth water samples for chemical analyses were collected on the up-casts. The depths for sample collection were determined by the EPA Chief Scientist and based on real-time plots of the downcast profile data. In addition to discrete-depth samples throughout the water column, water for an integrated epilimnetic sample was mixed using equal amounts of water from the top, middle, and bottom of the epilimnion.

At all sites, water samples from all depths were analyzed for extracted chlorophyll a, total phosphorus (TP), total nitrogen (N), and dissolved silica (Si). At master stations (Fig. 1), water samples were also analyzed for particulate organic carbon (POC), particulate nitrogen (PN), and particulate phosphorus (PP) for an integrated epilimnetic sample and a discrete depth sample at the DCM depth, when present. Water for chlorophyll analysis was filtered and processed using EPA Standard Operating Procedure (SOP) LG404 (Revision 7, 2013) and frozen. Samples were analyzed for chlorophyll a by

the non-acidification method (Welschmeyer, 1994) according to the EPA SOP LG405 (Revision 9, 2013) using a calibrated Turner Designs 10-AU bench-top fluorometer. Because there are quality control concerns for the extracted chlorophyll data collected prior to 2002, we do not report extracted chlorophyll values for early years even though we did use the profile data in our analysis of the depths at which various peak features occurred. Nutrients and particulates data were available for 2000 – 2015. TN, TP, and Si concentrations were determined using the EPA SOPs LG203, LG204, and LG205. Particulates concentrations for POC, PN, and PP were measured using respective EPA SOPs. All SOPs are available to registered users via the EPA Great Lakes National Program Office portal website (https://login.glnpo.net). Nutrient and extracted chlorophyll presented herein were downloaded from the Great Lakes Environmental Database (GLENDA) via the US EPA central data exchange website (https://cdx.epa.gov/). Carbon to chlorophyll ratios (C:Chl) in g:g were calculated using the POC concentrations and extracted chlorophyll concentrations for the integrated epilimnion water and DCM water at master stations when particulates data were available.

Profile Processing

The raw profile data for chlorophyll, beam attenuation, O_2 and temperature were binned to 0.5-meter depth resolution using Seabird's SBE processing software, and only down-cast data were used for further analysis. Beam attenuation coefficients generated from transmissometer measurements offer a good proxy for particulate organic carbon (POC) concentrations in the water columns (Bishop, 1999; Fennel and Boss, 2003; Gardner et al., 2000), and O_2 saturation data provide indications of positive net ecosystem

production (NEP). Positive heterograde DO curves often co-occur with DCM in lakes (Matthews and Deluna, 2008; Parker et al., 1991; Scofield et al., 2017), which indicates likely positive net ecosystem production (NEP) at depth. O_2 saturation percentages were calculated from O_2 concentrations (mg/L) and temperature data (Baca and Arnett, 1976). The euphotic depth (z_{eu}) was defined as the depth at which 1% surface PAR occurred and was calculated using the light attenuation coefficient (K) for the site as follows: $z_{eu} = -\ln(.01)/K$, where K was determined from the log-transformed PAR profiles, where available. In approximately 1/3 of the daytime profiles, the PAR data quality was poor. This percentage was largely driven by bad data for the years 2004-2006 (accounting for 15% of profiles) and the rest were scattered throughout the time series. For these profiles, we used the secchi disk depth (SD) measurement from the same site to estimate the light attenuation coefficient based on the relationship: $K = 1.07/(SD) + 0.05$, and we calculated PAR values at depth based on surface PAR and K. The SD to K relationship was optimized based on paired light attenuation coefficients from high quality PAR profiles and secchi depths taken concurrently (Fig. S1). For stations sampled at night, we used an average secchi depth for the lake basin (Fig. 1) for that year to estimate K and calculate z_{eu} for comparison with DCM depths.

Non-photochemical quenching can cause in situ chlorophyll fluorescence measurements to be biased low, and factor calibrations do not fully account for variability in the relationship between in situ and extracted chlorophyll values. To field-calibrate the in situ chlorophyll a fluorometer data and to correct for non-photochemical quenching, we compared the in situ fluorometer data with the discrete-depth extracted chlorophyll values. Scofield et al. (2017) derived an equation for correcting the in situ chlorophyll

data for the effects of temperature and non-photochemical quenching on fluorescence response in Lake Ontario which we modified slightly to better fit all lakes (changed PAR cutoff for light adjustment from 18 to 25):

$$\text{Chl} = (\text{in situ chl}) * (a * \text{Temp} + b) * \frac{\max(\text{PAR}, 25)^c}{25^c} \quad (1)$$

Where Chl is corrected chlorophyll in µg/L, Temp is temperature in degrees C, PAR is photosynthetic active radiation in µE/(m^2s), and a, b, and c are fitted constants. We used data from all lakes and the years 2002 - 2017 to obtain the values for the parameters a, b and c that minimized the difference between corrected chlorophyll data and the extracted chlorophyll data. The coefficients from the model fit to data collected after 2002, years for which we have confidence in the quality of the extracted chlorophyll data, were also applied to data from 1996 – 2001 to correct for quenching. Data collected in 2011 were fitted separately, as there was an apparent instrument calibration issue such that in situ fluorescence measurements were biased high. Applying this correction resolved the observed bias in data with high PAR values, as well as corrected the fluorescence to chlorophyll correlation for instrument calibration issues (Table S1, Fig. S2). These corrections allow us to better approximate the shape of the chlorophyll profile and estimate true chlorophyll concentrations throughout the water column.

The profile data were then processed using algorithms developed to detect thermal structure (lower epilimnion and upper hypolimnion boundaries, and the thermocline), as well as the start, maximum, and end depths of maxima (Xu, 2017). Thermal structure was determined based on piecewise linear representation (PLR) using the bottom-up approach (Keogh et al., 2004). The epilimnion and hypolimnion layers

were determined based on the cutoff gradient value of $0.1°Cm^{-1}$, and the thermocline depth was defined as the mid-point of the linear segment with the strongest temperature gradient.

The peak-detection algorithm developed by Xu (2017) was applied to profiles of corrected chlorophyll to detect the DCM, BAT profiles to detect the DBM, and O_2 saturation profiles to detect the DO_{max}. For each profile, all peaks in the data were identified by noting points where the sign changed from positive to negative (with increasing depth). Individual peaks were then categorized as significant or non-significant based on threshold values for the peak magnitude (the maximum value of the peak) and the peak height (the difference between maximum and minimum values within a peak feature). The minimum thresholds for magnitude (x_{min}) and height (h_{min}) were calculated relative to the total range observed in the data, as follows:

$$x_{min} = \min(X) + 0.3 \times (\max(X) - \min(X))$$

$$h_{min} = 0.2 \times (\max(X) - \min(X))$$

where X is the set of values for the full profile of the variable (chlorophyll, BAT, or O_2). A peak was determined significant if both its magnitude and height exceeded the given thresholds (for further details on algorithm parameterization and performance, see Xu (2017)). Where more than one significant peak was detected within a profile, we used only the highest magnitude peak for the current analysis; the DCM, DBM, or DO_{max} was then defined by the depth at which the maximum value occurred within the largest significant peak. Two half Gaussian curves with standard deviations σ_1 and σ_2 were fit to

the data above and below each maximum point, respectively. The upper and lower boundaries of the peak were defined as the maximum depth - $2.5\sigma_1$ and the maximum depth + $2.5\sigma_2$. The algorithm outputs were checked against the raw profile data for all variables, and manual corrections were applied where the algorithm detection was problematic based on expert opinion.

RESULTS

Profile processing

In total, 1879 profiles were available from across the Great Lakes from 1996 – 2017. Profiles from western Lake Erie (129 profiles) were excluded from further analysis because the western basin does not form a DCM due to the fact that it is eutrophic, shallow, and often well-mixed rather than stratified. After performing visual quality checks on the profiles for all variables of interest, a total of 1,707 profiles were used from Lakes Erie (335), Ontario (224), Michigan (396), Huron (350), and Superior (402). Only minor manual corrections were required to the algorithms used to detect thermal structure and peak features (Fig. 2). Thermal structure was detected consistently, as were the peak depths of the DCM, DBM, and DO_{max}. The few issues that did occur with detection were primarily associated with the presence of multiple peaks or especially noisy profiles, as there were some inconsistencies where the top and bottom of maxima features were detected when multiple peaks were present. In such cases, we made manual adjustments to the DCM range to encompass the appropriate extent of a DCM feature, based on expert opinion and the algorithm performance on typical profiles.

DCM characteristics across lakes

DCM were most common in Lakes Superior and Huron (93% and 91% of all profiles analyzed, respectively), frequent in Lakes Michigan and Ontario (78% and 62% respectively), and less often observed in central and eastern Lake Erie (26% and 29%, respectively) (Table 3). Lack of a DCM was associated with either unstratified conditions or high epilimnetic chlorophyll concentrations. The occurrence of multiple significant peaks was most common in Lakes Michigan and Huron, where they were present in approximately 25% of the sites with a DCM. DCM depths were shallowest in central Lake Erie (14.5 ± 2.6 m, 1 SD), when present, followed by Lake Ontario (17.4 ± 4.5 m 1 SD) and eastern Lake Erie (19.3 ± 3.7 m, 1 SD). DCM were significantly deeper in Lakes Michigan and Superior (27.8 ± 8.7 m and 28.1 ± 7.3 m 1D, respectively) and deepest in Lake Huron (34.8 ± 10.1 m, 1 SD). Shallow DCM were associated with higher chlorophyll concentration and were narrower than deep DCM, which tended to be weaker and broader. The DCM chlorophyll concentrations were highest in Lake Ontario (mean 3.5 µg/L, max 8.7 µg/L) and lowest in Lakes Superior and Huron, which were not significantly different from each other (both mean 1.6 µg/L), although there was a greater range of values is Lake Huron (max 4.1 µg/L) than in Lake Superior (max 3.0 µg/L). The shapes of the chlorophyll profiles were more variable in Lakes Michigan and Huron (Fig. 3) than in Lakes Erie, Ontario, and Superior, likely due to both the higher occurrence of multiple peaks and changing DCM characteristics over the study period. The thickness of chlorophyll peak features increased with level of oligotrophy, as DCM were narrowest in Lake Erie (7.2 ± 4.7 m) and broadest in Lake Superior (39.2 ± 11.8 m). The distribution of DCM depths aligned with that of the thermocline in Lake Erie, peaked between the

thermocline and the z_{eu} in Lake Ontario and Lake Superior, and better matched the z_{eu} in Lakes Huron and Michigan (Fig. 4). Furthermore, the changes in the depth of the DCM in Lakes Huron and Michigan associated with changes in z_{eu} for the period 1996-2017 (Fig. 5).

Both DBM and DO_{max} were also common for all of the five lakes (except Lake Erie: Table 3), although DO_{max} were observed more frequently than DBM. The depths at which DBM occurred were more variable than DCM depths (Fig. 3). O_2 saturation minimum features were frequently observed in Lakes Erie and Ontario, where O_2 depletion sometimes occurred near the metalimnion-hypolimnion boundary. In Lakes Michigan, Huron, and Superior, O_2 supersaturation often extended deeper in the water column. While maxima of all three variables were often observed, the depths at which the peaks occurred did not always coincide. In Lakes Erie and Ontario, the overall distribution of observed peak features overlapped almost entirely. In the upper lakes (Lakes Michigan, Huron and Superior), however, there were differences in the peak distributions. The distributions of DO_{max} were shallowest, followed by DBM, and DCM exhibited the deepest distribution (Fig 4). However, this pattern changed over time in Lakes Michigan in Huron, where there was greater peak overlap in first decade of the time series (1996 – 2005) and divergence of the chlorophyll and beam attenuation peaks in the most recent decade (2008-2017) (Fig. 4). In general, when DCM were relatively shallow as in Lake Erie and Lake Ontario, the peaks were closely aligned. The differences between the DCM and the other peaks increased with DCM depth (Fig. 6).

Temporal trends & abiotic drivers

Water clarity likely affected the DCM depth and thickness, DCM chlorophyll concentration, as well as the degree of photoadaptation of phytoplankton. Overall, the euphotic depth was positively correlated with DCM depth ($p < 0.01$, $R^2 = 0.28$, N=833, Fig.7), although the DCM often occurred shallower than the z_{eu}. DCM chlorophyll concentration (for 2002 – 2017) exhibited a significant negative nonlinear response to z_{eu} ($p < 0.01$, N =580), such that higher water clarity was associated with lower magnitude DCM. Data for particulate organic carbon (POC) from master stations indicate that photoadaptation is important when water clarity is high, as there were greater differences in the ratio of POC to chlorophyll (C:Chl) between the epilimnion and DCM in Lakes Huron (mean diff = -97.0, $p < 0.01$, N = 31), Michigan (mean diff = -79.0, $p < 0.01$, N = 33), and Superior (mean diff = -72.8, $p < 0.01$, N = 33) than in Lake Ontario (mean diff = -24.1, $p = 0.01$, N = 21). There was no significant difference between depth layers in Lake Erie, which had a small sample size due to infrequent formation of a DCM at the master stations ($p = 0.26$, N = 4). While C:Chl within the DCM was not significantly different across lakes (except Lake Erie, N = 4 DCM samples), there were differences in the epilimnetic C:Chl across the lakes. The epilimnetic C:Chl was significantly higher in Lakes Michigan (N = 35), Huron (N = 36), and Superior (N = 35) than in Lake Ontario (N = 22, all $p < 0.01$) and Lake Erie (N = 32, all $p < 0.05$), but there was no significant difference in epilimnetic C:Chl in Lakes Ontario and Erie ($p = 1.0$) (Fig. 8).

Over the period 1996-2017, z_{eu} increased in Lakes Michigan ($p < 0.01$, slope = 0.94 m/year, $R^2 = 0.43$, N = 191) and Huron ($p < 0.01$, slope = 0.74 m/year, $R^2 = 0.18$, N = 237), which likely contributed to the observed deepening of the DCM in Lake

Michigan ($p = 0.03$, slope = 0.17 m/year, N = 166) (Fig. 9). Furthermore, the DCM feature became broader in Lake Michigan ($p < 0.01$, slope = 0.47 m/year, N = 166) as the end depth of peak features deepened at a faster rate ($p < 0.01$, slope = 0.41 m/year, N = 166) than the peak. Surprisingly, there were no significant changes in the depth or thickness of DCM in Lake Huron over the study period, despite increasing water clarity. The z_{eu} became slightly shallower in Lake Superior over the study period ($p < 0.01$, slope = -0.39 m/year, $R^2 = 0.05$, N = 210), and the bottom depth of the DCM became shallower at the same rate ($p < 0.01$, slope = -0.31 m/year, $R^2 = 0.03$, N = 278). Thus, there was a decrease in the thickness of the DCM over time in Lake Superior ($p < 0.01$, slope = -0.39 m/year, $R^2 = 0.04$, N = 278). Though there were few significant trends in DCM depth, DBM deepened in Lakes Michigan ($p < 0.01$, slope = 0.21 m/year) and Superior ($p = 0.01$, slope = 0.15 m/year, $R^2 = 0.03$, N = 376), and DBM broadened in all lakes except Lake Erie as the end depths of the DBM deepened (Fig. 9). DO_{max} depths, however, did not change consistently across lakes. DO_{max} features became shallower in Lake Michigan ($p < 0.01$, slope = -0.26 m/year) and narrower in Lake Superior ($p < 0.01$, slope = -0.88 m/year). While the depth of the DCM did not exhibit significant change except for in Lake Michigan, the chlorophyll concentration at the DCM significantly decreased in Lakes Ontario ($p < 0.01$, slope = -0.12), Michigan ($p < 0.01$, slope = -0.12), Huron ($p < 0.01$, slope = -0.11), and Superior ($p < 0.01$, slope = -.033) (Fig. 10). However, based on POC data from master stations, only Lake Huron has experienced a significant decrease in POC within the DCM over the study period ($p = 0.02$, slope = -0.003), while there has been a slight increase in DCM POC in Lake Superior ($p = 0.01$, slope = 0.003).

Epilimnetic POC decreased significantly in Lakes Ontario ($p = 0.03$, slope = -.006) and Michigan ($p < 0.01$, slope = -0.006).

Thermal structure did not vary greatly across lakes, but there was a significant deepening of the lower epilimnion in eastern Lake Erie ($p = 0.02$, slope = 0.15 m/year) and a significant shallowing of the metalimnion in Lake Michigan, where the depths of the lower epilimnion, thermocline, and upper hypolimnion all decreased over the study period (Fig. 9). There were differences in the strength of stratification across lakes, likely driven primarily by differing summer surface temperatures across latitudes (Table 2). Stratification was strongest in Lake Erie (-5.4 ± 2.3 °C/m) and weakest in Lake Superior (-1.7 ± 1.1 °C/m). Stratification strength increased slightly in eastern Lake Erie ($p = 0.01$, slope = 0.06 °C/m·year) and decreased slightly in Lake Michigan ($p = 0.02$, slope = -0.03 °C/m·year) over the study period. The only lake which exhibited a significant trend in water temperatures was Lake Huron, where surface temperatures increased over the study period ($p = 0.04$, slope = 0.05 °C/year).

Summer nutrient concentrations had significant temporal trends in both epilimnetic and DCM concentrations in several lakes (Fig. 10). Total phosphorus increased wherever there was a significant trend observed: TP increased in the epilimnia of all lakes except Lake Ontario and increased in the DCM of eastern Lake Erie, Lake Huron, and Lake Superior. Patterns in total nitrogen were more variable. TN decreased in the epilimnia of central and eastern Lake Erie, as well as the DCM of central Erie, eastern Erie, and Huron; it increased in the epilimnion and the DCM of Lakes Michigan and Superior. Dissolved silica concentrations increased significantly in both depth layers of Lakes Ontario, Michigan, and Huron, although the strongest increase was observed in

lake Michigan. Particulate phosphorus and particulate nitrogen showed different trends than the TP and TN data, however. PP at master stations significantly decreased in the Michigan ($p < 0.01$) and Huron ($p < 0.01$), while PN decreased in all lakes until 2012, after which it increased sharply in all lakes (Fig. 11).

DISCUSSION

DCM characteristics across lakes

There are clear patterns to the frequency of occurrence, depth, thickness, and chlorophyll concentration of DCM along the productivity gradient from Lake Erie and Lake Ontario to Lakes Michigan, Huron, and Superior. Overall, the patterns of DCM formation in the Great Lakes agrees with expectations based on stratified marine systems as described by Cullen (2015) and with previous observations in the Great Lakes (e.g. Moll and Stoermer, 1982). The DCM forms more often and typically becomes deeper, broader, and lower in chlorophyll as systems become increasingly oligotrophic. There were notable differences in DCM variables across basins in Lakes Erie, Ontario, while DCM features were more spatially consistent in Lakes Michigan, Huron, and Superior.

Differences in DCM among basins in Lake Erie is expected due to variation in the bottom depth and trophic status of different regions of the lake (Table 1). The western basin of Lake Erie generally does not have DCM because it is both eutrophic and shallow (sample sites 9 – 12 m); given that stable stratification is uncommon (due to wind-driven mixing events) and epilimnetic production is high, conditions for DCM formation typically do not occur, and it was excluded from further analysis. The central basin of Lake Erie is mesotrophic and does form a DCM, but it is much shallower than in eastern

Erie and the rest of the Great Lakes. Bottom depth may affect differences in DCM thickness across lakes (Leach et al., 2018), in part because depth affects stratification patterns and limits the maximum range of a DCM, but also because lake depth is negatively correlated with lake productivity (Carpenter, 1983). The DCM occurring in Lake Erie's central basin were generally very shallow and narrow, occurring near to the top of the thermocline. This agrees with expectations because relatively high epilimnetic production results in a shallow euphotic zone – thus, central Erie is near the threshold productivity where conditions for DCM formation occur. While DBM commonly co-occurred with DCM in both central and eastern basins of Lake Erie (Fig. 4), DO_{max} were much less common. Rather, O_2 minima were commonly observed within the metalimnion. Due to the higher productivity in these basins, high bacterial decomposition rates below the DCM could cause oxygen depletion (Fig. 3). Oxygen depletion is common in the central basin of Lake Erie, especially in the last decade (Rucinski et al., 2014; Scavia et al., 2014).

In Lake Ontario, the major difference between basins was in frequency of occurrence of DCM (71% of profiles in the western basin and 38% in the central). The thermocline depth was significantly deeper in central than in western Lake Ontario ($p < 0.01$), such that the z_{eu} was sometimes shallower than the thermocline depth in the central basin. In such cases, a DCM was generally absent. However, the timing of the summer surveys in August is rather late in the stratified season, especially for Lakes Erie and Ontario, which are at lower latitudes, and the thermocline generally deepens considerably in the central basin over the summer due prevailing wind and circulation patterns (Beletsky et al., 1999). Thus, the absence of a DCM in August is not necessarily

indicative of a lack of DCM formation in central Lake Ontario, and previous studies have shown a DCM to be almost ubiquitous in offshore lake Ontario during June through July (Scofield et al., 2017; Twiss et al., 2012; Watkins et al., 2015).

DCM in Lakes Michigan and Huron were characterized by greater variability in both depth and profile shape, with about a quarter of the profiles having multiple peaks (Table 3). Similar patterns were seen in the DBM, which often formed double peaks as well. These multiple peaks caused much greater variability in distributions of normalized chlorophyll and normalized beam attenuation (Fig. 3), as well as affected the relationship between the DCM and DBM. For example, in some cases both chlorophyll and beam attenuation profiles would have multiple peaks, but the deeper peak would have a higher chlorophyll magnitude while the shallower peak had a higher beam attenuation coefficient. This suggests that the processes contributing to chlorophyll peaks are also variable with depth, not simply across systems. Shallower peaks within one profile may be associated with greater biomass and production, while the chlorophyll maximum may occur very deep within the water column and be driven largely by lower C:Chl ratio in those algae. More detailed investigations of profiles with multiple peaks will improve our understanding of DCM in oligotrophic lakes and the phytoplankton communities that contribute to such features.

The average DCM depth in Lake Superior was significantly shallower (28.1 m) than those in Lake Huron (34.6 m), despite similar levels of oligotrophy based on springtime water quality data (Table 1). This may seem counter to the broad shape determined for profiles in Lake Superior (Table 3), but the thickness variable in Lake Superior was largely driven by a skewed shape with a long tail below the maximum,

where chlorophyll levels were quite low but decreased gradually over an extended range (Fig. 9). Lake Huron did have significantly greater z_{eu} than Lake Superior during the summer (39.9 m vs. 35.6 m, respectively, $p < 0.01$), despite similar chlorophyll and nutrient concentrations, which likely accounts for this difference in DCM depth.

Mechanisms of DCM formation & Long-term change

Our results suggest that the processes contributing to the DCM vary across the productivity gradient in the Great Lakes. We base this assertion on the occurrence and distributions of DBM and DO_{max} as related to the DCM. Overall, the DO_{max} tended to occur shallowest and remain within the thermocline, while DBM were somewhat deeper, and DCM occurred below both the other peaks (Fig 4). The shallower depth of the DO_{max} relative to the DCM is consistent with the fact that both higher light intensity and higher temperature will increase photosynthetic rates even under nutrient stressed conditions. However, DO_{max} were often present even when peaks were not detected in the other variables. Physical processes likely contribute to the observed metalimnetic oxygen peaks, as has been observed in other lakes (Wilkinson et al., 2015). Solar warming of metalimnetic water cut-off from atmospheric exchange can lead to supersaturation of O_2 below the thermocline, even in the absence of positive net ecosystem production (NEP). However, supersaturation of oxygen did occur over a broad depth range below the thermocline in Lakes Michigan, Huron, and Superior, rather than just near the thermocline, suggesting that there is positive NEP occurring at depth (Fig. 3). Based on the observed overlap of these peak features, our results suggest that the DCM is closely associated with biomass peaks and is productive in Lakes Erie and Ontario, while the DCM depth in Lakes Michigan, Huron, and Superior is more strongly affected by

photoadaptation. The concentration of POC in the DCM was still significantly higher than in the epilimnion for the upper lakes, however, indicating that photoadaptation is not the sole cause of the observed DCM. The discrepancies in depth between DCM, DBM, and DO_{max} suggest that the distributions of phytoplankton biomass and production within the water column are regulated by different processes than those that affect chlorophyll, causing a divergence of peak productivity, biomass, and chlorophyll in the more oligotrophic systems.

Euphotic depth does appear to be a strong driver of differences in DCM characteristics, including depth, thickness, and chlorophyll concentration. DCM depth is often near z_{eu}, although some DCM in the upper lakes occur considerably shallower than the z_{eu} (Fig. 4). These discrepancies mostly occur in Lake Michigan and Lake Superior. In Lake Michigan, there was a significant increase in DCM depth over the study period (Fig. 5, $p = 0.02$), but there is greater variability in the DCM depth and a slower rate of change than for the z_{eu}. In Lake Superior, the DCM often occurs shallower than the z_{eu}, perhaps due to weaker stratification (Table 3), which may result in a higher nutrient flux to the thermocline and allow for shallowing of the DCM and greater production. Chlorophyll concentration at the DCM exhibits an exponential decay response to z_{eu}, indicating that DCM tend to decrease in magnitude with increasing water clarity. The importance of water clarity agrees with previous work in both freshwater and marine systems (Cullen, 2015; Leach et al., 2018).

Thermal structure does not appear to directly regulate DCM characteristics. Thermal structure did not differ greatly across the lakes, but the strength of stratification did. In systems with weak stratification, such as Lake Superior, increased nutrient flux to

the euphotic zone could lead to a shoaling of the DCM and greater production than might be expected based on trophic status alone. Furthermore, the relationship between z_{eu} and DCM depth may break down when transparency increases without further reduction in nutrient concentrations. For example, the change in DCM depth in Lake Michigan has not been nearly as strong as the increase in z_{eu} over the study period. This may be in part due to continued increasing water clarity, perhaps due to effects of dreissenid mussels, despite a stabilization of nutrient levels in recent years. TP and TN concentrations within the DCM of Lake Michigan have actually increased (Fig. 10), and, given that greater light is reaching the DCM depth with increasing water clarity, phytoplankton growth may not be changing significantly at the DCM despite decreasing chlorophyll. Particulates data further support this trade-off, as there has not been a significant decrease in POC within the DCM in Michigan even as chlorophyll has decreased and thus the C:Chl may have increased ($p = 0.08$).

In some cases, especially where multiple chlorophyll peaks form, additional processes such as phytoplankton migration for nutrient acquisition (e.g. Heaney and Eppley 1981; Baek et al. 2009), variable phytoplankton sinking rates (Steele and Yentsch, 1960), and nutrient excretion by migrating zooplankton (Oliver et al., 2014) may be important factors in DCM formation. Further information about the phytoplankton community making up DCMs would be useful for evaluating differences in DCM dynamics, especially in the context of the frequency of multiple peaks across a productivity gradient. For example, some phytoplankton may undergo partial diel migrations, or there could be community differences with depth related to fine-scale niche partitioning.

Previous work on phytoplankton community structure suggests that the DCM is often a unique phytoplankton community from that of the epilimnion with larger-bodied forms of siliceous algae (diatoms and chrysophytes) in the DCL compared to the epilimnion (Bramburger and Reavie, 2016; Scofield et al., 2017; Twiss et al., 2012). These comparisons have largely been based on discrete depth DCM samples compared to integrated epilimnetic samples; fluoroprobe profile data would provide phytoplankton community structure data at greater depth resolution, which is important for understanding bottom-up impacts on zooplankton grazers (Twiss et al., 2012)

Food web impacts

Differences in DCM characteristics are important to consider when evaluating the food web implications of phytoplankton distribution within the water column. While chlorophyll data alone are not sufficient to predict the importance of subsurface phytoplankton to total water column biomass or production, improving our framework for how DCM characteristics change along a trophic gradient does allow for improved interpretation of chlorophyll data. For example, the temperatures at which DBM occur affect bioenergetic trade-offs for zooplankton grazers, with deeper (and thus typically colder) DBM favoring large-bodied cold-adapted zooplankton species such as several large calanoid copepods (e.g. *Senecella calanoides*, *Limnocalanus macrurus*). Significant changes to the zooplankton community have occurred in Lakes Ontario, Michigan, and Huron over the past two decades, as calanoid copepod biomass has increased while species that prefer warmer surface waters have declined (Barbiero et al., 2014, 2012). This vertical redistribution of resources may favor native fish species, such as coregonids,

over non-native alewife as a forage fish base and has implications for both restoration efforts and the economics of the Great Lakes fisheries (Dettmers et al., 2012).

Conclusions

Our results extend previous work in the Laurentian Great Lakes by providing the first long-term cross-lake comparison using standardized methods. This is important for improving our understanding of DCM dynamics in this system. In short, DCMs became deeper, broader, and lower in chlorophyll concentration with oligotrophication. The DCM was shallowest, sharpest, and highest in chlorophyll in eastern Lake Erie and Lake Ontario, while DCM in Lakes Michigan, Huron, and Superior were typically deeper, broader, and lower in chlorophyll.

The time series presented here provides additional evidence that Lakes Michigan and Huron have undergone continued oligotrophication and converged toward Lake Superior. Lake Michigan is the only lake which shows significant trends across all variables in the past two decades, suggesting the processes occurring in Lake Michigan may be unique. Lake Michigan has both high densities of dreissenid mussels and low productivity, which may interact to increase the effect on the DCM. Lake Huron also shows a significant increase in z_{eu}, and the DCM has become broader in response, even though the DCM peak depth has not changed significantly. Lakes Michigan and Superior are now quite similar in terms of DCM properties, while Lake Huron DCM properties suggest that lake is now more oligotrophic than Lake Superior. Lakes Erie, Ontario, and Superior have not undergone major changes in spring TP concentrations (as an indicator of productivity) or DCM characteristics over the past two decade, except for decreasing chlorophyll concentrations at the DCM. However, these changes do not necessarily

represent declines in DCM productivity or deep algal biomass, as C:Chl ratios may also change in response to increasing light levels at the nutricline (as in Lake Michigan).

The overall patterns we observed in the distributions of biomass and productivity maxima, based on proxy variables, are consistent with expectations based on previous observations in the Great Lakes, other large lakes, and marine systems (Coon et al., 1987; Cullen, 2015; Moll and Stoermer, 1982). Our study shows that the processes contributing to the DCM likely change with productivity, given that peaks in proxies for production, biomass, and chlorophyll diverge as DCM deepen; photoadaptation contributes more to differences in chlorophyll between the epilimnion and DCM when water clarity is high. Especially in oligotrophic systems, the relative importance of different DCM-forming processes such as phytoplankton growth, phytoplankton sinking, and photoadaptation, change across the broad depth range within the euphotic zone. Thus, the depths at which productivity maxima, biomass maxima, and chlorophyll maxima occur are regulated by different processes. Chlorophyll profiles must therefore be interpreted with caution, and the use of other proxy variables for phytoplankton biomass, such as beam attenuation coefficients from transmissometer data, may be better suited to evaluating phytoplankton biomass distribution within the water column in oligotrophic systems.

REFERENCES

Baca, R.G., Arnett, R.C., 1976. A limnological model for eutrophic lakes and impoundments. Battelle, Pacific Northwest Laboratories.

Baek, S.H., Shimode, S., Shin, K., Han, M.-S., Kikuchi, T., 2009. Growth of dinoflagellates, *Ceratium furca* and *Ceratium fusus* in Sagami Bay, Japan: The role of vertical migration and cell division. Harmful Algae 8, 843–856. https://doi.org/10.1016/J.HAL.2009.04.001

Banse, K., 1987. Clouds, deep chlorophyll maxima and the nutrient supply to the mixed layer of stratified water bodies. J. Plankton Res. 9, 1031–1036. https://doi.org/10.1093/plankt/9.5.1031

Barbiero, R.P., Lesht, B.M., Warren, G.J., 2014. Recent changes in the offshore crustacean zooplankton community of Lake Ontario. J. Great Lakes Res. 40, 898–910. https://doi.org/10.1016/j.jglr.2014.08.007

Barbiero, R.P., Lesht, B.M., Warren, G.J., 2012. Convergence of trophic state and the lower food web in Lakes Huron, Michigan and Superior. J. Great Lakes Res. 38, 368–380. https://doi.org/10.1016/j.jglr.2012.03.009

Barbiero, R.P., Little, R.E., Tuchman, M.L., 2001. Results from the U.S. EPA's biological open water surveillance program of the Laurentian Great Lakes: III. Crustacean zooplankton. J. Great Lakes Res. 27, 167–184. https://doi.org/10.1016/S0380-1330(01)70630-2

Barbiero, R.P., Tuchman, M.L., 2004. The deep chlorophyll maximum in Lake Superior. J. Great Lakes Res. 30, 256–268. https://doi.org/10.1016/S0380-1330(04)70390-1

Barbiero, R.P., Tuchman, M.L., 2001a. Results from the U.S. EPA's biological open water surveillance program of the Laurentian Great Lakes: I. Introduction and phytoplankton results. J. Great Lakes Res. 27, 134–154. https://doi.org/10.1016/S0380-1330(01)70628-4

Barbiero, R.P., Tuchman, M.L., 2001b. Results from the U.S. EPA's biological open water surveillance program of the Laurentian Great Lakes: II. Deep chlorophyll maxima. J. Great Lakes Res. 27, 155–166. https://doi.org/10.1016/S0380-1330(01)70629-6

Beckmann, A., Hense, I., 2007. Beneath the surface: Characteristics of oceanic ecosystems under weak mixing conditions – A theoretical investigation. Prog. Oceanogr. 75, 771–796. https://doi.org/10.1016/J.POCEAN.2007.09.002

Beletsky, D., Saylor, J.H., Schwab, D.J., 1999. Mean circulation in the Great Lakes. J. Great Lakes Res. 25, 78–93.

Bishop, J.K.B., 1999. Transmissometer measurement of POC. Deep Sea Res. Part I Oceanogr. Res. Pap. 46, 353–369.

Boyd, J.D., 1980. Metalimnetic oxygen minima in Lake Ontario, 1972. J. Great Lakes Res. 6, 95–100. https://doi.org/10.1016/S0380-1330(80)72087-7

Bramburger, A.J., Reavie, E.D., 2016. A comparison of phytoplankton communities of the deep chlorophyll layers and epilimnia of the Laurentian Great Lakes. J. Great Lakes Res. 42, 1016–1025. https://doi.org/10.1016/J.JGLR.2016.07.004

Brooks, A.S., Torke, B.G., 1977. Vertical and seasonal distribution of chlorophyll a in Lake Michigan. J. Fish. Res. Board Canada 34, 2280–2287. https://doi.org/10.1139/f77-306

Bunnell, D.B., Barbiero, R.P., Ludsin, S.A., Madenjian, C.P., Warren, G.J., Dolan, D.M., Brenden, T.O., Briland, R., Gorman, O.T., He, J.X., Johengen, T.H., Lantry, B.F., Lesht, B.M., Nalepa, T.F., Riley, S.C., Riseng, C.M., Treska, T.J., Tsehaye, I., Walsh, M.G., Warner, D.M., Weidel, B.C., 2014. Changing ecosystem dynamics in the Laurentian Great Lakes: Bottom-up and top-down regulation. Bioscience 64, 26–39. https://doi.org/10.1093/biosci/bit001

Camacho, A., 2006. On the occurrence and ecological features of deep chlorophyll

maxima (DCM) in Spanish stratified lakes. Limnetica 25, 453–478.

Carpenter, S.R., 1983. Lake geometry: Implications for production and sediment accretion rates. J. Theor. Biol. 105, 273–286. https://doi.org/10.1016/S0022-5193(83)80008-3

CDX Home | Central Data Exchange | US EPA [WWW Document], n.d. URL https://cdx.epa.gov/ (accessed 7.19.18).

Coon, T.G., Lopez, M.M., Richerson, P.J., Powell, T.M., Goldman, C.R., 1987. Summer dynamics of the deep chlorophyll maximum in Lake Tahoe. J. Plankton Res. 9, 327–344. https://doi.org/10.1093/plankt/9.2.327

Cullen, J.J., 2015. Subsurface chlorophyll maximum layers: Enduring enigma or mystery solved? Ann. Rev. Mar. Sci. 7, 207–239. https://doi.org/10.1146/annurev-marine-010213-135111

Cullen, J.J., 1982. The deep chlorophyll maximum: Comparing vertical profiles of chlorophyll a. Can. J. Fish. Aquat. Sci. 39, 791–803. https://doi.org/10.1139/f82-108

Dettmers, J.M., Goddard, C.I., Smith, K.D., 2012. Management of Alewife using Pacific Salmon in the Great Lakes: Whether to manage for economics or the ecosystem? Fisheries 37, 495–501. https://doi.org/10.1080/03632415.2012.731875

Dove, A., 2009. Long-term trends in major ions and nutrients in Lake Ontario. Aquat. Ecosyst. Health Manag. 12, 281–295. https://doi.org/10.1080/14634980903136388

Dove, A., Chapra, S.C., 2015. Long-term trends of nutrients and trophic response variables for the Great Lakes. Limnol. Oceanogr. 60, 696–721. https://doi.org/10.1002/lno.10055

Estrada, M., Marrasé, C., Latasa, M., Berdalet, E., Delgado, M., Riera, T., 1993. Variability of deep chlorophyll maximum characteristics in the Northwestern Mediterranean. Mar. Ecol. Prog. Ser. 92, 289–300.

Fahnenstiel, G., Pothoven, S., Vanderploeg, H., Klarer, D., Nalepa, T., Scavia, D., 2010. Recent changes in primary production and phytoplankton in the offshore region of southeastern Lake Michigan. J. Great Lakes Res. 36, 20–29. https://doi.org/10.1016/j.jglr.2010.03.009

Fahnenstiel, G.L., Scavia, D., 1987. Dynamics of Lake Michigan phytoplankton: the deep chlorophyll layer. J. Great Lakes Res. 13, 285–295. https://doi.org/10.1016/S0380-1330(87)71652-9

Fee, E.J., 1976. The vertical and seasonal distribution of chlorophyll in lakes of the Experimental Lakes Area, northwestern Ontario: Implications for primary production estimates. Limnol. Oceanogr. 21, 767–783. https://doi.org/10.4319/lo.1976.21.6.0767

Fennel, K., Boss, E., 2003. Subsurface maxima of phytoplankton and chlorophyll: Steady-state solutions from a simple model. Limnol. Oceanogr. 48, 1521–1534. https://doi.org/10.4319/lo.2003.48.4.1521

Gardner, W.D., Richardson, M.J., Smith, W.O., 2000. Seasonal patterns of water column particulate organic carbon and fluxes in the Ross Sea, Antarctica. Deep. Res. II 47, 3423–3449.

Geider, R.J., 1993. Quantitative phytoplankton physiology: implications for primary production and phytoplankton growth. ICES Mar. Sci. Symp. 197, 52–62.

Giling, D.P., Staehr, P.A., Grossart, H.P., Andersen, M.R., Boehrer, B., Escot, C., Evrendilek, F., Gómez-Gener, L., Honti, M., Jones, I.D., Karakaya, N., Laas, A., Moreno-Ostos, E., Rinke, K., Scharfenberger, U., Schmidt, S.R., Weber, M., Woolway, R.I., Zwart, J.A., Obrador, B., 2017. Delving deeper: Metabolic processes in the metalimnion of stratified lakes. Limnol. Oceanogr. 62, 1288–1306. https://doi.org/10.1002/lno.10504

Hamilton, D.P., O'Brien, K.R., Burford, M.A., Brookes, J.D., McBride, C.G., 2010.

Vertical distributions of chlorophyll in deep, warm monomictic lakes. Aquat. Sci. 72, 295–307. https://doi.org/10.1007/s00027-010-0131-1

Heaney, S.I., Eppley, R.W., 1981. Light, temperature and nitrogen as interacting factors affecting diel vertical migrations of dinoflagellates in culture. J. Plankton Res. 3, 331–344. https://doi.org/10.1093/plankt/3.2.331

Hemsley, V.S., Smyth, T.J., Martin, A.P., Frajka-Williams, E., Thompson, A.F., Damerell, G., Painter, S.C., 2015. Estimating oceanic primary production using vertical irradiance and chlorophyll profiles from ocean gliders in the North Atlantic. Environ. Sci. Technol. 49, 11612–11621. https://doi.org/10.1021/acs.est.5b00608

Herbland, A., Voituriez, B., 1979. Hydrological structure analysis for estimating the primary production in the tropical Atlantic Ocean. J. Mar. Res. 37, 87–101.

Jamart, B.M., Winter, D.F., Banse, K., Anderson, G.C., Lam, R.K., 1977. A theoretical study of phytoplankton growth and nutrient distribution in the Pacific Ocean off the northwestern U.S. coast. Deep Sea Res. 24, 753–773. https://doi.org/10.1016/0146-6291(77)90498-2

Keogh, E., Chu, S., Hart, D., Pazzani, M., 2004. Segmenting time series: a survey and novel approach, in: Last, M., Kandel, A., Bunke, H. (Eds.), Data Mining in Time Series Databases. World Scientific, pp. 1–21. https://doi.org/10.1142/9789812565402_0001

Koops, M.A., Munawar, M., Rudstam, L.G., 2015. The Lake Ontario ecosystem: An overview of current status and future directions. Aquat. Ecosyst. Health Manag. 18, 101–104. https://doi.org/10.1080/14634988.2015.1004028

Leach, T.H., Beisner, B.E., Carey, C.C., Pernica, P., Rose, K.C., Huot, Y., Brentrup, J.A., Domaizon, I., Grossart, H.-P., Ibelings, B.W., Jacquet, S., Kelly, P.T., Rusak, J.A., Stockwell, J.D., Straile, D., Verburg, P., 2018. Patterns and drivers of deep chlorophyll maxima structure in 100 lakes: The relative importance of light and

thermal stratification. Limnol. Oceanogr. 63, 628–646. https://doi.org/10.1002/lno.10656

Madenjian, C.P., Fahnenstiel, G.L., Johengen, T.H., Nalepa, T.F., Vanderploeg, H.A., Fleischer, G.W., Schneeberger, P.J., Benjamin, D.M., Smith, E.B., Bence, J.R., Rutherford, E.S., Lavis, D.S., Robertson, D.M., Jude, D.J., Ebener, M.P., 2002. Dynamics of the Lake Michigan food web, 1970-2000. Can. J. Fish. Aquat. Sci. 59, 736–753. https://doi.org/10.1139/f02-044

Matthews, R., Deluna, E., 2008. Metalimnetic oxygen and ammonium maxima in Lake Whatcom, Washington (USA). Northwest Sci. 82, 18–29. https://doi.org/10.3955/0029-344X-82.1.18

Mills, E., Casselman, J., Dermott, R., Fitzsimons, J., Gal, G., Holeck, K., Hoyle, J., Johannsson, O., Lantry, B., Makarewicz, J., Millard, E., Munawar, I., Munawar, M., Owens, R., Rudstam, L., Schaner, T., Stewart, T., 2003. Lake Ontario: food web dynamics in a changing ecosystem (1970–2000) 1. Can. J. Fish. Aquat. Sci. 60, 471–490. https://doi.org/10.1139/F03-033

Moll, R.A., Brahce, M.Z., Peterson, T.P., 1984. Phytoplankton dynamics within the subsurface chlorophyll maximum of Lake Michigan. J. Plankton Res. 6, 751–766. https://doi.org/10.1093/plankt/6.5.751

Moll, R.A., Stoermer, E.F., 1982. A hypothesis relating trophic status and subsurface chlorophyll maxima of lakes. Arch. für Hydrobiol. 94, 425–440.

NOAA, Laboratory, G.L.E.R.L., 2016. About Our Great Lakes : Lake by Lake Profiles [WWW Document]. URL https://www.glerl.noaa.gov/education/ourlakes/lakes.html (accessed 7.27.18).

Oliver, S.K., Branstrator, D.K., Hrabik, T.R., Guildford, S.J., Hecky, R.E., 2014. Nutrient excretion by crustacean zooplankton in the deep chlorophyll layer of Lake Superior. Can. J. Fish. Aquat. Sci. 72, 390–399. https://doi.org/10.1139/cjfas-2014-0209

Parker, B.C., Wenkert, L.J., Parson, M.J., 1991. Cause of the metalimnetic oxygen maximum in Mountain Lake, Virginia. J. Freshw. Ecol. 63, 293–303. https://doi.org/10.1080/02705060.1991.9665306

Pothoven, S.A., Fahnenstiel, G.L., 2013. Recent change in summer chlorophyll a dynamics of southeastern Lake Michigan. J. Great Lakes Res. 39, 287–294. https://doi.org/10.1016/j.jglr.2013.02.005

Reavie, E.D., Barbiero, R.P., Allinger, L.E., Warren, G.J., 2014. Phytoplankton trends in the Great Lakes, 2001-2011. J. Great Lakes Res. 40. https://doi.org/10.1016/j.jglr.2014.04.013

Rucinski, D.K., DePinto, J. V., Scavia, D., Beletsky, D., 2014. Modeling Lake Erie's hypoxia response to nutrient loads and physical variability. J. Great Lakes Res. 40. https://doi.org/10.1016/j.jglr.2014.02.003

Rudstam, L.G., Holeck, K.T., Watkins, J.M., Hotaling, C., Lantry, J.R., Bowen, K.L., Munawar, M., Weidel, B.C., Barbiero, R., Luckey, F.J., Dove, A., Johnson, T.B., Biesinger, Z., 2017. Nutrients, phytoplankton, zooplankton, and macrobenthos, in: O'Gorman, R. (Ed.), GLFC Special Publication. pp. 10–32.

Scavia, D., David Allan, J., Arend, K.K., Bartell, S., Beletsky, D., Bosch, N.S., Brandt, S.B., Briland, R.D., Daloğlu, I., DePinto, J. V., Dolan, D.M., Evans, M.A., Farmer, T.M., Goto, D., Han, H., Höök, T.O., Knight, R., Ludsin, S.A., Mason, D., Michalak, A.M., Peter Richards, R., Roberts, J.J., Rucinski, D.K., Rutherford, E., Schwab, D.J., Sesterhenn, T.M., Zhang, H., Zhou, Y., 2014. Assessing and addressing the re-eutrophication of Lake Erie: Central basin hypoxia. J. Great Lakes Res. 40, 226–246. https://doi.org/10.1016/j.jglr.2014.02.004

Scofield, A.E., Watkins, J.M., Weidel, B.C., Luckey, F.J., Rudstam, L.G., 2017. The deep chlorophyll layer in Lake Ontario: extent, mechanisms of formation, and abiotic predictors. J. Great Lakes Res. 43, 782–794. https://doi.org/10.1016/j.jglr.2017.04.003

Stadelmann, P., Moore, J.E., Pickett, E., 1974. Primary production in relation to temperature structure, biomass concentration, and light conditions at an inshore and offshore station in Lake Ontario. J. Fish. Res. Board Canada 31, 1215–1232. https://doi.org/10.1139/f74-145

Steele, J., 1964. A study of production in the Gulf of Mexico. MIAMI UNIV FLA MARINE LAB.

Steele, J.H., Yentsch, C.S., 1960. The vertical distribution of chlorophyll. J. mar. biol. Ass. U.K 39, 217–226.

Twiss, M.R., Ulrich, C., Zastepa, A., Pick, F.R., 2012. On phytoplankton growth and loss rates to microzooplankton in the epilimnion and metalimnion of Lake Ontario in mid-summer. J. Great Lakes Res. 38, 146–153. https://doi.org/10.1016/j.jglr.2012.05.002

Watkins, J.M., Weidel, B.C., Rudstam, L.G., Holeck, K.T., 2015. Spatial extent and dissipation of the deep chlorophyll layer in Lake Ontario during the Lake Ontario lower foodweb assessment, 2003 and 2008. Aquat. Ecosyst. Health Manag. 18, 18–27. https://doi.org/10.1080/14634988.2014.937316

Welschmeyer, N.A., 1994. Fluorometric analysis of chlorophyll a in the presence of chlorophyll b and pheopigments. Limnol. Oceanogr. 39, 1985–1992. https://doi.org/10.4319/lo.1994.39.8.1985

Weston, K., Fernand, L., Mills, D.K., Delahunty, R., Brown, J., 2005. Primary production in the deep chlorophyll maximum of the central North Sea. J. Plankton Res. 27, 909–922. https://doi.org/10.1093/plankt/fbi064

White, B., Matsumoto, K., 2012. Causal mechanisms of the deep chlorophyll maximum in Lake Superior: A numerical modeling investigation. J. Great Lakes Res. 38, 504–513. https://doi.org/10.1016/j.jglr.2012.05.001

Wilkinson, G.M., Cole, J.J., Pace, M.L., Johnson, R.A., Kleinhans, M.J., 2015. Physical

and biological contributions to metalimnetic oxygen maxima in lakes. Limnol. Oceanogr. 60, 242–251. https://doi.org/10.1002/lno.10022

Xu, W., 2017. Sensor data analytics and web applications to improve monitoring and understanding of lake processes. University of Illinois at Urbana-Champaign.

Yentsch, C.S., 1980. Phytoplankton growth in the sea, in: Falkowski, P.G. (Ed.), Primary Productivity in the Sea. Plenum Press, New York, pp. 17–32. https://doi.org/10.1007/978-1-4684-3890-1_2

Yentsch, C.S., 1974. The influence of geostrophy on primary production. Tethys 6, 111–118.

Table 1. Spring & summer water quality variables indicative of lake trophy, including secchi disk depth, chlorophyll concentration (Chl), and total phosphorus (TP). N is the number of samples for spring chlorophyll measurements. Springtime values for Chl and TP are measurements for samples integrated from three depths within the top 20 meters of the water column. Summertime values are for integrated epilimnetic water and discrete depth water samples from the deep chlorophyll maximum (DCM). Values given are the mean ± two standard errors. All available years of quality-approved data were used for each variable. Data source EPA-GLNPO GLENDA data base (https://cdx.epa.gov/).

	N	Secchi Depth (m) 1996-2015		Chlorophyll (µg/L) 2002 - 2016			Total Phosphorus (µg/L) 1996 - 2014			Trophic State
		Spring	Summer	Spring 20-meter	Summer		Spring 20-meter	Summer		
					Epilimnion	DCM		Epilimnion	DCM	
Erie	369	3.4 ± 0.4	5.3 ± 0.3	4.54 ± 0.41	4.01 ± 0.37	2.59 ± 1.07	6.39 ± 0.46	3.34 ± 0.22	3.05 ± 0.21	Eutrophic to Oligotrophic
Western	97	1.2 ± 0.2	2.1 ± 0.3	3.42 ± 0.48	6.80 ± 0.90	---	7.96 ± 1.33	4.59 ± 0.51	---	Eutrophic
Central	189	2.7 ± 0.3	6.2 ± 0.3	6.24 ± 0.69	3.04 ± 0.21	2.97 ± 1.79	5.18 ± 0.36	2.83 ± 0.20	3.18 ± 0.27	Mesotrophic
Eastern	83	8.3 ± 1.2	6.8 ± 0.5	2.09 ± 0.37	2.31 ± 0.22	2.05 ± 0.49	7.03 ± 0.55	2.73 ± 0.45	2.91 ± 0.32	Meso-Oligotrophic
Ontario	231	13.7 ± 0.9	6.4 ± 0.3	1.55 ± 0.12	2.87 ± 0.18	3.51 ± 0.35	2.97 ± 0.15	2.52 ± 0.13	2.56 ± 0.18	Oligotrophic
Western	116	13.2 ± 1.1	6.8 ± 0.4	1.63 ± 0.18	2.92 ± 0.26	3.77 ± 0.48	2.90 ± 0.21	2.38 ± 0.23	2.54 ± 0.27	
Central	115	14.2 ± 1.5	6.1 ± 0.5	1.48 ± 0.16	2.82 ± 0.25	3.20 ± 0.48	3.05 ± 0.21	2.63 ± 0.15	2.58 ± 0.24	
Michigan	326	13.2 ± 0.9	11.9 ± 0.7	1.01 ± 0.05	0.97 ± 0.06	2.11 ± 0.15	2.06 ± 0.11	1.51 ± 0.08	1.65 ± 0.09	Ultra-oligotrophic
Northern	146	13.7 ± 1.1	10.8 ± 0.8	0.96 ± 0.07	1.18 ± 0.10	2.47 ± 0.23	2.16 ± 0.16	1.55 ± 0.12	1.52 ± 0.10	
Southern	180	12.6 ± 1.3	13.0 ± 1.0	1.01 ± 0.08	0.81 ± 0.06	1.82 ± 0.17	2.00 ± 0.15	1.49 ± 0.12	1.76 ± 0.14	
Huron	363	13.3 ± 0.8	15.0 ± 0.5	0.76 ± 0.03	0.59 ± 0.04	1.57 ± 0.12	1.46 ± 0.07	1.30 ± 0.08	1.42 ± 0.08	Ultra-oligotrophic
Superior	533	15.0 ± 0.4	12.1 ± 0.3	0.70 ± 0.03	1.05 ± 0.06	1.57 ± 0.07	1.60 ± 0.07	1.39 ± 0.08	1.47 ± 0.07	Ultra-oligotrophic

Table 2. Summer physical variables for the Great Lakes based on data collected during summer survey from 1996-2017, including average site depth, thermal structure (epilimnion, thermocline, and hypolimnion), and euphotic depth (z_{eu}), defined as the depth where photosynthetically active radiation (PAR) is 1% of surface PAR calculated from the light extinction coefficient. For euphotic depth, only daytime sites were included in the analysis. Values given are mean depths ± two standard errors for all profiles.

	N sites	N profiles	Site Depth (m)	Epilimnion (m)	Thermocline (m)	Hypolimnion (m)	Thermal Gradient (°C/m)	Euphotic Depth (1% PAR)
Erie	22	369	24.2 ± 5.7	12.7 ± 0.4	15.5 ± 0.5	20.6 ± 0.8	4.0 ± 0.3	17.1 ± 0.9
Western	6	97	10.4 ± 0.5	5.5 ± 0.5	5.9 ± 0.5	5.7 ± 0.5	0.3 ± 0.1	8.1 ± 0.8
Central	11	189	22.0 ± 1.1	13.2 ± 0.4	15.9 ± 0.3	17.6 ± 0.3	5.9 ± 0.3	19.3 ± 0.7
Eastern	5	83	45.4 ± 8.0	14.3 ± 0.8	18.8 ± 0.7	29.1 ± 1.0	4.3 ± 0.4	22.1 ± 1.5
Ontario	12	231	89.9 ± 30.4	11.3 ± 0.6	14.6 ± 0.7	32.5 ± 1.4	2.8 ± 0.2	18.9 ± 0.8
Western	7	116	84.4 ± 35.2	9.5 ± 0.7	11.9 ± 0.9	28.3 ± 1.4	2.9 ± 0.3	19.3 ± 1.1
Central	5	115	97.6 ± 53.1	12.8 ± 0.9	17.4 ± 0.9	37.5 ± 2.2	2.6 ± 0.3	18.7 ± 1.1
Michigan	20	326	97.7 ± 26.3	11.8 ± 0.5	16.5 ± 0.5	34.3 ± 1.0	2.6 ± 0.1	32.4 ± 1.6
Northern	11	146	113.5 ± 42.4	11.9 ± 0.7	17.9 ± 1.0	34.9 ± 1.5	2.4 ± 0.1	29.4 ± 1.8
Southern	9	180	78.3 ± 20.6	11.7 ± 0.6	16.1 ± 0.7	33.7 ± 1.2	3.0 ± 0.2	35.0 ± 2.3
Huron	16	363	80.9 ± 13.9	11.9 ± 0.4	16.6 ± 0.6	34.9 ± 1.0	2.6 ± 0.1	42.1 ± 1.6
Superior	19	533	184.4 ± 19.4	12.0 ± 0.5	17.1 ± 0.8	32.6 ± 1.3	1.7 ± 0.1	35.4 ± 1.5

Table 3. Summary of deep chlorophyll maxima (DCM), deep biomass maxima (DBM), and deep oxygen maxima (DO_{max}) characteristics in the Laurentian Great Lakes, based on profiles in August 1996 – 2017, organized by lake and basin (see Fig. 1). N = the number of profiles analyzed; DCM present = the proportion of the profiles for which a DCM was observed; Multiple Peaks = the proportion of profiles with a DCM which also had two or more peaks present. DCM depth = the depth of the highest magnitude chlorophyll within the DCM; DCM thickness = the depth range of the peak feature; DCM chlorophyll = the chlorophyll concentration at the DCM based on profile data. DBM depth = the depth at which the highest magnitude peak occurred in transmissometer data. DBM coefficient = the beam attenuation coefficient at the peak. DO_{max} depth = the depth at which the highest magnitude peak occurred in dissolved oxygen saturation data. DO_{max} saturation = the dissolved oxygen saturation percentage at the peak. All values shown are the mean ± one standard deviation.

	N	DCM present (%)	Multiple peaks (%)	DCM depth (m)	DCM thickness (m)	DCM chlorophyll (µg/L)	DBM present (%)	DBM depth (m)	DBM (coeff)	DO_{max} present (%)	DO_{max} depth (m)	DO_{max} saturation (%)
Erie	335	27	1	16.1 ± 3.8	7.2 ± 4.7	4.8 ± 2.58	27	18.1 ± 4.8	1.74 ± 1.13	11	20.3 ± 4.2	99 ± 9
Central	233	26	0	14.5 ± 2.6	5.3 ± 2.4	4.89 ± 2.62	19	15 ± 2.7	2.03 ± 1.29	2	14 ± 1	102 ± 8
Eastern	102	29	4	19.3 ± 3.7	11 ± 5.8	4.53 ± 2.42	47	21 ± 4.4	1.45 ± 0.83	33	21.1 ± 3.8	98 ± 9
Ontario	224	62	11	17.4 ± 4.5	17.4 ± 6.8	5.69 ± 3.17	54	18.7 ± 5	1.91 ± 1.32	72	17.8 ± 7.9	116 ± 13
Western	112	80	8	17 ± 4.3	17.8 ± 6.2	6.13 ± 2.97	71	18.4 ± 4.7	2 ± 1.31	87	16.5 ± 9.2	121 ± 13
Central	112	43	13	18.2 ± 4.8	16.5 ± 7.7	5 ± 3.33	38	19.3 ± 5.4	1.74 ± 1.32	57	19.8 ± 5.1	110 ± 11
Michigan	396	78	26	27.8 ± 8.7	25.8 ± 12.5	2.73 ± 3.3	66	25.3 ± 6.8	1.32 ± 1.37	91	20.6 ± 6	119 ± 9
Northern	169	60	18	26.3 ± 8.5	27.4 ± 12	2.77 ± 1.85	53	25.6 ± 7	1.31 ± 1.04	82	21.9 ± 7.7	114 ± 9
Southern	137	91	33	29.6 ± 8.3	24 ± 11.4	2.74 ± 4.75	74	25.5 ± 6.1	1.23 ± 0.96	99	20.3 ± 3.8	123 ± 8
Huron	350	91	25	34.8 ± 10.1	26.4 ± 11.8	2.21 ± 1.27	78	31.3 ± 8.8	1.01 ± 0.86	98	22.6 ± 6.1	123 ± 44
Superior	402	93	18	28.1 ± 7.3	39.2 ± 11.8	2.19 ± 0.99	83	24.6 ± 8.3	1.17 ± 2.08	89	21.9 ± 14.1	111 ± 8

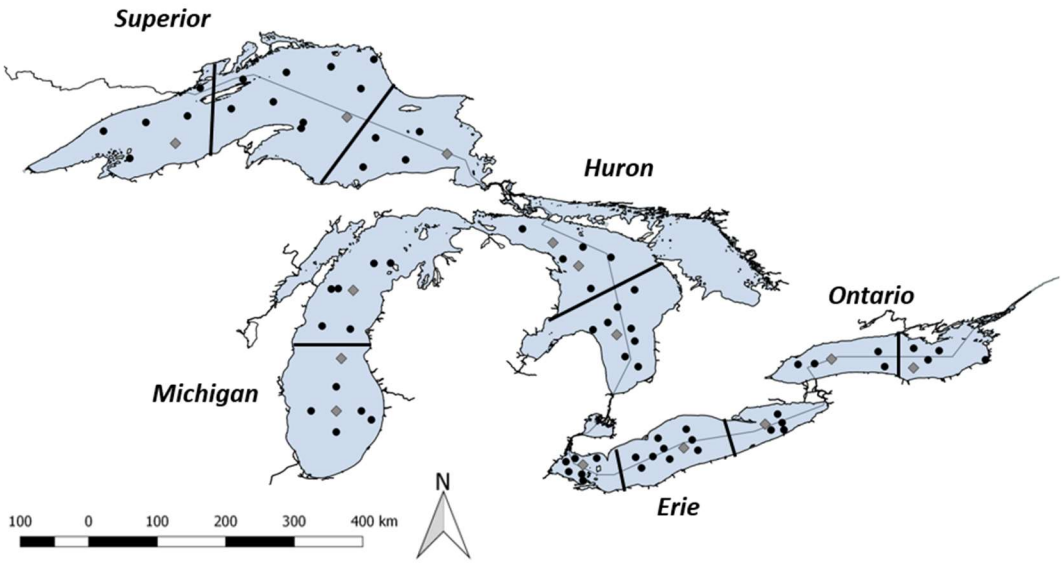

Figure 1. Map of the Laurentian Great Lakes showing station locations for the Great Lakes National Program Office (GLNPO) long-term monitoring program. Solid lines in each lake denote basin boundaries

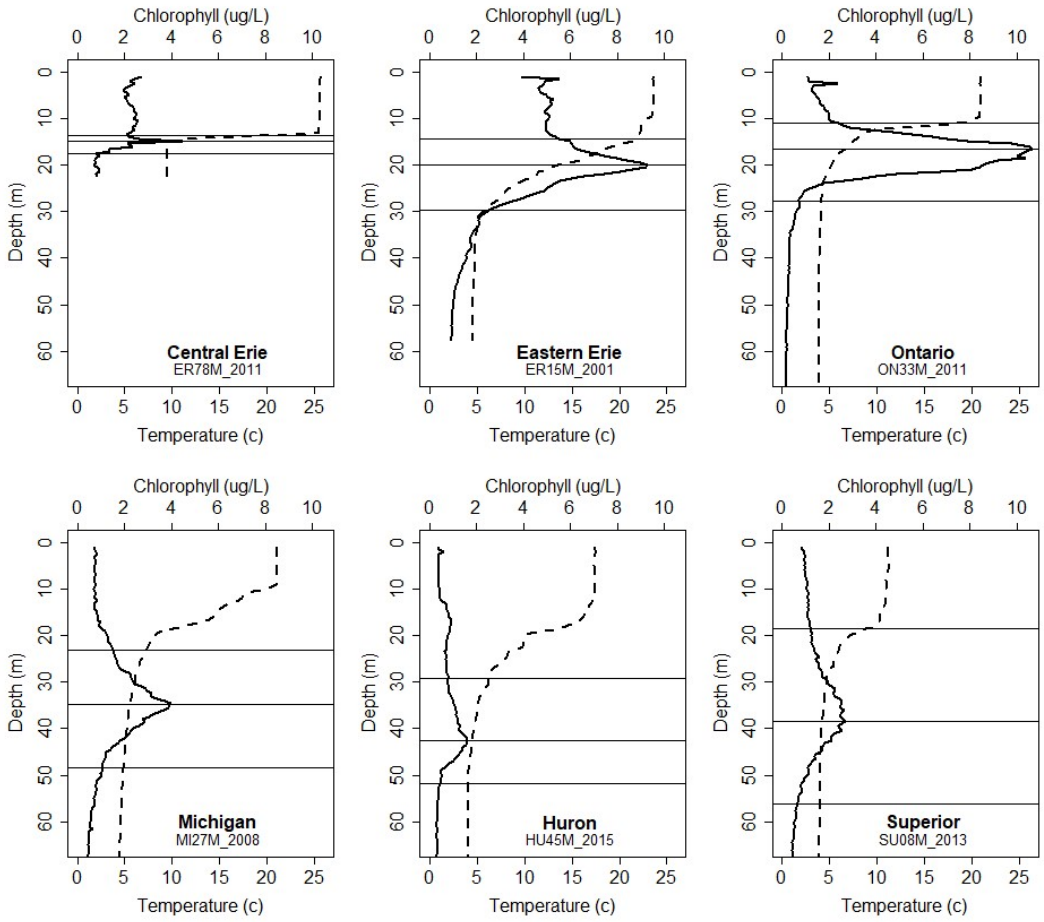

Figure 2. Examples of common deep chlorophyll maximum (DCM) shapes observed in the Laurentian Great Lakes. The dashed vertical line shows temperatures, and the solid line shows quenching-corrected chlorophyll concentrations. Horizontal lines indicate the algorithm detection for the start, peak, and end depths of the DCM.

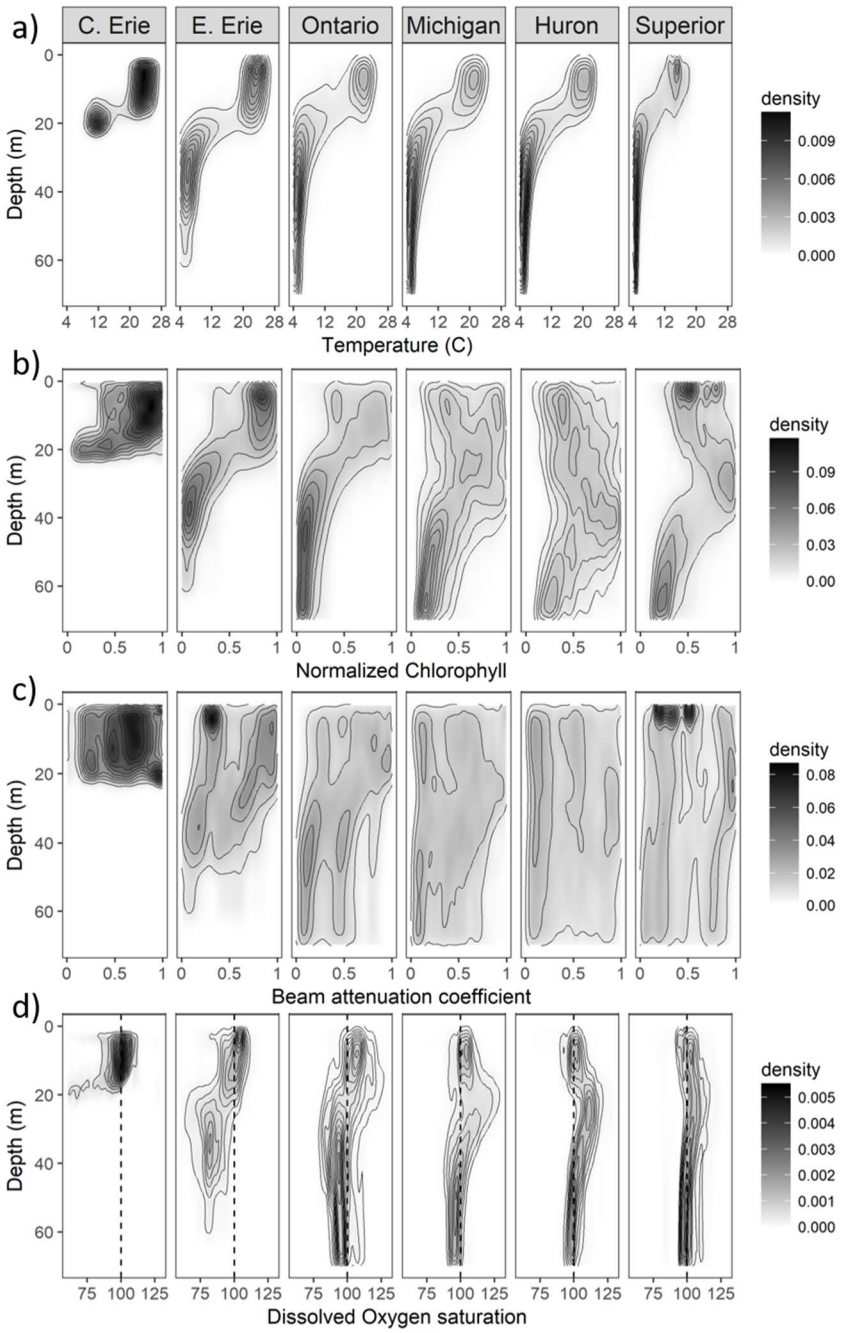

Figure 3. Density plots for all profile data, binned to 0.5-meter intervals. High density regions indicate where profiles are similar for that depth, while diffuse regions suggest greater variability in the data. **a)** temperature (°C), **b)** normalized chlorophyll (maximum of 1), **c)** normalized beam attenuation coefficient (maximum of 1), and **d)** dissolved oxygen saturation percent, with 100% saturation indicated by the dotted line. Data shown includes all profiles generated at all standard sampling sites from 1996 – 2017.

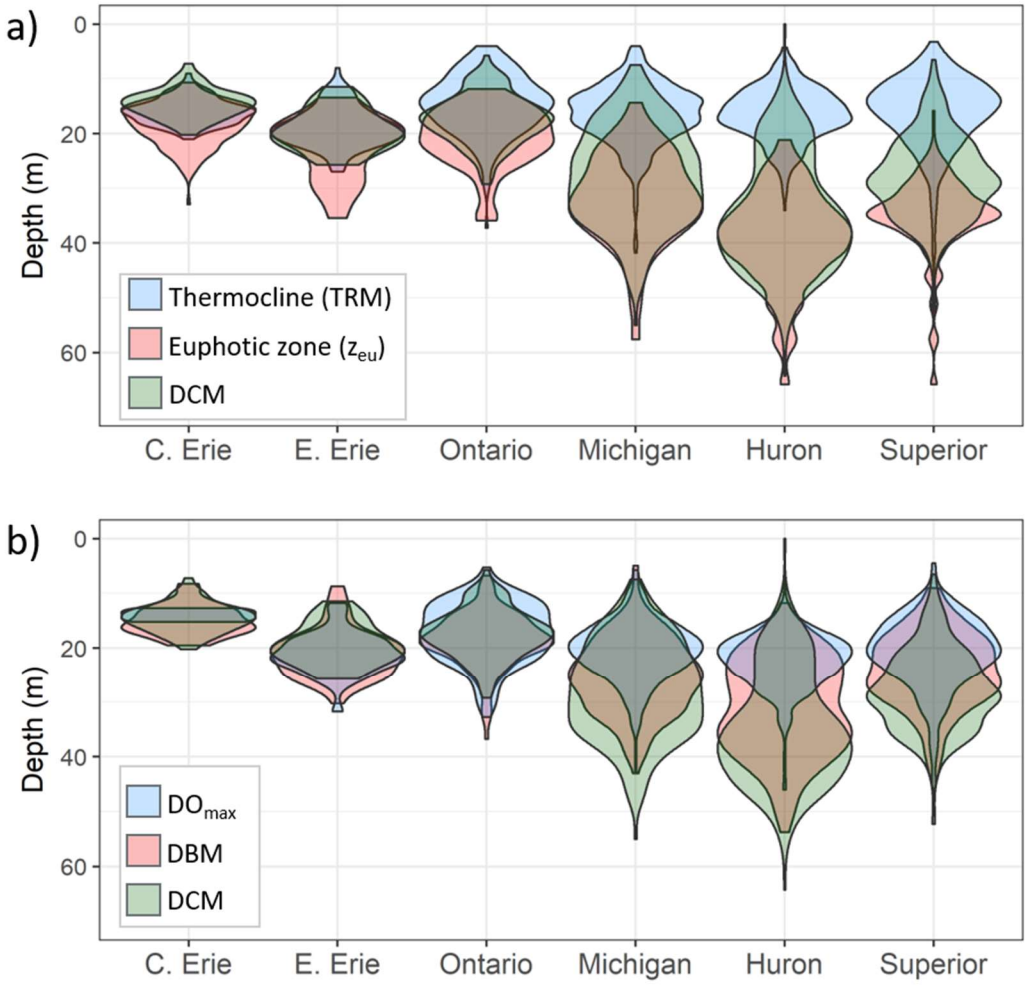

Figure 4. Violin plots showing the distribution of data for the depths of the **a)** thermocline (TRM, blue), euphotic zone (z_{eu}, red), and deep chlorophyll maximum (DCM, green), and **b)** deep oxygen maximum (DO_{max}, blue), deep biomass maximum (DBM, red), and DCM (green). Data shown are for all sites sampled from 1996 – 2017. Regions with overlap of distributions have intermediate colors: TRM/DO_{max} & DCM (blue-green); DO_{max} & DBM (purple); z_{eu}/DBM & DCM (brown); all three distributions (gray).

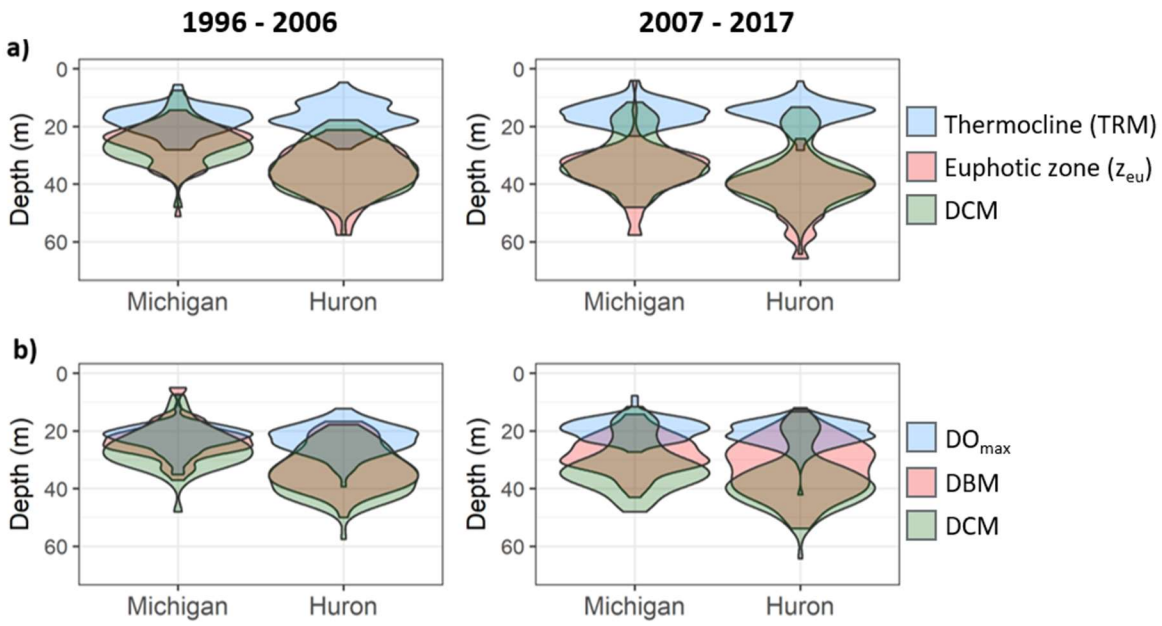

Figure 5. Violin plots showing the distribution of data in Lakes Michigan and Huron, which exhibit significant change in water clarity over time, split by decade (1996-2006, and 2007 – 2017) for the depths of the **a)** thermocline (TRM), euphotic zone (z_{eu}), and deep chlorophyll maximum (DCM), and **b)** deep oxygen maximum (DO_{max}), deep biomass maximum (DBM), and DCM. Regions with overlap of distributions have intermediate colors: TRM/DO_{max} & DCM (blue-green); DO_{max} & DBM (purple); z_{eu}/DBM & DCM (brown); all three distributions (gray).

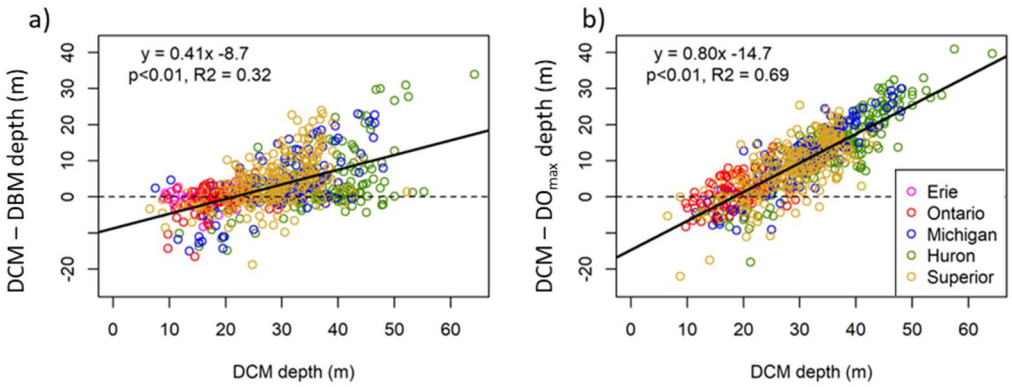

Figure 6. The differences between the DCM depth and **a)** the DBM depth, **b)** DO_{max} depth plotted against DCM depth. The dotted line marks the zero line, where the DCM and DBM/DO_{max} occur at the same depth, and the solid line is the linear regression.

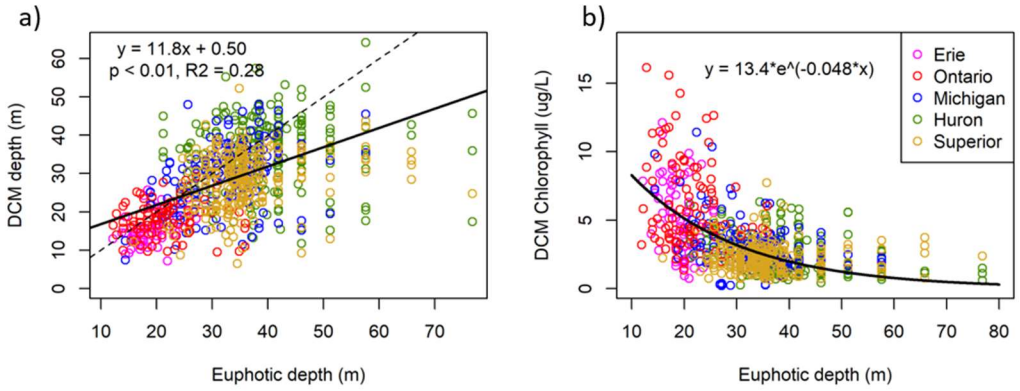

Figure 7. Euphotic depth as a predictor for **a)** deep chlorophyll maximum (DCM) depth, with the 1:1 line indicated (dotted line) and linear regression; **b)** DCM chlorophyll (ug/L) with a nonlinear fit for exponential decay. The dotted line marks the 1:1 relationship.

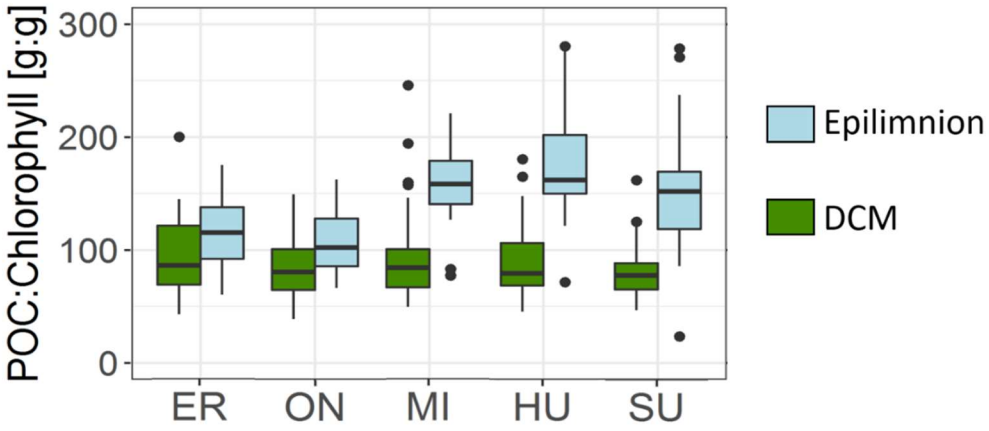

Figure 8. Particular Organic Carbon (POC) to chlorophyll ratios for the epilimnion (light blue) and DCM (green) by lake, based on extracted chlorophyll and particulate organic carbon concentrations at master stations (see Fig. 1) from 2000 - 2014. Boxes show the first and third quartiles with the median (line), whiskers extend to most extreme data point within 1.5 times the interquartile range from the box, and dots show outliers.

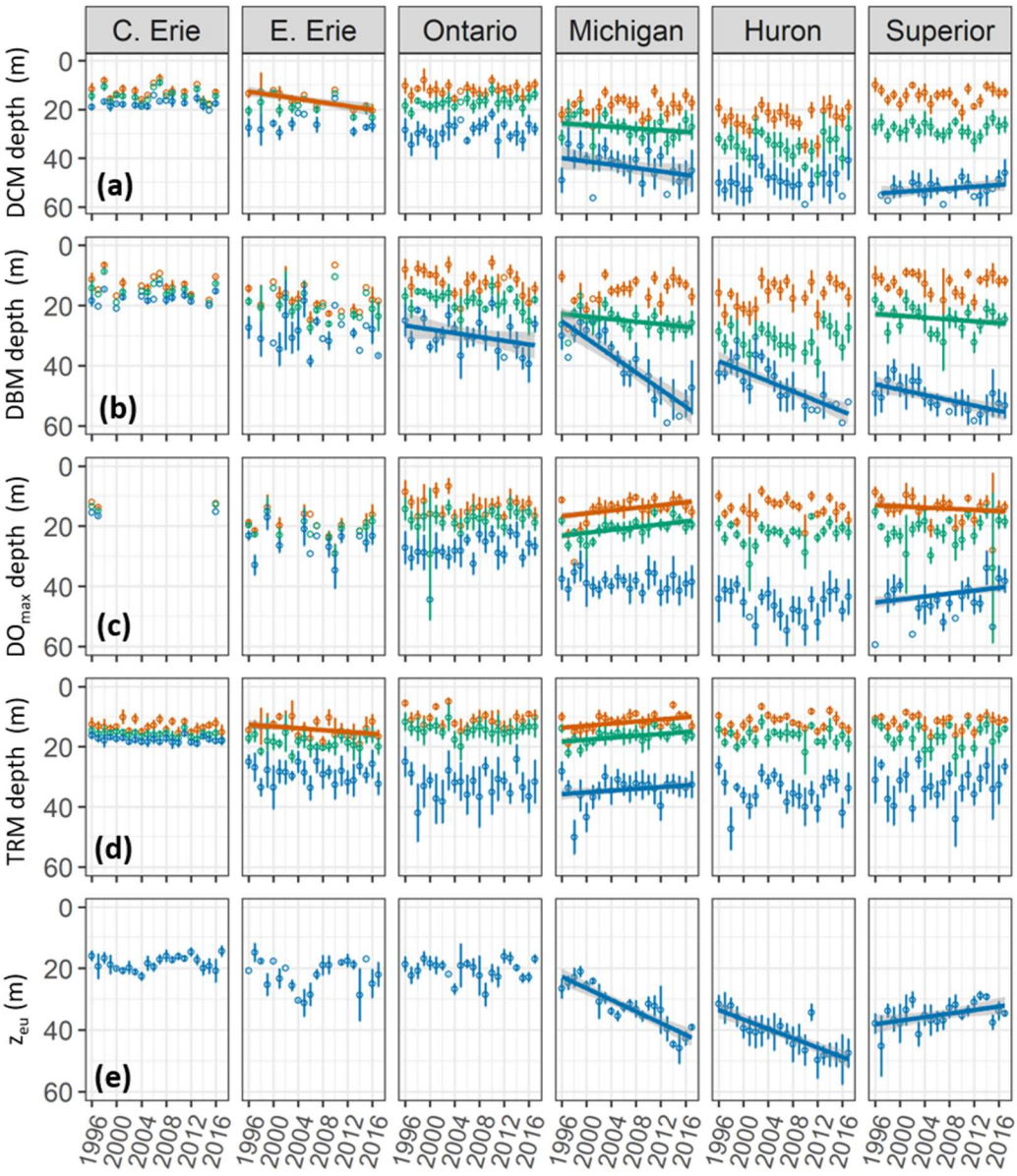

Figure 9. Summer time series plots for the start (orange), maximum (green), and bottom (blue) of features for **a)** deep chlorophyll maxima (DCM), **b)** deep biomass maxima (DBM), using beam attenuation coefficient (BAT) as a proxy for phytoplankton biomass, and **c)** deep oxygen saturation maxima (DO_{max}) **d)** thermoclines (TRM) **c)** euphotic zone (z_{eu}, 1% light level). Points mark the mean value, bars show ± two standard errors, and lines show significant linear trends.

Figure 10. Summer time series for data for **a)** chlorophyll concentration, **b)** total phosphorus, **c)** total nitrogen, and **d)** dissolved silica. Data are shown for the integrated epilimnetic water (orange) and water sampled at the deep chlorophyll maximum (green). Points show the mean value for the given year, and error bars extend to ± two standard errors. Significant linear trends are shown. Data source EPA-GLNPO GLENDA data base (https://cdx.epa.gov/)

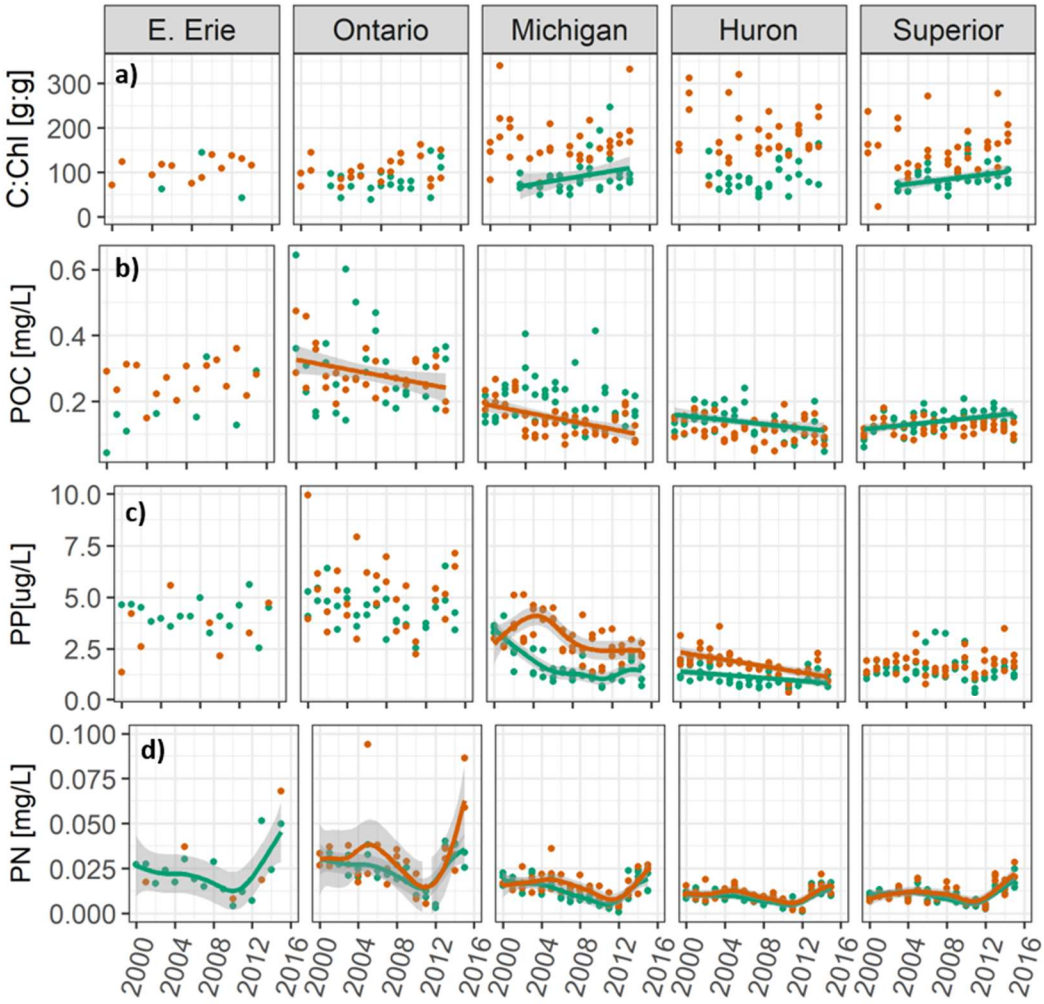

Figure 11. Summer time series from master stations (see Fig. 1) for data for the **a)** carbon to chlorophyll ratio (C:Chl), **b)** particulate organic carbon (POC) concentration, **c)** particulate phosphorus (PP) concentration, and **d)** particulate nitrogen (PN) for the integrated epilimnion (orange) and the deep chlorophyll maximum (green). Lines show significant linear trends or generalized additive model smoother lines with a significant year effect when a linear relationship was not appropriate for the full time series. Only eastern Erie is included (one master station) because DCM samples were not routinely collected in central Erie.

CHAPTER 1
SUPPLEMENTARY MATERIAL

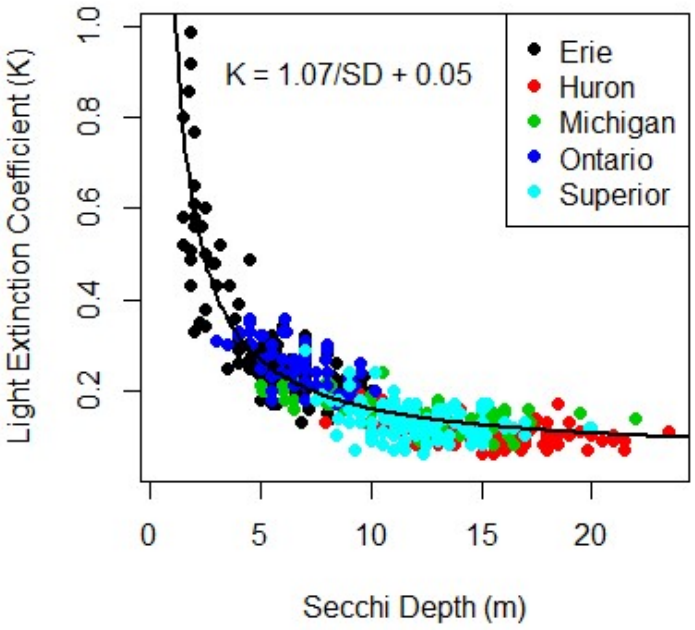

Figure S1. Relationship of the light extinction coefficient (K) to the secchi disk depth (meters) for all sites with paired secchi disk measurements and profiles of photosynthetically active radiation (PAR). K values were calculated from the slope of the linear relationship between the natural log transformed PAR vs. depth.

Table S1. Parameter fits for the quenching correction model for data subsets: 2002 – 2017, and 2011 (fit separately as the calibration constant was entered incorrectly that year). The parameters fitted for data from 2002 – 2017 were also applied to data from 1996 – 2001, for which there are concerns about the quality of the extracted chlorophyll data. Corrected profiles were then run through the peak detection algorithm.

Parameter	Estimate	Std. Error	t value	Pr(>|t|)
2002 – 2017 fit				
a	0.0466	0.001680	27.75	< 0.001
b	0.9658	0.016236	59.48	< 0.001
c	0.1425	0.007157	19.91	< 0.001
2011 fit				
a	0.0008	0.0010	0.7310	0.466
b	0.4942	0.0165	29.998	< 0.001
c	0.1719	0.0108	15.906	< 0.001

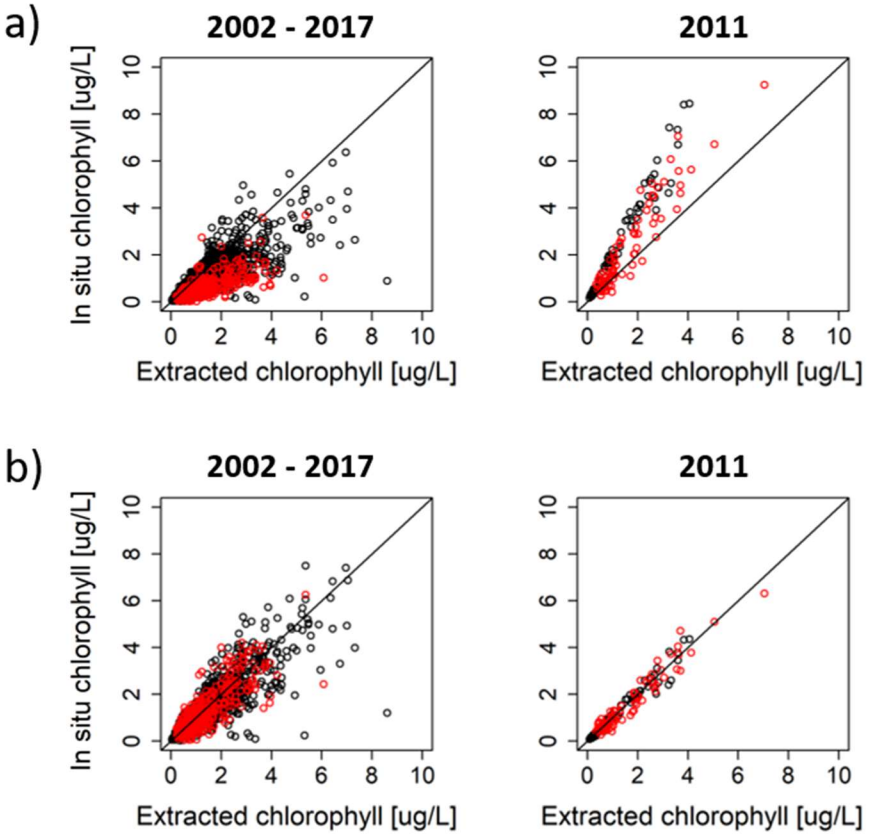

Figure S2. Scatter plots of in situ chlorophyll measurements versus extracted values for discrete depth water samples taken throughout the water column **a)** before quenching corrections were applied, and **b)** after quenching corrections were applied. Black dots indicate points where the PAR measurement was less than 25 µE/m^{2}s, and red dots indicate points with greater than 25 µE/m^{2}s PAR measurements, which are biased low prior to the correction. Only data from 2002 onward (through 2017) were used for the calibration because of quality control issues for extracted chlorophyll in earlier years. The model was optimized separately for 2011, when in situ fluorometer values were biased upward relative to other years (likely a calibration issue). All other years showed a similar relationship and thus were pooled to fit the quenching equation parameters.

CHAPTER 3

VARIABILITY IN ZOOPLANKTON DIEL VERTICAL MIGRATIONS IN SOUTHERN LAKE MICHIGAN

ABSTRACT

In oligotrophic lakes with a deep chlorophyll maxima (DCM), zooplankton food resources are often more abundant below the epilimnion, thereby invalidating accepted mechanisms driving standard diel vertical migration: ascending to higher food resources in the epilimnion at night when predation risk is lower than during the day. The existence and direction of zooplankton DVM in these lakes may therefore vary with size groups and season. We investigated seasonal patterns in DVM in southern Lake Michigan using stratified net tows, fine-scale spatial variability in DVM among zooplankton size groups using laser optical plankton (LOPC) transects, and potential drivers of DVM using data on the vertical structure of temperature, chlorophyll, and predators. We found that temperature and mean chlorophyll depth are important predictors of zooplankton depth distributions across taxa. We observed high variability in DVM patterns among size groups of zooplankton across seasons and locations, which were associated with strong differences in thermal structure, chlorophyll distribution, and predator densities. Copepodites, small diaptomids (*Leptodiaptomus ashlandi, L. minutus*), and the cyclopoid *Diacyclops thomasi* consistently migrated to surface waters at night, even when phytoplankton were less abundant in the epilimnion. However, this standard DVM This pattern is likely driven by a combination of a preference for warm temperatures and

avoidance of predation by *Limnocalanus* and *Mysis*, which migrate to the metalimnion at night and feed on smaller zooplankton taxa.

INTRODUCTION

Many pelagic organisms exhibit diel vertical migration (DVM) in stratified waters, ascending to the surface waters at night and descending during the day. This "standard" DVM pattern is generally believed to be a response to the trade-offs between favorable conditions for growth in the epilimnion and higher predation risk from visually feeding predators during the day (e.g. Bollens et al., 1992; Lampert, 1989; Zaret and Suffern, 1976) and can be induced by changes in light levels and by predator kariomones (Lampert, 1993; Peacor et al., 2005; Ringelberg, 1964). Further support for this explanation is the observation of reduced or lack of DVM in *Daphnia* population in lakes without fish predators (Gliwicz, 1986). While this "standard DVM" pattern is commonly observed, the mechanisms generally assumed to explain the DVM may not operate in oligotrophic systems where phytoplankton resources are concentrated in deep chlorophyll maxima (DCMs) rather than in surface waters. Furthermore, the presence of predators which are effective in low light environments may alter DVM behavior from the normal pattern of movement downward at dawn and upward at dusk. Thus, a range of non-standard migration behaviors have been observed across aquatic systems, including reverse vertical migration (Hairston, 1980; Ohman et al., 1983) and horizontal migration (Burks et al., 2002).

Seasonal shifts in DVM patterns are common at temperate and northern latitudes, due to changes in thermal structure, seasonal succession of phytoplankton and zooplankton species, and variable predator densities. Often, migration behavior is strongest in summer months when resources are vertically stratified and predator abundances are high (Bollens et al., 1992). In lakes where extended studies have been conducted to discern seasonal patterns in DVM, including Lake Constance in Germany/Austria/Switzerland (Geller, 1986; Stich and Lampert, 1981), Lake Maarsseveen in The Netherlands (Ringelberg et al., 1991a, 1991b), and Lake Mondsee in Austria (Nauwerck, 1993), zooplankton migration generally starts in late spring to early summer, strengthens during summer months, and ends during fall. Individual species of zooplankton also show different DVM patterns even in the same environments, with some groups undergoing migration year-round and others showing strong seasonal changes in migration (Monika Winder et al., 2003). This variability is a challenge but also an opportunity to test theory. Ideally, a universal DVM theory should be able to predict when DVM will occur, which species or life history stages are involved, and what the magnitude of DVM will be. This requires system-specific studies that includes both the distribution of the different zooplankton species and information on the distribution of the possible drivers.

In oligotrophic to ultra-oligotrophic lakes, food resources are often distributed in a way that would not favor standard DVM. Such low-productivity lakes often have low phytoplankton densities in the epilimnion and form DCM that may have greater food abundance and quality than the epilimnion (Barbiero and Tuchman, 2001; Camacho, 2006; Coon et al., 1987; Kelly et al., 2017). When food resources for zooplankton are

greater in the meta- and/or hypolimnion, species which prefer warmer temperatures, such as *Daphnia*, experience a trade-off between food availability and optimal temperature (Kessler and Lampert, 2004; Lampert et al., 2003; Williamson et al., 1996). This may affect the magnitude of migrations and ultimately exert selection pressure against warm-adapted species. Furthermore, the high transparency of oligotrophic lakes forces zooplankton to migrate deep during the day to both avoid light-dependent predation and the negative effects of damaging solar radiation (Fischer et al., 2015; Hairston, 1980; Williamson et al., 2011). Thus, species which prefer cooler temperatures have a competitive advantage in deep oligotrophic lakes and the average depth of zooplankton biomass in the water column may be deeper than in eutrophic systems.

However, many deep lake communities include predatory invertebrates or vertebrates which are effective in low-light environments and migrate from the hypolimnion into the metalimnion at night. Therefore, standard DVM may be driven by increased predation risk at night, even when food conditions are less favorable in the epilimnion. For example, *Mysis diluviana* is common in deep lakes, migrates into the metalimnion at night (Beeton, 1960), exerts strong predation pressure on zooplankton (Bunnell et al., 2011; Gal et al., 2006; Lasenby et al., 1986; O'Malley et al., 2017), and can induce standard migration in prey species of zooplankton (Peacor et al., 2005).

Lake Michigan is an example of an oligotrophic lake where the assumption of greater food availability in surface waters is violated, as DCM commonly form and contribute significantly to total summer production (Moll et al., 1984; Moll and Stoermer, 1982). Furthermore, Lake Michigan has undergone significant change over the past

several decades, largely due to oligotrophication and the impacts of nonnative species such as dreissenid mussels and predatory cladocerans (*Cercopagis pengoi* and *Bythotrephes longimanus*) (Cuhel and Aguilar, 2013; Madenjian et al., 2015; Vanderploeg et al., 2015). Increasing water clarity and decreasing epilimnetic chlorophyll have likely contributed to the observed changes in zooplankton community structure, including a decrease in cladoceran biomass and an increase in the relative contribution of calanoid copepods, especially *Limnocalanus macrurus*, to total zooplankton biomass (Barbiero et al., 2009; Barbiero and Tuchman, 2004; Doubek and Lehman, 2011; Vanderploeg et al., 2012). *Bythotrephes* may also have contributed to such changes, as it can significantly alter zooplankton community structure (Barbiero and Tuchman, 2004) through direct predation and indirect effects such as driving its prey species to deeper depths during the day (Bourdeau et al., 2011). While Lake Michigan has undergone changes lake-wide, there can be considerable heterogeneity in thermal structure, productivity, and zooplankton community due to the location of large riverine inputs, circulation patterns, upwellings (Beletsky and Schwab, 2001; Chen et al., 2002), and seiche activity. Such variability in the offshore environment likely affects zooplankton DVM patterns across time and space; thus, zooplankton DVM on finer spatial scales is an important aspect of evaluating the food web implications of a changing zooplankton community, including the availability and distribution of prey for planktivorous fishes (Bunnell et al., 2015).

Large-scale patterns and drivers of zooplankton DVM have been extensively studied across systems, including in Lake Michigan, using stratified sampling of the water column with equipment such as closing nets and discrete-depth sampling

techniques (Beeton, 1960; Bourdeau et al., 2015; Carter and Goudie, 1986; Vanderploeg et al., 2012), as well as with laboratory experiments (e.g. Boscarino, 2009; Peacor et al., 2005). However, investigations of finer-scale zooplankton distributions are less common, as they have only become possible with recent technological advances. Fine-scale measurements of in situ zooplankton distributions have become practical through the development of sensors such as the laser optical plankton counter (LOPC), which has become an increasingly popular tool for evaluating zooplankton distributions in the Great Lakes (Liebig et al., 2006; Sprules et al., 1998; Vanderploeg et al., 2015; Watkins et al., 2017; Yurista et al., 2009).

In this study, we investigate spatio-temporal patterns in zooplankton DVM in the offshore region of southern Lake Michigan during 2015 using stratified net tow data and a laser optical plankton counter (LOPC). Specifically, our objectives are to: 1) describe seasonal patterns in species-specific diel vertical migration, 2) investigate spatial heterogeneity in migration among zooplankton groups when the water column was stratified (July and September) using LOPC transects, and 3) consider potential drivers of observed spatio-temporal differences in migration patterns, including the vertical structure of temperature, phytoplankton, and predatory zooplankton.

METHODS

Study system

Lake Michigan is a deep ultra-oligotrophic lake which is the second-largest of the Laurentian Great Lakes by volume and the third largest by area (58,030 km^2). It has a mean depth of 85 m (maximum 281 meters) and an estimated residence time of 62 years

(Quinn, 1992). In southern lake Michigan, the eastern side of the basin tends to be more productive than the western side, due to relatively high nutrient inputs from the rivers including the Grand River, Kalamazoo River, and St. Joseph River. Lake Michigan, like the other Great Lakes, underwent cultural eutrophication during the mid-20th century, but nutrient loading has been reduced since the 1972 Great Lakes Water Quality agreement. In combination with nutrient decreases, invasive dreissenid mussels have contributed to increasing water clarity and decreasing chlorophyll in Lake Michigan. As lake productivity has decreased, the zooplankton community has also shifted so that in recent years it has been dominated by calanoid copepods. The most common zooplankton taxa now include *Leptodiatomus sicilis, L. minutus L. ashlandi*, *Senecella calanoides*, and *Limnocalanus macrurus* (Barbiero et al., 2018). The cyclopoid *Diacyclops thomasi* is also common, while cladocerans make up a relateively small portion of total biomass during summer. When herbivorous cladocerans are present, *Daphnia mendotae* and *Bosmina longirostris* are the most common taxa. The planktonic larvae of *Dreissena* spp. are also common in Lake Michigan since the population expansion of the invasive mussels *Dreissenapolymorpha* and *D. bugensis* (Griffiths et al., 1991). The predatory zooplankton community is primarily made up of *Limnocalanus*, *Mysis*, and the invasive predatory cladocerans *Bythotrephes longimanus* and *Cercopagi pengoi* (common in late summer to fall). Major planktivorous fish species are alewife (*Alosa pseudoharengus*), bloater (*Coregonus hoyi*) and rainbow smelt (*Osmerus mordax*) (Bunnell et al., 2014).

Sampling efforts

The data presented herein were collected through sampling activities organized by the Cooperative Science and Monitoring Initiative (CSMI), a binational effort to coordinate science across the Great Lakes and address lake-specific management needs with intensive monitoring. Sampling efforts were conducted aboard the United States Environmental Protection Agency's R/V Peter Wise Lake Guardian during May 19-22, July 6-11, and September 10-15, 2015. To investigate spatial variability in zooplankton distributions and diel vertical migration, we sampled three transects in southern Lake Michigan offshore from Racine, WI, Saugatuck, MI, and St. Joseph, MI (Fig. 1). Transects were visited during both day and night, weather permitting.

Field sampling

To assess the offshore zooplankton community structure, stratified net tows were completed at the offshore end-point of each transect. Prior to the net tows, we deployed a rosette assembly equipped with a Seabird CTD, Seapoint chlorophyll a fluorometer (Seapoint Sensors, Inc., Exeter, NH), transmissometer (WETlab C-Star) with 660 nm wavelengths, and Biospherical/Licor sensor to measure photosynthetically available radiation (PAR). The depths over which to collect stratified tows were determined from profiles of temperature and chlorophyll immediately prior to sampling. Zooplankton tows were taken for the hypolimnion, metalimnion, and epilimnion using a 64 µm mesh closing net equipped with a flow meter (Tsurumi-Seiki Co., Ltd). At night, net tows were also completed to calculate densities of *Mysis diluviana* in the water column using a 1-meter diameter 1000-µm mesh net towed from 2 meters off the bottom to the surface at a

speed of 0.5 m/second. Note 100% efficiency was assumed for the larger-mesh size net and a flow meter was not used. Upon retrieval of each tow, the contents of the cod-end were sieved through 53 µm mesh to concentrate the zooplankton, narcotized with soda water, and preserved in 70% ethanol within one hour of collection.

Preserved zooplankton samples were later counted at the University of Wisconsin Superior (Dr. Mary Balcer). Large zooplankton (*Mysis diluviana*, *Cercopagis pengoi*, and *Bythotrephes longimanus*) were removed prior to sub-sampling, and all individuals of these species were counted and measured. The remaining zooplankton sample was rinsed through a 53-µm sieve with deionized water, brought to a known volume, mixed, and subsampled using 1-mL wide-bore Henson-Stempel pipette. Crustacean zooplankton were counted in multiple subsamples for each sample until a minimum of 200 organisms (excluding veligers and nauplii) were enumerated. Due to high abundance, veligers and nauplii were only counted in the first subsample. For each tow, up to twenty individuals of each observed taxon were measured. For *Mysis* samples, all individuals were counted and measured. Taxon-specific equations were used to convert length data to dry weight biomass in micrograms (Bottrell et al., 1976; Burgess et al., 2015) (Bottrell et al., 1976; Dumont et al., 1975; McCauley, 1984, Burgess et al. 2015, see SOP LG403 version 8, 2017). For stratified zooplankton tows, the volume of water filtered by the tow was obtained from flow meter readings and used to calculate volumetric biomass, which was multiplied by the tow depth to calculate areal biomass. Weighted depths for each taxon were then calculated by multiplying the mid-point depth of each layer by the proportion of the total areal biomass within each layer. Migration distance at each site was calculated for each species by subtracting the day weighted depth from the night

weighted depth. For *Mysis* tows, areal density in mg/m^2 was calculated by dividing the total biomass collected in the net by the area of the net opening (0.785 m^2).

Triaxus deployments

During each transect visit, we towed a Triaxus (McArtney) instrument array at a speed of four knots with undulations between 5 meters and 60 meters. The Triaxus was equipped with a Seabird CTD, Fluoroprobe (BBE Moeldaenke), transmissometer (WETlab C-Star) with 660 nm wavelengths, and a laser optical plankton counter (LOPC, Rolls Royce). Triaxus data from May sampling were not used due to inconsistent tow patterns related to a malfunction of the depth sensor. In July, the Racine, Saugatuck, and St. Joseph transects were successfully sampled during both daytime and nighttime. In September, foul weather led to delays and safety concerns and therefore, there were limited Triaxus deployments: only the Racine transect (night) and the Saugatuck transect (day and night) were sampled. In this study, we limited the Triaxus dataset to all points where the Triaxus was towed to its greatest possible depth range (approximately 60 meters) to focus on the offshore environment. Thus, undulations over depth ranges too shallow to safely sample down to 60 meters were excluded from analysis.

LOPC data processing

Triaxus data streams were parsed and cleaned using a Shiny application run from within R, which was developed to processes towed undulating vehicle data (Xu et al., 2017). The LOPC detects zooplankton particles as they travel through a 70 mm wide sampling tunnel and uses internal image processing to count and measure particles (Herman et al., 2004). The LOPC output counts particles ranging from an equivalent

spherical diameter (ESD) of 0.075 to 1.920 mm, grouped into 123 size bins of 0.015 mm each. Data streams for position data and depth data, temperature, beam attenuation coefficient, and fluoroprobe chlorophyll, and LOPC bin counts were aligned prior to further processing and data were binned to a 0.5-meter depth interval.

Prior to LOPC biomass calculations, the equivalent spherical diameter (ESD) size bins of interest were determined from length measurements on zooplankton collected in stratified net tows. The length data were converted to ESD measurements using previously-established ratios for Lake Michigan zooplankton (Liebig and Vanderploeg, 2008). Density plots weighted by the proportion of total zooplankton biomass for each taxon group, in terms of areal densities (for each site sampled in July and September) were used to inform bin-cut off values (Fig. 2). Bin sizes were chosen to the nearest sample interval to the desired cut-off (bin breaks range from 0.075 mm to 1.920 mm by intervals of 0.015 mm). The size bins break points chosen were 0.075 (lower limit), 0.180, 0.495, 0.960, and 1.92 mm (upper limit), resulting in four size bins. Herein, we use the following terms for the size groups: small (0.75 – 0.180 mm ESD), medium (0.180-0.495 mm ESD), large (0.495-0.960), x-large (0.960-1.92 mm ESD), which were each related to specific zooplankton taxa/stages by sample occasion (Table 1).

The zooplankton volume (ZV) for each size bin was calculated from particle counts using the midpoint of each ESD bin. Because zooplankton are better represented as ellipsoids than as spheres, a length-width ratio shape factor (f) was included in the spherical volume calculation, according to the following equation:
$ZV = (\pi/6) * (ESD^2 * 10^{-6})/f^2$ (Yurista et al., 2009). ZV was converted to wet

weight biomass (µg) assuming a biomass specific density of 1.0 g per cm^3 (value for water), which is commonly used for LOPC data processing (Liebig and Vanderploeg, 2008; Watkins et al., 2017; Yurista et al., 2009). To estimate volume filtered (m^3), flow rates through the LOPC were calculated from the transit times of small particles (< 300 µm) passing through a 1 mm element of the LOPC tunnel. The average transit time (total time / # particles) is nonlinearly related to flow speed and yields estimates of volume filtered (LOPC manual notes by A. Herman, November 2004). Wet volumetric biomass was converted to dry biomass using a 10% conversion factor (Bottrell et al., 1976).

Data Analysis

To test for overall differences in migration behavior across months, we used a two-way analysis of variance (ANOVA) on zooplankton weighted mean depth (WMD) calculated from the net tow data with time of day and month as independent variables. We then tested for differences within each month across time of day, transect, and species using a 3-way ANOVA. Tukey Honest Statistical Differences (HSD) were used post-hoc to identify which transects/species were significantly different.

The Triaxus data were visualized in Ocean Data View (ODV; Schlitzer, 2015) using simple inverse-distance weighting interpolation. After processing of the Triaxus data stream, we split the data into upcasts/downcasts for calculation of water column profile data. The temperature profiles were analyzed by calculating the magnitude of temperature change for each meter of depth and a cut-off temperature gradient of 1 °C/m was used to define the epilimnion depth. The thermocline was defined as the depth at which the maximum temperature gradient occurred. Epilimnetic temperature and

chlorophyll values were calculated for each profile by taking the mean of all values which were shallower than the epilimnion depth. The chlorophyll maximum (Chl_{max}) was defined as the depth where chlorophyll concentration was the highest for the entire profile, regardless of whether it was above or below the epilimnion. The weighted mean depths (WMD) of chlorophyll, beam attenuation coefficient, and zooplankton biomass (by size group) were calculated for each profile by weighting each depth by the relative magnitude of the variable and then taking the mean of weighted depths. WMD was calculated using data from the depth range 6 to 50 meters because some transects had profiles where there were no data above or below that range (September data available to a maximum of 50 meters).

To test for differences in zooplankton distributions across sample occasions, time of day, and size groups, we used a generalized additive model (GAMM) on the LOPC data with a smoothed depth variable and month, transect, time of day, and size group as additional predictors. We then tested for DVM at each location in two ways: 1. For each sample occasion, we used a one-way ANOVA on the integrated zooplankton calculation within each layer to test for an effect of time of day on zooplankton biomass for each size group. 2. For each sample occasion, we used a two-way ANOVA on zooplankton WMD (calculated from the LOPC data) with time of day and size group as independent variables. Tukey HSD were used post-hoc to identify if distributions for each size group were different between day and night.

To investigate the importance of phytoplankton distribution on day/night zooplankton depths, we tested the WMD of both chlorophyll and beam attenuation

coefficient (BAT) as predictor variables for zooplankton depth using simple linear regression (by time of day). BAT is highly correlated with particulate organic carbon (POC) in oligotrophic systems (e.g. Bishop, 1999; Fennel and Boss, 2003; Gardner et al., 2000). BAT is sometimes a better proxy for phytoplankton biomass than is chlorophyll due to photoacclimation of phytoplankton cells to low light (decreased C:Chl) at the DCM. We used Akaike's Information Criterion (AIC) to determine the best-fitting model.

RESULTS

Zooplankton Community

Based on zooplankton net tow data, total zooplankton biomass peaked in July and was typically lowest at the Racine transect, intermediate at the Saugatuck transect, and highest at the St. Joseph transect (Fig. 2, Fig. 3). Overall, the zooplankton community biomass was dominated by calanoid copepods including *L. minutus, L. ashlandi, L. sicilis,* and *Limnocalanus* (Fig. 3). During May, the calanoid community was a mix of copepodites I-V and adult diaptomids. *Limnocalanus* populations were mostly immature copepodites in May. In July, there were few large adult diaptomids (*L. sicilis* decreased) and the community was dominated by copepodites I-V and adult *L. ashlandi*, and *L. minutus*. By July, most of the *Limnocalanus* population was mature. In September, there was an increase in adult *L. sicilis* and increased diversity in the zooplankton community overall. The cyclopoid copepod *D. thomasi* was uncommon during May to July but increased in September. Herbivorous cladocerans were rare, but *Bosmina longirostris* and *Daphnia mendotae* did increase in September. Invasive predatory Cladocera including

Cercopagis pengoi and *Bythotrephes longimanus* were common in July to September (Fig. 3, Table 2)

Net tow weighted mean depths

There was a significant difference in average zooplankton WMD in May compared to July ($p < 0.01$) and September ($p < 0.01$) based on net tow data (Fig. 4). Results of Tukey HSD tests indicate that zooplankton depths in May were significantly deeper than in July (5.9 m difference, $p < 0.01$) and September (7.0 m difference, $p < 0.01$). Thus, each month was tested separately for depth differences among species, locations, and time of day (Table 1). Results of the 3-way ANOVA indicate that time of day, species, and location are all highly significant factors affecting zooplankton mean depth in May ($p < 0.01$ for all factors). The Tukey HSD tests show that mean depths were significantly deeper (mean difference 5.1 m) at night than during the day ($p < 0.01$). Biomass was generally shallower at the Racine transect than the Saugatuck transect (difference 5.7 m, $p < 0.01$) and St. Joseph transect (difference 6.0 m, $p < 0.01$). In July, there was standard migration of total zooplankton biomass, which on average was 3.0 meters shallower at night ($p < 0.01$). There was no significant difference in day/night depths in September ($p = 0.46$). The significant species term in all months was largely driven by deeper depth distributions of *S. calanoides* and *Limnocalanus* compared to other taxa (Table 2).

LOPC weighted mean depths

The ANOVA with Tukey HSD tests on WMD of total zooplankton biomass (Fig. 5) indicated significant standard DVM at the Racine transect in July (4.2 m shallower at

night, $p < 0.01$) and the Saugatuck transect in September (4.6 m shallower at night, $p < 0.01$). Day/night differences in the depth of total zooplankton biomass at the Saugatuck and St. Joseph transects in July were not significant. When split into size categories, however, it was clear that there are differences in DVM among size groups that was not detectable in the changes in WMD of total zooplankton biomass.

Different DVM patterns were observed across size classes (Fig. 5). In July, both small (0.75 – 0.180 mm ESD) and medium zooplankton (0.180-0.495 mm ESD) exhibited significant reverse migration at the Racine transect (2.3 m and 3.3 m deeper at night, respectively, $p < 0.01$) and the Saugatuck transect (1.8 m and 1.5 m deeper at night, respectively, $p < 0.01$). Large zooplankton (0.495-0.960) showed no significant migration for any transect in July, while x-large zooplankton (0.960-1.96 mm ESD) showed significant standard migration at all three transects sampled: Racine (8.8 m shallower at night, $p < 0.01$), Saugatuck (1.2 m shallower at night, $p = 0.02$), and St. Joseph (2.2 m shallower at night, $p < 0.01$). In September, all size groups had significant standard migration (small 2.3 m, $p < 0.01$; medium 4.0 m, $p < 0.01$; large 4.7 m, $p < 0.01$; x-large 5.9 m, $p < 0.01$)

LOPC zooplankton distributions

The GAM results for zooplankton distributions indicated that month, transect, and all size groups were highly significant parameters ($p < 0.01$), while time of day was not significant for the full model ($p = 0.70$) (Figure 8). Thus, each sample occasion was treated separately for further analysis. Based on day/night differences in integrated biomass for each depth layer (Table 5), there were notable differences in migration

patterns among size groups and across sample occasions. In July, significant upward migration of total zooplankton biomass occurred at the Racine transect, where there was an increase in biomass in both epilimnion and metalimnion at night ($p = 0.007$ and $p = 0.002$, respectively). However, the standard migration was driven by large and x-large zooplankton: large zooplankton increased in the epilimnion at night ($p = 0.01$), and x-large zooplankton increased in both the epilimnion ($p < 0.01$) and metalimnion ($p < 0.01$). Other size groups (small, medium, and large), however, all decreased in the epilimnion at night ($p = 0.03$, $p = 0.01$, $p = 0.01$, respectively). At the Saugatuck transect, the only significant day/night difference for total zooplankton biomass was in a decrease in the metalimnion at night ($p < 0.01$). This difference was driven by medium and large zooplankton, both of which decreased in the metalimnion at night (both $p < 0.01$). There were also significant changes in the epilimnion for all sizes except medium zooplankton: small zooplankton decreased ($p = 0.02$), while large and x-large zooplankton increased (both $p < 0.01$). In addition, total biomass increased in the hypolimnion at night, but the only size group with a significant difference was the small zooplankton ($p = 0.03$). At the St. Joseph transect, total metalimnetic zooplankton decreased at night ($p < 0.01$), which was driven by decreases in both medium and large zooplankton (both $p < 0.01$). As at Saugatuck, differences among size groups masked an overall effect for epilimnetic biomass: small and large zooplankton decreased at night ($p = 0.02$ and $p = 0.04$, respectively) and medium zooplankton increased ($p = 0.02$).

In September at the Saugatuck transect, total zooplankton biomass increased in the epilimnion ($p < 0.01$) and metalimnion ($p < 0.01$) at night. This was a consistent pattern for all sizes except small zooplankton in the epilimnion, which did not show

significant change ($p = 0.88$, all others $p < 0.01$). There was no measurable change in hypolimnetic zooplankton overall, but small and x-large zooplankton increased ($p = 0.01$ and $p = 0.03$, respectively) while large zooplankton decreased ($p = 0.04$). Medium zooplankton increased but the change was marginally non-significant ($p = 0.06$).

Visualizations across the full transect further clarify the differences among taxa, provide context for the analysis of integrated zooplankton biomass, and highlight the spatial heterogeneity present in the offshore environment (Fig. 6 -8, Fig. S2 – S6). Overall, small zooplankton (veligers, nauplii) did not appear to exhibit strong migrations. Medium zooplankton (immatures, *L. minutus, L, ashlandi*) often migrated from the bottom of the epilimnion / thermocline (typically in concentrated layers) to surface waters at night and dispersed. In some case, medium zooplankton likely moved upward out of the Triaxus depth range, given that whole water column integrated biomass decreased at night in some cases (Table 6). Whole water column biomass of large zooplankton (primarily *L. sicilis* and immatures of *Limnocalanus*) was also lower at night at the Saugatuck and St. Joseph transects (both $p < 0.01$), even though this group did not generally show strong migration based on other metrics. Based on full transect visualizations, there was typically some dispersal and weakening of the biomass layer at night for large zooplankton, which may not be captured by WMD or even integrated biomass. The x-large zooplankton (*Limnocalanus*) showed strong upward movement at the Racine transect, but movement at other transects was less apparent. In September, total biomass measured by the LOPC was much higher at both the Racine (night only) and the Saugatuck transect (day and night) than it was in July. Compared to July,

zooplankton were concentrated much shallower (near the surface) at the Racine transect at night, but zooplankton were deeper in the water column at the Saugatuck transect.

Abiotic variables and predator abundance

In May, the water column was not yet stratified and thus there were not strong vertical gradients in temperature or chlorophyll. Values reported in text are night data (see Table 8 for day and night values). In July, there was variation in thermal structure and phytoplankton distributions among transects. At Racine, there was weak stratification with cool epilimnetic temperatures (mean 10.7, 1 SD 0.5 °C) and a relatively shallow epilimnion depth (10.9, 3.4 m). Chlorophyll concentrations were low in the epilimnion (1.2, 0.1 µg/L) and higher within the DCM (3.4, 0.3 µg/L), which was relatively deep (40.2, 4.0 m). At the Saugatuck transect, there were warmer surface temperatures (14.4, 0.5 °C) and a deeper epilimnion (15.2, 4.7 m). Epilimnetic and DCM chlorophyll concentrations were higher (2.6, 0.3 and 4.5, 1.2 µg/L, respectively) than at the Racine transect, and the DCM was shallower (29.3, 4.9 m). St. Joseph had the warmest epilimnion (16.1, 0.1 °C) and highest chlorophyll concentrations in July. Epilimnetic chlorophyll concentrations were high (3.9, 0.4 µg/L) and the Chl_{max} was at the bottom of the epilimnion / top of the thermocline (epilimnion depth 15.5, 0.3 m, Chl_{max} depth 13.9, 9.1 m). There was a DCM feature (Fig. 8, Fig. 9), but total chlorophyll was less at the DCM than at the bottom of the epilimnion at St. Joseph.

In September, surface temperatures at both the Racine and Saugatuck transects were much warmer (17.9, 0.7 and 19.1, 0.5 °C, respectively; Fig. 8). At Racine, there was not a well-defined epilimnion, as the thermocline started very near the surface, and the

DCM was shallower (13.5, 3.4 m) than it was in July (40.2, 4.0 m). The epilimnion at Saugatuck was 2-3 meters deeper (16.4, 2.5 m) than it was in July, but the DCM was shallower (18.1, 2.7 m). Chlorophyll concentrations in the epilimnion and DCM were considerably higher in September than July at the Racine transect (1.9, 0.2 and 3.7, 0.5 µg/L, respectively). At the Saugatuck transect, September epilimnetic chlorophyll (2.7, 0.7 µg/L) and DCM chlorophyll (4.55, 0.9 µg/L) were comparable to July values.

The phytoplankton community structure was also different among transects, based on the fluoroprobe profiles generated on the Triaxus tows (Fig. 9); the GAM results for fluoroprobe data indicated that month, transect, and phytoplankton group were highly significant parameters ($p < 0.01$). Across transects, the DCM was typically dominated by diatoms. At the Racine transect in July, however, there was also a high concentration of green algae at the DCM, while at the Saugatuck and St. Joseph transect, green algae were highest in surface waters. Cryptophytes and bluegreen algae concentrations were low in July overall, but cryptophytes were more common in September. Cryptophytes were higher in the hypolimnion than the epilimnion or metalimnion across sites.

Both chlorophyll and BAT coefficient WMD were significant predictors of zooplankton depth during day and night ($p < 0.001$ for both variables, Fig. 10). However, BAT coefficient was a significantly better predictor at both times of day (based on AIC difference > 2) than was chlorophyll. Both chlorophyll and BAT explained more of the variation in zooplankton depths during the night than during the day, based on R^2 values (Fig. 10).

On average, predator biomass generally increased from spring to fall (Table 3). In May, *Mysis* densities were relatively low across transects (98-179 mg/m^2). They were higher in July at Saugatuck (234 mg/m^2) and St. Joseph (207 mg/m^2), but lower at Racine (25 mg/m^2). In September, *Mysis* densities increased drastically at the Racine transect (338 mg/m^2) but decreased at Saugatuck (107 mg/m^2). Predatory cladocerans including *Cercopagis* and *Bythotrephes* were absent in May and at Racine in July, but they were present at both Saugatuck and St. Joseph in July. In September, some *Cercopagis* occurred at the Racine transect, and *Bythotrephes* made up a notable portion of total zooplankton biomass at the Saugatuck transect (Fig. 3, Table 2).

DISCUSSION

Seasonal patterns in DVM

The net tow data offered insights into seasonal differences in zooplankton DVM based on sampling in May, July and September. Overall, the vertical distribution of zooplankton was deepest in the water column in May, which is likely due to greater water clarity in the spring (Table 7). In addition, the DVM of all taxa were different in May (lack of migration or reverse migration) than in July and September (standard migration in most cases, Fig. 4). This suggests that factors beyond light-dependent predation avoidance are driving behavior in the spring. Previous observations of reverse DVM have been described in systems with highly diverse conditions (e.g. Cunningham, 1972; Hairston, 1980; Hutchinson, 1967; Ohman et al., 1983), and a definitive conclusion as to the ultimate cause of the behavior across different circumstances has not been reached (Ringelberg, 2009). However, the most compelling evidence for an ultimate cause of

reverse migration is consistent with the major driver of standard migration: reduction of predation risk. For example, Ohman et al. (1983) observed reverse DVM of the marine copepod *Pseudocalanus* in response to standard DVM of nocturnal invertebrate predators in Dabob Bay, Washington. Reduced spatial overlap with predators may decrease mortality rate and thus provide a benefit to migration regardless of direction within the water column. Planktivorous fishes also often show standard DVM to limit predation by visually-feeding piscivores in surface waters (Hensler and Jude, 2007; Hrabik et al., 2006; Janssen and Brandt, 1980). Thus, it may benefit zooplankton to move in the opposite direction to limit spatial overlap with their predators.

In Lake Michigan, the primary predatory invertebrate in spring is *Mysis*, which undergoes standard migration. However, *Mysis* biomass was relatively low in May compared to July and September (Table 3). Furthermore, *Mysis* typically would likely induce standard migrations in their prey rather than reverse migrations because they remain primarily in deep water near the bottom sediment during the day and migrate upward at night (typically to the upper hypolimnion or metalimnion). Given their deep depth range it is unlikely they would induce reverse migrations in their prey. Predatory cladocerans, especially the nonnative species *Cercopagis pengoi* and *Bythotrephes*, are another group of predatory invertebrates which could affect migration patterns; however, they also had low densities in May and only increased in summer to fall (Table 3). This leaves predation risk by planktivorous fishes as a possible driver of the observed reverse migration pattern in May. For example, round goby larvae exhibit diel vertical migration in Lake Erie (Hayden and Miner, 2009; Hensler and Jude, 2007), and rainbow smelt also undergo standard DVM (Carter and Goudie, 1986). In the absence of vertical gradients in

temperature or phytoplankton concentrations, predation avoidance by fishes which undergo standard migration may drive reverse DVM behavior. We did not quantify the density of planktivorous fishes in our study; inclusion of acoustics data to quantity fish densities and more spatially-explicit *Mysis* densities would improve our ability to assess the impact of predators on zooplankton distributions.

In July, net tow data indicated that there was significant standard migration overall (all sites and species included) (WMD 2.97 m shallower at night); there was no significant difference in zooplankton WMD from day to night in September (Table 2, Fig 4). The lack of significant migration in September may be due in part to fewer available data since the St. Joseph transect was not sampled (because of inclement weather). The LOPC data from July and September allow us to investigate DVM in greater detail as well as to test differences among transects and zooplankton groups using a larger sample size (Table 4). Based on LOPC data, significant standard migration of total zooplankton WMD was observed only at the Racine transect in July and the Saugatuck transect in September – half of the total transects with day & night Triaxus data available (Table 4). What these two transects have in common is a relatively deep euphotic zone (52 m and 61 m, respectively), suggesting light avoidance may drive zooplankton deeper during the day.

Differences among size groups

By separating the LOPC data into size groups, we can assess the role of various taxa in driving overall patterns in total biomass DVM. For example, the significant overall migration at Racine in July was driven only by the x-large zooplankton (primarily

Limnocalanus); other size groups showed no migration or even indications of reverse migration (Table 4). At Saugatuck in September, however, all zooplankton size groups had a significant day-night difference (standard migrations). At the Saugatuck transect in July, size groups showed significant day-night differences in opposite directions, such that total biomass did not show a significant change overall.

Small (nauplii and veligers) and medium zooplankton (copepodites, *L. minutus*, *L. ashlandi*, *D. thomasi* where present), both had a significant reverse migration based on WMD at two sites in July. This result is somewhat surprising given previous observations. The DVM patterns of dreissenid veligers is not well-known, but previous studies have reported a lack of migration in nauplii (Bourdeau et al., 2015; Watkins et al., 2017). Furthermore, the significant reverse migration of medium-sized zooplankton was unexpected, given previous observations of standard migration in the major taxa comprising this group. For example, small diaptomids (*L. ashlandi & L. minutus)* have previously been shown to favor upper strata in Lake Michigan, moving near the surface at night (Wells, 1960). More recent studies in Lake Michigan and Huron have shown that diaptomids inhabit the metalimnion during the day and may exhibit strong migrations to reach warm surface waters at night (Bourdeau et al., 2015; Nowicki et al., 2017). While our data does often show a dense layer of medium-sized zooplankton in the metalimnion during the day, there is not clear evidence for an increase in epilimnetic densities during night.

However, one of the limitations of the LOPC towed on the Triaxus vehicle is the lack of data for the top several meters of the water column. In several instances, there was

a decrease in total zooplankton biomass from day to night, suggesting movement of zooplankton to depth zones outside of the LOPC range (Table 6). For example, integrated zooplankton biomass data provide evidence that the significant increases in WMD for small zooplankton were driven by decreases in the epilimnetic biomass at night with no corresponding increase in the metalimnion or hypolimnion (Table 5), suggesting upward movement of small zooplankton. Furthermore, in both instances where reverse migration of medium-sized zooplankton was significant, there was also a significant decrease in integrated medium-sized zooplankton biomass for the whole Triaxus depth range; this did not occur at transects where no migration or standard migration was detected. It is likely that these zooplankton are migrating to shallow depths (< 6 meters) at night and escaping the range of the LOPC. This inference is consistent with previous reports on the depth distributions of small diaptomid copepods. In addition to immatures and small diaptomids, *D. thomasi* has been shown to undergo standard DVM in Lakes Michigan, Huron, and Ontario (Bourdeau et al., 2015; Nowicki et al., 2017; Watkins et al., 2017). *D. thomasi* did not make up a large proportion of zooplankton biomass during our study period, but it did undergo DVM when present, based on net tow data. Given that it generally falls into the same size bin as copepodites and small diaptomids, it is likely that *D. thomasi* is responsible for some of the upward migration observed in the medium-sized LOPC category as well – especially in September when it was more abundant (Fig. 3, Fig 4., Fig. S6).

Large zooplankton (primarily *L. sicilis*) generally did not show significant migrations in the LOPC WMD data. However, using the strata-specific biomass integrations suggested that there were significant increases in epilimnetic biomass at

three out of four sample occasions (St. Joseph in July non-significant) which indicates some upward movement. Overall, the x-large zooplankton (primarily *Limnocalanus)* exhibited significant standard migration for all sampling events, which was consistent with expectations and previous observations that they typically undergo standard DVM.

In general, data from the LOPC suggest that there are often vertical movements which cannot be captured by the coarse scale of stratified net tows or summary statistics such as WMD, including migrations within a depth layer (bottom to top of epilimnion or metalimnion). For example, the LOPC WMD data indicate significant ($p < 0.05$) upward migration in September for all size categories (Table 4, Fig. 5), but visualization of the full profiles clarifies this pattern. It appears that much of this change was driven by zooplankton concentrating in a narrower band within the metalimnion at night than during the day (Fig. 7, Fig. S6), rather than significant movement of zooplankton upward into the epilimnion. In particular, large zooplankton were distributed in the lower metalimnion to upper hypolimnion during the day and moved into the metalimnion at night, narrowing their range and weighting biomass toward shallower depths. Examination of the full distribution of zooplankton data is more informative than the use of summary statistics (such as weighted mean depth or even strata-specific integrations) alone.

Possible drivers of migration

Depth changes on the scale of a few meters within the water column may have significant implications for the bioenergetics of zooplankton (especially near the thermocline) and predation risk. Previous studies have identified temperature as a

primary driver of zooplankton DVM in warm-adapted species which benefit from increased temperatures in surface waters (Dawidowicz and Loose, 1992; Williamson et al., 1996; Winder et al., 2003). Our observations of dense zooplankton layers within the metalimnion during the daytime and dispersal at night are consistent with these observations and agree with those recently documented in Lake Ontario (Watkins et al. 2017), where the authors concluded temperature was an important factor determining nighttime distributions. Across all sites, temperature appears to be a factor affecting the magnitude and depth of migration patterns; for example, the strongest standard migration overall occurred at the Racine transect, which had a shallower and colder epilimnion (combined with high water clarity). Given that the observed migration was primarily due to the x-large size group, cooler surface temperatures likely allowed for *Limnocalanus* to migrate shallower to access preferred zooplankton prey items. *L. macurus* prefers nauplii prey but will also consume larger zooplankton such as copepodites (Warren, 1985). *Mysis* are also abundant in Lake Michigan and can consume a greater size range of zooplankton prey, including large copepods such as *Limnocalanus*. We can infer (from the decrease in total integrated biomass at night) that small and medium zooplankton migrated to surface waters (< 6 m) at night, possibly to access warmer temperatures for demographic benefits (McLaren, 1974) or escape predation risk from *Limnocalanus*. At stations where temperature was warmer (for example, St. Joseph in July and Saugatuck in September), zooplankton tended to remain at the bottom of the epilimnion or within the metalimnion at night rather than migrating to shallower depths. The warm epilimnion may have offered a refuge for small zooplankton to escape the temperature range inhabited by *Limnocalanus* and *Mysis*. The biomass measured above the thermocline at these transects

was likely large predatory Cladocera (*Cercopagis and Bythotrephes*), which increased in July and would drive zooplankton deeper during the day. Small and medium zooplankton formed a dense layer within the thermocline at both of these transects, and they may be facing predation risk from above and below.

In addition to temperature and predation risk, previous studies of zooplankton DVM have often focused on epilimnetic chlorophyll as a potential driver of behavior. There is evidence that chlorophyll affects zooplankton nighttime distributions even in the absence of other factors such as warmer temperatures. For example, Nowicki et al. (2017) found that epilimnetic chlorophyll was an important factor for *Bosmina* spp. but not for *Daphnia* or copepods. We used whole water column chlorophyll distributions to calculate WMD and found that chlorophyll WMD was a significant predictor of zooplankton depth ($p < 0.01$, Fig. 10) during day and night ($R = 0.10$ and $R = 0.50$, respectively). However, BAT was a significantly better predictor of zooplankton distributions for both times of day than was chlorophyll (AIC difference > 2). This is likely due to two factors: 1. Quenching of chlorophyll fluorescence in the surface waters during the day (decreased fluorescence response in high light) creates a diel signal in the chlorophyll concentration WMD (with artificially deep daytime values) 2. Photoacclimation causes the chlorophyll to carbon ratio to differ with depth (see Ch.2), and thus chlorophyll is not an optimal predictor of phytoplankton biomass distribution. The BAT data may be better correlated with phytoplankton carbon, and the signal is not affected by differing ambient light environments as is chlorophyll (Scofield et al., 2017). In addition, the R^2 value for BAT as a predictor variable was higher for night data than for day ($R^2 = 0.74$ and $R^2 = 0.58$, respectively). This suggests that overall, zooplankton may not be distributed according to

optimum food conditions during the day and then move to preferred feeding habitat at night, when light-dependent predation risk is lower. Given that *Limnocalanus* makes up a large portion of the zooplankton biomass (Fig. 3), this relationship is likely be driven by *Limnocalanus* migrating upward to the depth of the DCM at night (Oliver et al., 2014; Watkins et al., 2017), where they may feed on algae or microzooplankton.

Phytoplankton community structure may also affect depth preferences of herbivorous zooplankton. The GAM distributions of all fluoroprobe profiles were significantly different ($p < 0.01$) across phytoplankton groups and sample occasion. At most sites, green algae were highest in surface waters and diatoms made up the bulk of phytoplankton chlorophyll within the DCM (Fig. 9). The one exception is the Racine transect in July, when the DCM also had high concentrations of green algae. *Limnocalanus* and *Mysis* are known to graze on large diatoms, so higher diatom density within the DCM may lead to increased herbivory and reduce the need for strong migrations to predate on smaller zooplankton within the metalimnion.

Ultraviolet and other short-wave length radiation may also be a cause for migration out of surface waters during the day, and avoidance of damaging solar radiation may drive some of the fine-scale (on the order of a few meters) migrations observed in small taxa. Several studies have established the importance of photodamaging radiation as a driver of zooplankton migration in high transparency systems (Fischer et al., 2015; Hairston, 1976, 1980; Urmy et al., 2016; Williamson et al., 2011). Although we did not directly evaluate ultraviolet radiation in this study, the two transects with significant overall DVM (based on LOPC biomass WMD) were those sites

with the highest water clarity (Table 7). UV radiation likely plays a role in driving variability in daytime surface avoidance.

Conclusions

Our observations of fine-scale zooplankton DVM patterns across a range of conditions in offshore Lake Michigan provide insights into the complexity of zooplankton DVM in oligotrophic lakes. We found that the distributions of temperature, food resources, and predation are all likely to affect DVM, and teasing apart ultimate drivers would be quite complex given that all drivers tended to co-vary. That being said, we did consistently observe standard DVM of several zooplankton taxa in Lake Michigan during summer stratification, despite the fact that food resource in the epilimnion are generally less abundant than in the metalimnion to hypolimnion. However, much of the measurable differences in day/night depths were due to the upward migration of zooplankton greater than 0.96 mm ESD, which were primarily *Limnocalanus* adults; their movements were often from the hypolimnion into the metalimnion where food resources are abundant. The current conditions in Lake Michigan likely favor such cold-adapted species. However, zooplankton diversity increased from spring to fall; where there was strong thermal stratification and warm surface temperatures, calanoid copepods and cladocerans were much more common. Such conditions may provide a thermal refuge from predation by *Limnocalanus* or *Mysis*.

It is important, going forward, to recognize that the offshore environment does have a high degree of spatial variability and that zooplankton depth distributions can vary greatly in response to changing stressors over the course of the stratified season. We

observed significant differences in behavior among size groups of zooplankton, often on scales which are not measurable with traditional stratified net tows or discrete-depth sampling methods. Even fine-scale variation in environmental conditions may have significant demographic consequences for zooplankton species and may ultimately affect zooplankton community structure. Relationships between known taxa size distributions at the time of sampling can inform our interpretation of LOPC results and provide a wealth of information that offers potential for future modeling approaches to assess DVM behavior in the offshore environment. Continued use of LOPC technology will allow for further insights into the potential impacts of changing conditions in Lake Michigan, including increasing water clarity, oligotrophication, invasive species impacts, and warming temperatures.

REFERENCES

Barbiero, R.P., Bunnell, D.B., Rockwell, D.C., Tuchman, M.L., 2009. Recent increases in the large glacial-relict calanoid *Limnocalanus macrurus* in Lake Michigan. J. Great Lakes Res. 35, 285–292. doi:10.1016/j.jglr.2008.12.006

Barbiero, R.P., Lesht, B.M., Warren, G.J., Rudstam, L.G., Watkins, J.M., Reavie, E.D., Kovalenko, K.E., Karatayev, A.Y., 2018. A comparative examination of recent changes in nutrients and lower food web structure in Lake Michigan and Lake Huron. J. Great Lakes Res. doi:10.1016/j.jglr.2018.05.012

Barbiero, R.P., Tuchman, M.L., 2004. Changes in the crustacean communities of Lakes Michigan, Huron, and Erie following the invasion of the predatory cladoceran *Bythotrephes longimanus*. Can. J. Fish. Aquat. Sci. 61, 2111–2125. doi:10.1139/f04-149

Barbiero, R.P., Tuchman, M.L., 2001. Results from the U.S. EPA's biological open water surveillance program of the Laurentian Great Lakes: II. Deep chlorophyll maxima. J. Great Lakes Res. 27, 155–166. doi:10.1016/S0380-1330(01)70629-6

Beeton, A.M., 1960. The vertical migration of *Mysis relicta* in Lakes Huron and Michigan. J. Fish. Res. Board Canada 17, 517–539. doi:10.1139/f60-037

Beletsky, D., Schwab, D.J., 2001. Modeling circulation and thermal structure in Lake Michigan: annual cycle and interannual variability. J. Geophys. Res. 106, 19745–19771. doi:10.1029/2000JC000691

Bishop, J.K.B., 1999. Transmissometer measurement of POC. Deep Sea Res. Part I Oceanogr. Res. Pap. 46, 353–369.

Bollens, S.M., Frost, B.W., Thoreson, D.S., Watts, S.J., 1992. Diel vertical migration in zooplankton: field evidence in support of the predator avoidance hypothesis. Hydrobiologia 234, 33–39.

Boscarino, B.T., Rusdtam, L.G., Eillenberger, J.L., O'Gorman, R., 2009. Importance of light, temperature, zooplankton and fish in predicting the nighttime vertical distribution of *Mysis diluviana*. Aquat. Biol. 5, 263–279. doi:10.3354/ab00161

Bottrell, H.H., Duncan, A., Grygierek, E., Herzig, A., Hillbricht-Ilkowska, A., Kurosawa, H., Larsson, P., Weglenska, T., 1976. A review of some problems in zooplankton production studies. Norw J. Zool. 24, 419–456.

Bourdeau, P.E., Pangle, K.L., Peacor, S.D., 2015. Factors affecting the vertical distribution of the zooplankton assemblage in Lake Michigan: the role of the invasive predator *Bythotrephes longimanus*. J. Great Lakes Res. 41, 115–124. doi:10.1016/j.jglr.2015.09.017

Bourdeau, P.E., Pangle, K.L., Peacor, S.D., 2011. The invasive predator *Bythotrephes* induces changes in the vertical distribution of native copepods in Lake Michigan.

Biol. Invasions 13, 2533–2545. doi:10.1007/s10530-011-0073-0

Bunnell, D.B., Barbiero, R.P., Ludsin, S.A., Madenjian, C.P., Warren, G.J., Dolan, D.M., Brenden, T.O., Briland, R., Gorman, O.T., He, J.X., Johengen, T.H., Lantry, B.F., Lesht, B.M., Nalepa, T.F., Riley, S.C., Riseng, C.M., Treska, T.J., Tsehaye, I., Walsh, M.G., Warner, D.M., Weidel, B.C., 2014. Changing ecosystem dynamics in the Laurentian Great Lakes: bottom-up and top-down regulation. Bioscience 64, 26–39. doi:10.1093/biosci/bit001

Bunnell, D.B., Davis, B.M., Chriscinske, M.A., Keeler, K.M., Mychek-Londer, J.G., 2015. Diet shifts by planktivorous and benthivorous fishes in northern Lake Michigan in response to ecosystem changes. J. Great Lakes Res. 41, 161–171. doi:10.1016/j.jglr.2015.07.011

Bunnell, D.B., Davis, B.M., Warner, D.M., Chriscinske, M.A., Roseman, E.F., 2011. Planktivory in the changing Lake Huron zooplankton community: *Bythotrephes* consumption exceeds that of *Mysis* and fish. Freshw. Biol. 56, 1281–1296. doi:10.1111/j.1365-2427.2010.02568.x

Burgess, S., E. W. Jackson, L. Schwarzman, N. Gezon, and J. T. Lehman. 2015. Improved estimates of calanoid copepod biomass in the St. Lawrence Great Lakes. Journal of Great Lakes Research 41:484-491.

Burks, R.L., Lodge, D.M., Jeppesen, E., Lauridsen, T.L., 2002. Diel horizontal migration of zooplankton: costs and benefits of inhabiting the littoral. Freshw. Biol. 47, 343–365. doi:10.1046/j.1365-2427.2002.00824.x

Camacho, A., 2006. On the occurrence and ecological features of deep chlorophyll maxima (DCM) in Spanish stratified lakes. Limnetica 25, 453–478.

Carter, J.C.H., Goudie, K.A., 1986. Diel vertical migrations and horizontal distributions of *Limnocalanus macrurus* and *Senecella calanoides* (Copepoda, Calanoida) in lakes of Southern Ontario in relation to planktivorous fish. Can. J. Fish. Aquat. Sci.

43, 2508–2514. doi:10.1139/f86-309

Chen, C., Ji, R., Schwab, D.J., Beletsky, D., Fahnenstiel, G.L., Jiang, M., Johengen, T.H., Vanderploeg, H., Eadie, B., Budd, J.W., Bundy, M.H., Gardner, W., Cotner, J., Lavrentyev, P.J., 2002. A model study of the coupled biological and physical dynamics in Lake Michigan. Ecol. Modell. 152, 145–168. doi:10.1016/S0304-3800(02)00026-1

Coon, T.G., Lopez, M.M., Richerson, P.J., Powell, T.M., Goldman, C.R., 1987. Summer dynamics of the deep chlorophyll maximum in Lake Tahoe. J. Plankton Res. 9, 327–344. doi:10.1093/plankt/9.2.327

Cuhel, R.L., Aguilar, C., 2013. Ecosystem transformations of the Laurentian Great Lake Michigan by nonindigenous biological invaders. Annu. Rev. Mar. Sci 5, 289–320. doi:10.1146/annurev-marine-120710-100952

Cunningham, L., 1972. Vertical migration of *Daphnia* and copepods under the ice. Limnol. Oceanogr. 17, 301–303.

Dawidowicz, P., Loose, C.J., 1992. Metabolic costs during predator-induced diel vertical migration of *Daphnia*. Limnol. Oceanogr. 37, 1589–1595. doi:10.4319/lo.1992.37.8.1589

Dumont, H.J., Van de Velde, I. and Dumont, S., 1975. The dry weight estimate of biomass in a selection of Cladocera, Copepoda and Rotifera from the plankton, periphyton and benthos of continental waters. Oecologia, 19, 75-97.

Doubek, J.P., Lehman, J.T., 2014. Historical trophic position of *Limnocalanus macrurus* in Lake Michigan. J. Great Lakes Res. 40, 1027–1032. doi:10.1016/j.jglr.2014.09.003

Doubek, J.P., Lehman, J.T., 2011. Historical biomass of *Limnocalanus* in Lake Michigan. J. Great Lakes Res. 37, 159–164. doi:10.1016/j.jglr.2010.11.012

Fennel, K., Boss, E., 2003. Subsurface maxima of phytoplankton and chlorophyll: steady-state solutions from a simple model. Limnol. Oceanogr. 48, 1521–1534. doi:10.4319/lo.2003.48.4.1521

Fischer, J.M., Olson, M.H., Theodore, N., Williamson, C.E., Rose, K.C., Hwang, J., 2015. Diel vertical migration of copepods in mountain lakes: the changing role of ultraviolet radiation across a transparency gradient. Limnol. Oceanogr. 60, 252–262. doi:10.1002/lno.10019

Gal, G., Rudstam, L.G., Mills, E.L., Lantry, J.R., Johannsson, O.E., Greene, C.H., 2006. Mysid and fish zooplanktivory in Lake Ontario: quantification of direct and indirect effects. Can. J. Fish. Aquat. Sci. 63, 2734–2747.

Gardner, W.D., Richardson, M.J., Smith, W.O., 2000. Seasonal patterns of water column particulate organic carbon and fluxes in the Ross Sea, Antarctica. Deep. Res. II 47, 3423–3449.

Geller, W., 1986. Diurnal vertical migration of zooplankton in a temperate great lake (L. Constance): a starvation avoidance mechanism?. Arch. fuer Hydrobiol. Suppl. 74, 1–60.

Griffiths, R.W., Schloesser, D.W., Leach, J.H., Kovalak, W.P., 1991. Distribution and dispersal of the zebra mussel (*Dreissena polymorpha*) in the Great Lakes region. Can. J. Fish. Aquat. Sci. 48, 1381–1388.

Hairston, J.N.G., 1976. Photoprotection by carotenoid pigments in the copepod *Diaptomus nevadensis*. Proc. Natl. Acad. Sci. 73, 971–974.

Hairston, N.G.J., 1980. The vertical distribution of diaptomid copepods in relation to body pigmentation, in: Kerfoot, W.C. (Ed.), Evolution and Ecology of Zooplankton Communities. University Press of New England, Hanover, New Hampshire, pp. 98–110.

Hayden, T.A., Miner, J.G., 2009. Rapid dispersal and establishment of a benthic Ponto-Caspian goby in Lake Erie: diel vertical migration of early juvenile Round Goby. Biol. Invasions 11, 1767–1776. https://doi.org/10.1007/s10530-008-9356-5

Hensler, S.R., Jude, D.J., 2007. Diel vertical migration of Round Goby larvae in the Great Lakes. J. Gt. Lakes Res. 33, 295–302.

Herman, A.W., Beanlands, B., Phillips, E.F., 2004. The next generation of optical plankton counter: the Laser-OPC. J. Plankton Res. 26, 1135–1145. https://doi.org/10.1093/plankt/fbh095

Hrabik, T.R., Jensen, O.P., Martell, S.J.D., Walters, C.J., Kitchell, J.F., 2006. Diel vertical migration in the Lake Superior pelagic community. I. Changes in vertical migration of coregonids in response to varying predation risk. Can. J. Fish. Aquat. Sci. 63, 2286–2295. doi:10.1139/f06-124

Hutchinson, G.E., 1967. A treatise on Limnology, Vol II: Introduction to Lake Biology and the Limnoplankton. Wiley, New York.

Janssen, J., Brandt, S.B., 1980. Feeding ecology and vertical migration of adult Alewives (*Alosa pseudoharengus*) in Lake Michigan. Can. J. Fish. Aquat. Sci. 37, 177–184. doi:10.1139/f80-023

Kelly, P.T., Weidel, B.C., Paufve, M.R., O'Malley, B.P., Watkins, J.M., Rudstam, L.G., Jones, S.E., 2017. Concentration and biochemical gradients of seston in Lake Ontario. J. Great Lakes Res. 43, 795–803. doi:10.1016/J.JGLR.2017.03.007

Kessler, K., Lampert, W., 2004. Fitness optimization of *Daphnia* in a trade-off between food and temperature. Oecologia 140, 381–387. doi:10.1007/s00442-004-1592-5

Lampert, W., 1993. Ultimate causes of diel vertical migration of zooplankton: new evidence for the predator-avoidance hypothesis. Ergebnisse der Limnol. 39, 79–88.

Lampert, W., 1989. The adaptive significance of diel vertical migration of zooplankton. Funct. Ecol. 3, 21–27.

Lampert, W., McCauley, E., Manly, B.F.J., 2003. Trade–offs in the vertical distribution of zooplankton: ideal free distribution with costs? Proc. R. Soc. London B Biol. Sci. 270, 765–773. doi:10.1098/rspb.2002.2291

Lasenby, D.C., Northcote, T.., Furst, M., 1986. Theory, practice, and effects of *Mysis relicta* introductions to North American and Scandinavian lakes. Can. J. Fish. Aquat. Sci. 43, 1277–1284.

Liebig, J., Vanderploeg, H., 2008. Selecting optical plankton counter size bins to optimize zooplankton information in Great Lakes studies. NOAA Technical Memorandum GLERL-143, 1–16.

Liebig, J.R., Vanderploeg, H.A., Ruberg, S.A., 2006. Factors affecting the performance of the optical plankton counter in large lakes: insights from Lake Michigan and laboratory studies. J. Geophys. Res. Ocean. 111, 1–10. doi:10.1029/2005JC003087

Madenjian, C.P., Bunnell, D.B., Warner, D.M., Pothoven, S.A., Fahnenstiel, G.L., Nalepa, T.F., Tsehaye, I., Claramunt, R.M., Clark, R.D., 2015. Changes in the Lake Michigan food web following dreissenid mussel invasions: A synthesis. J. Great Lakes Res. 41, 217–231. doi:10.1016/j.jglr.2015.08.009

McCauley, E., 1984. The estimation of the abundance and biomass of zooplankton in samples, in: Downing, J.A. and Rigler, F.H. (Ed.), A manual on methods for the assessment of secondary productivity in fresh waters. Blackwell Scientific Publications, Oxford, pp.228-265.

McLaren, I. A. 1974. Demographic strategy of vertical migration by a marine copepod. The American Naturalist. 108, 91-102.

Moll, R., Stoermer, E., 1982. A hypothesis relating trophic status and subsurface

chlorophyll maxima of lakes. Arch. für Hydrobiol. 94, 425–440.

Nauwerck, A., 1993. Migration strategies of crustacean zooplanton in Lake Mondsee. Ergebnisse der Limnol. ERLIA 6, 39.

Nowicki, C.J., Bunnell, D.B., Armenio, P.M., Warner, D.M., Vanderploeg, H.A., Cavaletto, J.F., Mayer, C.M., Adams, J. V., 2017. Biotic and abiotic factors influencing zooplankton vertical distribution in Lake Huron. J. Great Lakes Res. 43, 1044–1054.

O'Malley, B.P., Rudstam, L.G., Watkins, J.M., Holda, T.J., Weidel, B.C., 2017. Effects of food web changes on *Mysis diluviana* diet in Lake Ontario. J. Great Lakes Res. 43, 813–822. doi:10.1016/J.JGLR.2017.02.003

Ohman, M.D., Frost, B.W., Cohen, E.B., 1983. Reverse diel vertical migration: an escape from invertebrate predators. Science. 220, 1404–1407. doi:10.1126/science.150.3692.28

Pangle, K.L., Peacor, S.D., 2006. Non-lethal effect of the invasive predator *Bythotrephes longimanus* on *Daphnia mendotae*. Freshw. Biol. 51, 1070–1078. doi:10.1111/j.1365-2427.2006.01555.x

Peacor, S.D., Pangle, K.L., Vanderploeg, H.A., 2005. Behavioral response of Lake Michigan *Daphnia mendotae* to *Mysis relicta*. J. Great Lakes Res. 31, 144–154.

Quinn, F.H., 1992. Hydraulic residence times for the Laurentian Great Lakes. J. Great Lakes Res. 18, 22–28. doi:10.1016/S0380-1330(92)71271-4

Ringelberg, J., 2009. Diel vertical migration of zooplankton in lakes and oceans: causal explanations and adaptive significances. Springer Science & Business Media. doi:10.1007/978-90-481-3093-1

Ringelberg, J., 1964. The positively phototactic reaction of *Daphnia magna straus*: a

contribution to the understanding of diurnal vertical migration. Netherlands J. Sea Res. 2, 319–406.

Ringelberg, J., Flik, B.J.G., Lindenaar, D., Royackers, K., 1991a. Diel vertical migration of *Daphnia hyalina* (*sensu latiori*) in Lake Maarsseveen: Part 1. Aspects of seasonal and daily timing. Arch. fuer Hydrobiol. 121, 129–145.

Ringelberg, J., Flik, B.J.G., Lindenaar, D., Royackers, K., 1991b. Diel vertical migration of *Daphnia hyalina* (*sensu latiori*) in Lake Maarsseveen: Part 2. Aspects of population dynamics. Arch. fuer Hydrobiol. 121, 129–145.

Schlitzer, R., 2015. Ocean Data View. http://odv.awi.de.

Scofield, A.E., Watkins, J.M., Weidel, B.C., Luckey, F.J., Rudstam, L.G., 2017. The deep chlorophyll layer in Lake Ontario: extent, mechanisms of formation, and abiotic predictors. J. Great Lakes Res. 43, 782–794. doi:10.1016/j.jglr.2017.04.003

Sprules, W.G., Jin, E.H., Herman, A.W., Stockwell, J.D., 1998. Calibration of an optical plankton counter for use in fresh water. Limnol. Oceanogr. 43, 726–733. doi:10.4319/lo.1998.43.4.0726

Stich, H.-B., Lampert, W., 1981. Predator evasion as an explanation of diurnal vertical migration by zooplankton. Nature 293, 396–398. doi:10.1038/293396a0

Urmy, S.S., Williamson, C.E., Leach, T.H., Schladow, S.G., Overholt, E.P., Warren, J.D., 2016. Vertical redistribution of zooplankton in an oligotrophic lake associated with reduction in ultraviolet radiation by wildfire smoke. Geophys. Res. Lett. 43, 3746–3753. doi:10.1002/2016GL068533

Vanderploeg, H.A., Pothoven, S.A., Fahnenstiel, G.L., Cavaletto, J.F., Liebig, J.R., Stow, C.A., Nalepa, T.F., Madenjian, C.P., Bunnell, D.B., 2012. Seasonal zooplankton dynamics in Lake Michigan: disentangling impacts of resource limitation, ecosystem engineering, and predation during a critical ecosystem transition. J. Great Lakes Res.

38, 336–352. doi:10.1016/j.jglr.2012.02.005

Vanderploeg, H.A., Pothoven, S.A., Krueger, D., Mason, D.M., Liebig, J.R., Cavaletto, J.F., Ruberg, S.A., Lang, G.A., Ptáčníková, R., 2015. Spatial and predatory interactions of visually preying nonindigenous zooplankton and fish in Lake Michigan during midsummer. J. Great Lakes Res.41, Supple, 125–142. doi:10.1016/j.jglr.2015.10.005

Warren, G.J., 1985. Predaceous feeding habits of *Limnocalanus macrurus*. J. Plankton Res. 7, 537–552. doi:10.1093/plankt/7.4.537

Watkins, J.M., Collingsworth, P.D., Saavedra, N.E., O'Malley, B.P., Rudstam, L.G., 2017. Fine-scale zooplankton diel vertical migration revealed by traditional net sampling and a Laser Optical Plankton Counter (LOPC) in Lake Ontario. doi:10.1016/j.jglr.2017.03.006

Wells, L., 1960. Seasonal abundance and vertical movements of crustacea in Lake Michigan. US Fish Wildl. Serv., Fish. Bull. 60, 343-369.

Williamson, C.E., Fischer, J.M., Bollens, S.M., Overholt, E.P., Breckenridge, J.K., 2011. Toward a more comprehensive theory of zooplankton diel vertical migration: integrating ultraviolet radiation and water transparency into the biotic paradigm. Limnol. Oceanogr. 56, 1603–1623. doi:10.4319/lo.2011.56.5.1603

Williamson, C.E., Sanders, R.W., Moeller, R.E., Stutzman, P.L., 1996. Utilization of subsurface food resources for zooplankton reproduction: implications for diel vertical migration theory. Limnol. Oceanogr. 41, 224–233.

Winder, M., Buergi, H.R., Spaak, P., 2003. Seasonal vertical distribution of phytoplankton and copepod species in a high-mountain lake. Arch. für Hydrobiol. 158, 197–213. doi:10.1127/0003-9136/2003/0158-0197

Xu, W., Collingsworth, P., Bailey, B., Carlson Mazur, M., Schaeffer, J., Minsker, B.,

2017. Detecting spatial patterns of rivermouth processes using a geostatistical framework for near-real-time analysis. Environmental 97, 72–85. doi:10.1016/j.envsoft.2017.06.049

Yurista, P.M., Kelly, J.R., Miller, S.E., 2009. Lake Superior zooplankton biomass: alternate estimates from a probability-based net survey and spatially extensive LOPC surveys. J. Great Lakes Res. 35, 337–346. doi:10.1016/j.jglr.2009.03.004

Zaret, T.M., Suffern, S., 1976. Vertical migration in zooplankton as a predator avoidance mechanism. Limnol. Oceanogr. 21, 804–813. doi:10.4319/lo.1976.21.6.0804

Table 1. Analysis of variance (ANOVA) table displaying the degrees of freedom (df), F-values, and P-values for the weighted mean depths (WMD) of zooplankton biomass (calculated by taxon) collected in stratified net tows for all factors tested. Because month was a significant factor (top), the 3-way ANOVA including time, transect, and species was applied for each month separately. Significant P-values are indicated in bold face (α = .05).

Independent Variable	df	F-value	P-value
All Months			
Time	1	0.015	0.901
Month	2	12.263	**<0.001**
Residuals	216	---	---
May			
Time	1	17.25	**< 0.001**
Transect	2	10.10	**< 0.001**
Species	14	6.95	**< 0.001**
Residuals	53	---	---
July			
Time	1	11.46	**0.001**
Transect	2	5.424	**0.006**
Species	16	20.29	**< 0.001**
Residuals	70	---	---
September			
Time	1	0.560	0.459
Transect	1	9.468	**0.004**
Species	17	29.88	**< 0.001**
Residuals	39	---	---

Table 2. Results of Tukey HSD tests on the 3-way analysis of variance (ANOVA) on zooplankton weighted mean depths (WMD), by month. Table includes the Tukey HSD difference and P-value for each pairwise comparison. All comparisons are shown for time and transect (significant P-values are indicated in gray shade, $\alpha = .05$). Only combinations which were significant in at least one month are shown for the species variable (all comparisons not shown were non-significant). Because *Limnocalanus macrurus* and *Senecella calanoides* were significantly deeper than most other species, not all species-specific differences are shown. Instead, the mean (standard deviation) of all differences, the number of significant pairwise differences with other taxa (N) and the highest of all p-values are reported. Positive values indicate that the first listed time of day / transect / species is deeper in the water column, and negative values indicate that it is shallower.

		May		July		September	
Independent Variable	**Difference calculated**	**Difference (WMD)**	**P-value**	**Difference (WMD)**	**P-value**	**Difference (WMD)**	**P-value**
Time	Night - Day	5.09	< 0.001	- 2.97	0.001	- 0.60	0.459
Transect	Racine - Saugatuck	- 5.71	0.001	1.85	0.221	- 2.46	0.004
	Racine – St. Joseph	- 6.02	0.001	- 1.55	0.351	---	---
	Saugatuck – St. Joseph	- 0.31	0.977	- 3.40	0.004	---	---
Species	*Limnocalanus* adults - *Limnocalanus* copepodites	---	---	- 10.34	p = .006	- 20.18	p < 0.001
	Limnocalanus copepodites - (others)	---	---	20.96 (2.75)	p < .002 (N = 13)	33.67 (2.54)	p < 0.001 (N = 14)
	Limnocalanus adults - (others)	---	---	11.59 (1.80)	p < .047 (N = 10)	14.04 (1.64)	p < 0.031 (N = 13)
	Senecella copepodites - (others)	17.19 (5.18)	p < .045 (N = 12)	18.15 (2.75)	p < .013 (N = 13)	28.60 (2.54)	p < 0.001 (N = 14)
	Senecella adults - (others)	18.59 (5.06)	p < .047 (N = 5)	17.48 (2.75)	p < .023 (N = 13)	- 32.29	p < 0.001 (N = 1) *
	Senecella adults - *Senecella* copepodites	---	---	---	---	- 27.21	p < 0.001
	Leptodiaptomus sicilis - *Dreissena* veliger	---	---	9.62	0.015	---	---
	Leptodiaptomus sicilis - *Epischura lacustris*	---	---	9.82	0.042	---	---
	Leptodiaptomus sicilis - *Leptodiaptomus ashlandi*	---	---	9.49	0.018	---	---
	Leptodiaptomus sicilis - *Leptodiaptomus minutus*	---	---	9.86	0.011	9.96	0.005
	Leptodiaptomus sicilis- copepod nauplii	---	---	---	---	8.25	0.041
	Leptodiaptomus sicilis - cyclopoid copepodites	---	---	---	---	8.6	0.027
	Leptodiaptomus sicilis - *Bosmina longirostris*	---	---	---	---	8.62	0.027
	Leptodiaptomus sicilis - *Cercopagis pengoi*	---	---	---	---	10.42	0.007

* only significant difference with *Limnocalanus* copepodites

Table 3. Species corresponding to equivalent spherical diameter (ESD) size bins for LOPC data by month (July, September) and transect in offshore southern Lake Michigan during 2015 (see Fig. 2 for full size distributions).

Month	Transect	.075 - .180 mm	.180-.495 mm	.495 - .960 mm	.960 – 1.92
July	Racine	*Veligers nauplii*	*Calanoid* copepodites	*L. sicilis* *Limnocalanus* copepodites	*Limnocalanus* *Mysis* immatures
	Saugatuck	*Veligers nauplii*	*Calanoid* copepodites *L. ashlandi* *L. minutus*	*L. sicilis* *Limnocalanus* copepodites.	*Limnocalanus* *Bythotrephes longimanus* *Mysis* immatures
	St. Joseph	*Veligers nauplii*	*Calanoid* copepodites *L. ashlandi* *L. minutus*	*L. sicilis* *Limnocalanus* copepodites.	*Limnocalanus* *Cercopagis pengoi* *Bythotrephes longimanus* *Mysis* immatures
September	Racine	*Veligers nauplii*	*Calanoid* copepodites *D. thomasi* *L. ashlandi* *L. minutus* *Bosmina longirostris*	*L. sicilis* *D. galaeta mendotae*	*Limnocalanus* *Cercopagis Pengoi*
	Saugatuck	*nauplii*	*Calanoid* copepodites *L. ashlandi* *L. minutus* *D. thomasi*	*L. sicilis* *D. galaeta mendotae*	*Limnocalanus* *Bythotrephes longimanus* *Cercopagis Pengoi*

Table 4. The weighted mean depths (WMD) of zooplankton biomass with standard deviations calculated from the laser optical plankton counter (LOPC) data by month, transect, and size group during the day (top) and night (bottom, bold). Significant differences

based on Tukey's honestly significant difference (HSD) are shown with shaded cells (α = .05) where blue indicates a decrease in depth from day to night (standard migration) and red indicates an increase in depth from day to night (reverse migration).

		N Triaxus profiles	Total Zooplankton WMD (m)	Small Zooplankton WMD (m)	Medium Zooplankton WMD (m)	Large Zooplankton WMD (m)	X-Large Zooplankton WMD (m)
July	Racine	16 13	30.6 (2.1) **26.2 (1.1)**	24.3 (2.3) **26.6 (1.2)**	21.9 (1.8) **25.2 (1.7)**	25.8 (2.0) **26.2 (1.6)**	35.2 (2.2) **26.4 (1.2)**
	Saugatuck	38 46	22.6 (1.2) **23.1 (1.7)**	21.5 (1.3) **23.3 (1.7)**	19.7 (1.6) **21.2 (2.1)**	19.1 (0.9) **18.9 (1.5)**	29.2 (1.8) **28.0 (2.6)**
	St. Joseph	19 19	23.5 (1.8) **23.2 (2.0)**	19.1 (1.9) **19.3 (2.5)**	22.3 (2.3) **22.2 (3.5)**	19.9 (0.9) **19.8 (1.6)**	28.8 (2.4) **26.7 (2.0)**
September	Racine	-- 25	--- **20.9 (1.9)**	--- **22.1 (1.1)**	--- **25.0 (1.4)**	--- **15.4 (1.6)**	--- **22.3 (2.6)**
	Saugatuck	44 18	28.3 (2.9) **23.6 (2.1)**	26.1 (3.0) **23.8 (2.0)**	29.4 (3.2) **25.4 (1.9)**	26.2 (2.2) **21.5 (1.3)**	30.5 (3.8) **24.6 (4.5)**

Table 5. Integrated zooplankton biomass (mg/m^2) calculated from the laser optical plankton counter (LOPC) data by month, transect, depth layer, and zooplankton size group during day (top) and night (bottom, bold). Values reported are the mean (standard deviation). Significant differences (α = .05) based on Tukey honestly significant differences (HSD) are shown with shading, where red indicates an increase and blue indicates a decrease from day to night.

Month	Transect	Sample Size (N)	Depth Stratum	All Zooplankton	Small	Medium	Large	X-Large
July	Racine	Day: N = 16 Night: N = 13	Epilimnion	135 (61) **216 (87)**	11 (6) **6 (4)**	74 (31) **45 (17)**	49 (27) **83 (42)**	1 (2) **82 (38)**
			Metalimnion	288 (85) **608 (355)**	22 (8) **22 (17)**	89 (22) **57 (31)**	167 (53) **137 (72)**	11 (12) **391 (267)**
			Hypolimnion	1872 (172) **1690 (585)**	53 (20) **51 (21)**	151 (35) **136 (40)**	417 (71) **367 (101)**	1251 (152) **1136 (457)**
	Saugatuck	Day: N = 38 Night: N = 46	Epilimnion	1660 (495) **1892 (564)**	161 (29) **141 (44)**	652 (193) **640 (181)**	714 (264) **910 (328)**	133 (54) **201 (88)**
			Metalimnion	2385 (853) **1298 (562)**	126 (46) **117 (45)**	638 (265) **329 (136)**	1169 (315) **486 (199)**	453 (465) **365 (315)**
			Hypolimnion	2147 (768) **2133 (729)**	141 (64) **167 (78)**	357 (175) **427 (179)**	345 (166) **352 (124)**	1304 (580) **1186 (622)**
	St. Joseph	Day: N = 19 Night: N = 19	Epilimnion	2870 (389) **2821 (319)**	618 (96) **552 (68)**	1176 (176) **1298 (138)**	689 (109) **615 (103)**	388 (91) **356 (77)**
			Metalimnion	1663 (744) **920 (272)**	166 (76) **130 (46)**	668 (290) **310 (128)**	557 (229) **275 (76)**	272 (197) **205 (73)**
			Hypolimnion	3399 (753) **4011 (647)**	310 (97) **390 (124)**	1234 (381) **1531 (590)**	430 (103) **460 (62)**	1424 (438) **1630 (644)**
Sept	Racine	Day: N = 0 Night: N = 25	Epilimnion	--- **201 (227)**	--- **2 (2)**	--- **37 (47)**	--- **105 (123)**	--- **58 (67)**
			Metalimnion	--- **4248 (842)**	--- **244 (72)**	--- **716 (250)**	--- **2032 (418)**	--- **1256 (436)**
			Hypolimnion	--- **4338 (1291)**	--- **204 (31)**	--- **1120 (288)**	--- **643 (157)**	--- **2372 (1336)**
	Saugatuck	Day: N = 44 Night: N = 18	Epilimnion	1137 (380) **3194 (1362)**	181 (83) **177 (107)**	472 (216) **804 (336)**	382 (133) **1451 (496)**	102 (43) **761 (695)**
			Metalimnion	6492 (2128) **9366 (3659)**	264 (123) **455 (163)**	1446 (613) **2384 (1422)**	3458 (1048) **4369 (1263)**	1324 (529) **2158 (990)**
			Hypolimnion	6245 (2046) **5484 (537)**	266 (66) **311 (48)**	1868 (444) **2109 (456)**	1903 (955) **1418 (450)**	2208 (993) **1646 (546)**

Table 6. Results of Tukey honestly significant difference (HSD) tests on the analysis of variance (ANOVA) on whole water column (6 m– 60 m) integrated zooplankton biomass (mg/m^2) calculated from the laser optical plankton counter (LOPC) data by month, transect, and zooplankton size group. The table includes the Tukey HSD difference and P-value for each pairwise comparison. Significant differences (night - day) are indicated with shading ($\alpha = .05$) where blue indicates net movement out of the LOPC range from day to night and red indicates a net movement into the range of the LOPC from day to night.

		Total Biomass		Small		Medium		Large		X-large	
Month	**Transect**	**Diff (N-D)**	**P-value**	**Diff (D-N)**	**P-value**	**Diff (N-D)**	**P-value**	**Diff (D-N)**	**P-value**	**Diff (N-D)**	**P-value**
July	Racine	219	0.013	-6	0.484	-77	<0.001	-44	0.07	346	<0.001
	Saugatuck	-869	< 0.001	-3	0.828	-249	<0.001	-479	<0.001	-138	0.238
	St. Joseph	-180	0.359	-21	0.317	62	0.63	-326	<0.001	106	0.540
Sept	Saugatuck	4170	< 0.001	231	<0.001	1512	<0.001	1495	<0.001	931	0.002

Table 7. Site data for the offshore stations: station bottom depth, epilimnion temperature (based on seabird profile), epilimnion chlorophyll (extracted measurements on integrated water from four depths within the epilimnion), euphotic depth (calculated from profiles of photosynthetically available radiation). Zooplankton biomass was calculated by multiplying the biomass concentration (mg/m^3) within each layer by the tow depth range and summing across all depth layers. *Bythotrephes* and *Cercopagis* densities were calculated using the same method, but for density instead of biomass. For zooplankton data, regular face indicates day values, and bold face numbers are night values. *Mysis* biomass was calculated from whole water column net tows taken at night.

		Station Bottom Depth (m)	Epilimnion Temp (°C)	Epilimnion Chlorophyll (µg/L)	Euphotic Depth (m)	Zooplankton Biomass dry weight (mg/m^2)	*Bythotrephes* Density ($\#/m^2$)	*Cercopagis* Density ($\#/m^2$)	*Mysis* Biomass dry weight (mg/m^2)
May	**Racine**	89	3.6	0.40	78.6	1564 / **1705**	42 / **0**	0 / **0**	**98**
	Saugatuck	108	3.5	0.59	66.7	1017 / **1594**	8 / **0**	0 / **0**	**158**
	St. Joseph	108	3.6	0.51	49.4	3658 / **2877**	0 / **7**	0 / **0**	**124**
July	**Racine**	90	9.5	0.53	51.9	1155 / **1597**	16 / **36**	0 / **0**	**25**
	Saugatuck	108	14.5	1.25	38.4	1919 / **3786**	72 / **106**	532 / **508**	**234**
	St. Joseph	108	16.3	2.42	38.5	3032 / **3964**	62 / **87**	8114 / **3805**	**307**
Sept	**Racine**	89	17.5	1.52	49.5	1459 / **1510**	0 / **0**	678 / **478**	**338**
	Saugatuck	108	19.5	0.53	61.3	1855 / **1976**	238 / **612**	0 / **6**	**107**

Table 8. Water column properties during the month of July and September at offshore transects in southern Lake Michigan. Values shown are the mean (standard deviation) calculated from the profiles generated from the Triaxus towed instrument array (N = number of profiles for each transect) during the day (top) and night (bottom). The epilimnion depth was determined based on a minimum temperature gradient threshold of 1°C/m. Epilimnion temperature and chlorophyll are the average of all measurements taken above the epilimnion depth for each profile. The chlorophyll maximum (Chl_{max}) depth and chlorophyll concentration values are for the depth where the chlorophyll concentration was highest. The weighted mean depths (WMD) for chlorophyll (Chl), beam attenuation coefficient (BAT), and total zooplankton (Zoop) biomass were calculated using data between 5 and 60 meters depth.

		N Triaxus profiles	**Epilimnion Depth (m)**	**Epilimnion Temp (°C)**	**Epilimnion Chl (µg/L) Fluoroprobe**	**Thermocline Depth (m)**	**Chl_{max} Depth (m)**	**Chl_{max} Chl (µg/L)**	**Chl WMD (m)**	**BAT WMD (m)**
July	Racine	16 13	12.1 (2.0) 10.9 (3.4)	11.0 (0.2) 10.7 (0.5)	0.91 (0.15) 1.22 (0.06)	15.5 (1.2) 15.4 (8.1)	41.7 (6.5) 40.2 (4.0)	3.35 (0.33) 3.35 (0.34)	32.3 (1.9) 31.3 (1.4)	26.9 (3.0) 27.9 (1.2)
	Saugatuck	38 46	16.1 (1.5) 15.2 (4.7)	14.2 (0.3) 14.4 (0.5)	2.30 (0.22) 2.64 (0.26)	17.8 (1.9) 18.8 (1.7)	22.3 (10.3) 29.3 (4.9)	4.05 (0.57) 4.47 (1.18)	28.6 (1.2) 27.2 (1.8)	22.8 (1.8) 23.6 (1.9)
	St. Joseph	19 19	17.0 (0.5) 15.5 (0.3)	16.5 (0.1) 16.6 (0.1)	3.72 (0.24) 3.90 (0.41)	17.5 (0.5) 16.0 (0.4)	14.8 (7.7) 13.6 (9.1)	5.35 (0.40) 4.80 (1.34)	27.0 (1.3) 25.7 (1.5)	22.7 (1.2) 23.0 (1.5)
Sept	Racine	-- 25	--- 5.8 (1.1)	--- 17.9 (0.7)	--- 1.86 (0.15)	--- 8.20 (2.2)	--- 13.5 (3.4)	--- 3.74 (0.46)	--- 23.20 (1.2)	--- 18.2 (1.7)
	Saugatuck	44 18	19.1 (3.2) 16.4 (2.5)	19.4 (0.5) 19.1 (0.5)	1.76 (1.93) 2.67 (0.61)	20.6 (2.3) 19.2 (1.5)	24.0 (7.4) 18.1 (2.7)	3.80 (2.68) 4.55 (0.90)	26.0 (3.1) 23.6 (1.3)	24.1 (3.7) 21.4 (2.3)

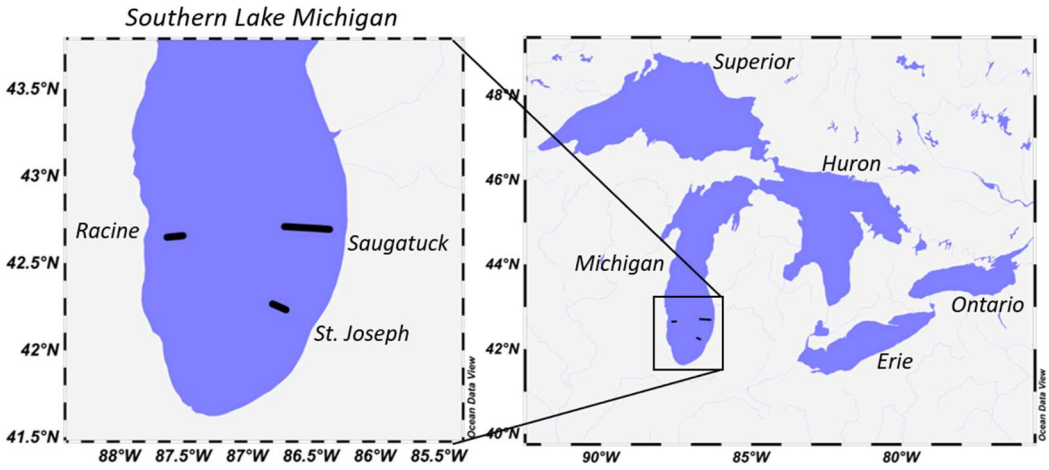

Figure 1. Map of the Laurentian Great Lakes and the location of the transects sampled in Southern Lake Michigan. The Triaxus array was towed from nearshore to offshore both day and night at each transect, and all data included in the "offshore" zone (bottom depth > 60 m) are shown. Stratified zooplankton net tows were completed at the offshore end-point of each transect.

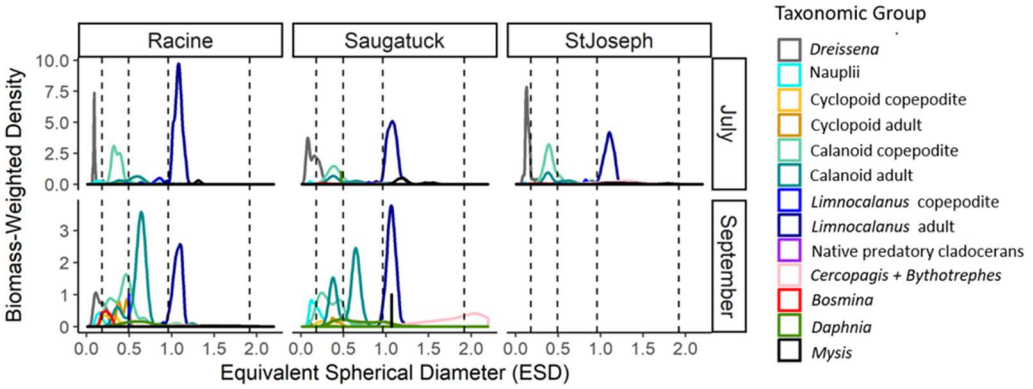

Figure 2. Distributions of zooplankton taxonomic group by equivalent spherical diameter (ESD) based on measurements of individuals from all net tows showing biomass-weighted density distributions by transect and month. Vertical dashed lines indicate the cut-off points for size bins used to distinguish among taxa. Size bins break points chosen were .075 (lower limit), .180, .495, .960, and 1.92 mm (upper limit). Bin sizes were chosen to the nearest sample interval to the desired cut-off (bin breaks range from 0.075 mm to 1.920 mm by intervals of 0.015 mm.

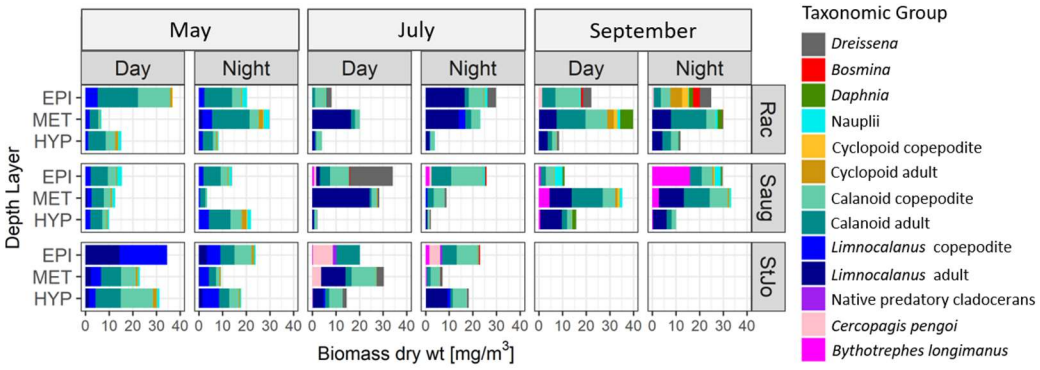

Figure 3. Zooplankton biomass. by taxonomic group for the epilimnion (EPI), metalimnion (MET), and hypolimnion (HYP) at offshore sites in Southern Lake Michigan (Fig. 1) in May, July, and September 2015. Bar plots show biomass dry weight in mg/m^3.

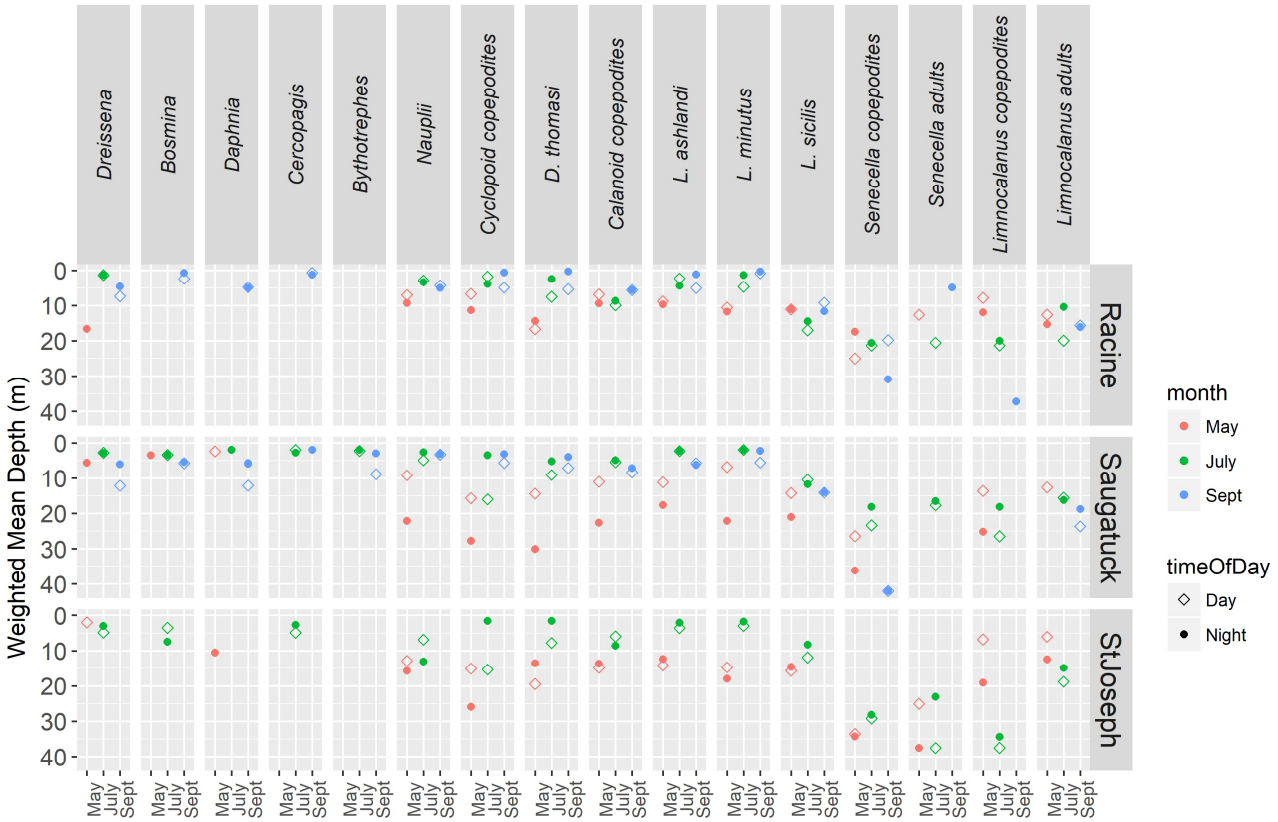

Figure 4. Biomass-weighted mean depths (WMD) of zooplankton species during the day and night for May, July, and September by transect (note no data for St. Joseph in September). Each data point is the WMD for one tow. Data are only shown where at least ten individuals were caught at the given site.

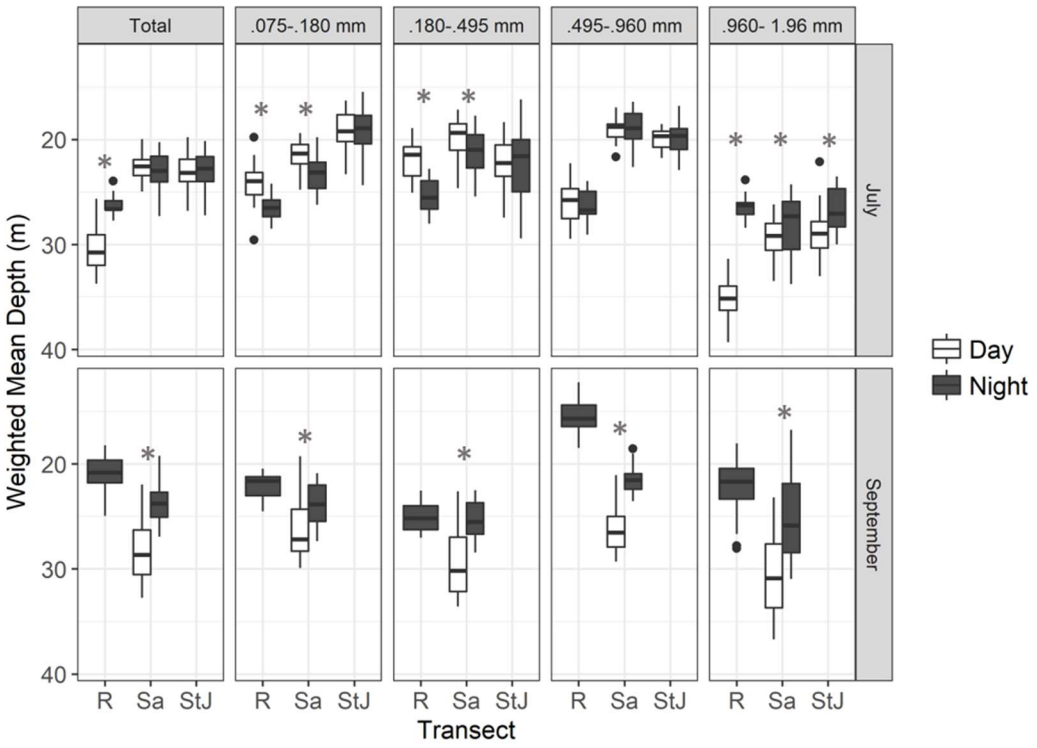

Figure 5. The weighted mean depths of zooplankton biomass from LOPC data, separated by size groups, during day (white) and night (dark gray) at the Racine (R), Saugatuck (Sa), and St. Joseph (StJ) transects in offshore lake Michigan (> 60 m bottom depth) during July and September 2015. Asterisks indicate sites with significant day/night differences in mean depth.

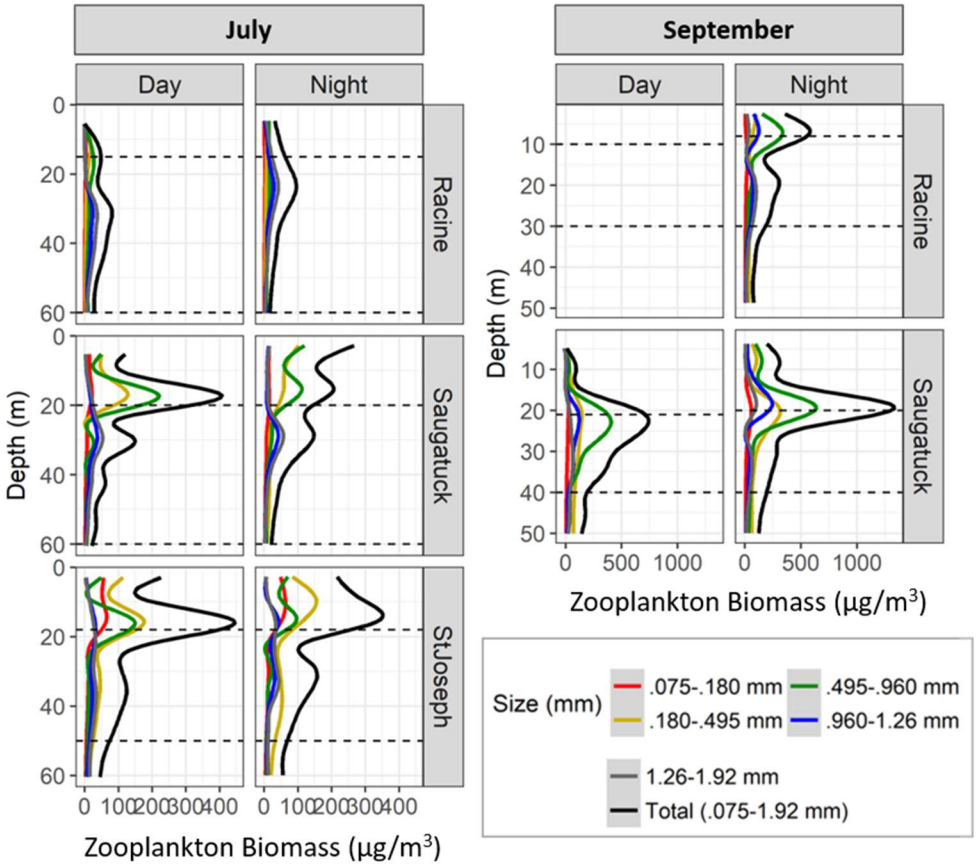

Figure 6. Zooplankton biomass wet weight (µg/m^3) by size category for the Racine, Saugatuck, and St. Joseph transects during day and night July and September 2015. Lines shown are the smoothed lines using a generalized additive model (gam) method with depth as the smoothed term. The horizontal dashed lines indicate the depths at which net tows were taken. Note that the LOPC data does not capture the hypolimnion below 60 meters.

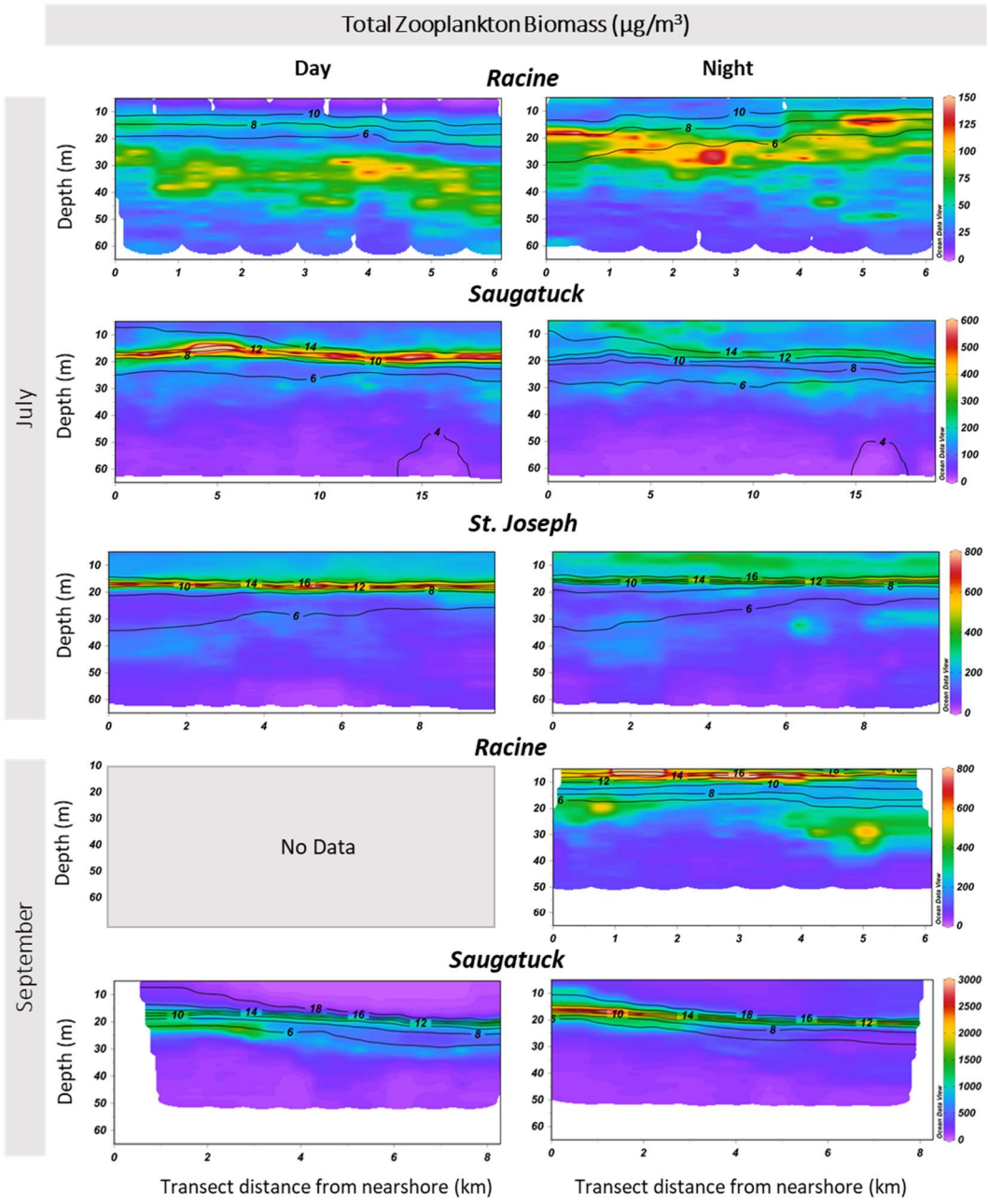

Figure 7. Depth distribution of total zooplankton biomass from laser optical plankton counter (LOPC) data during the day (left) and night (right) transects for the Racine, Saugatuck, and St. Joseph transects in offshore southern Lake Michigan during July 2015. The transect distance is from nearshore to offshore (Fig 1). The color scale indicates zooplankton biomass in µg wet weight biomass/m^3 (note the different scale maxima of 150 (Racine), 600 (Saugatuck), and 800 (St. Joseph). The contour lines with labels show isotherms to visualize the thermocline. Note different color scale and x-axis ranges.

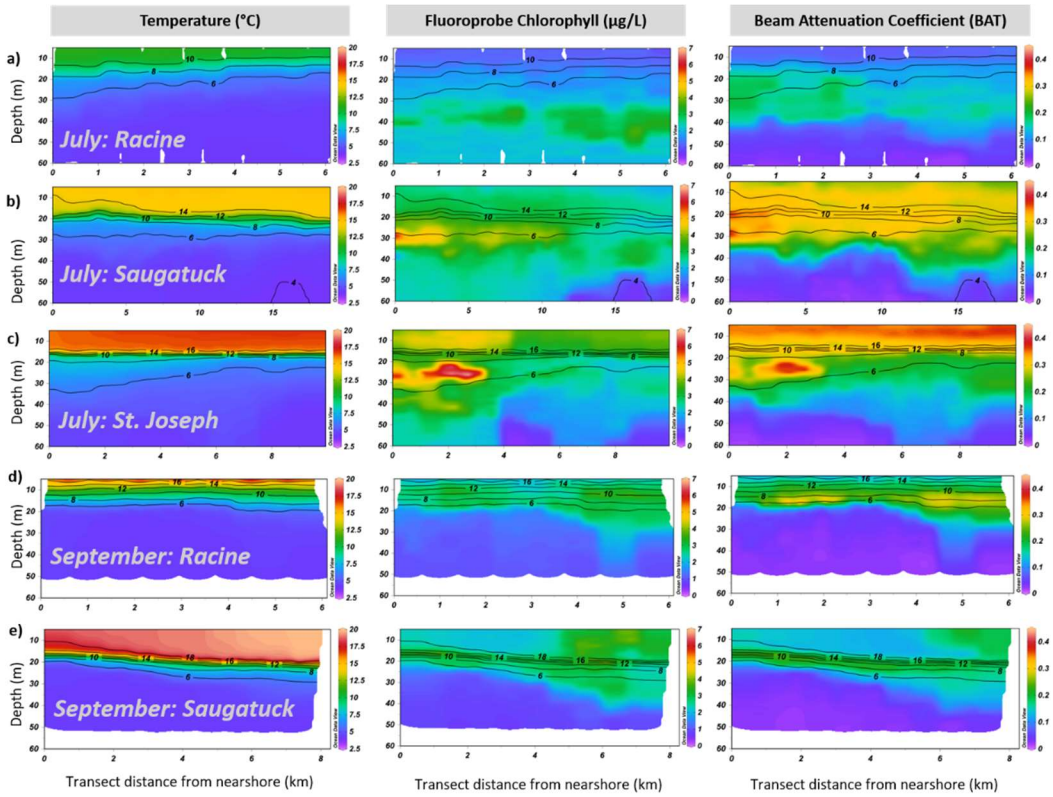

Figure 8. Temperature, chlorophyll, and beam attenuation coefficients (BAT) for night transects in July: **a)** Racine, **b)** Saugatuck, and **c)** St. Joseph transects and September: **d)** Racine, **e)** Saugatuck transects in offshore southern Lake Michigan during July 2015. The transect distance is from nearshore to offshore (Fig 1). The color scale is consistent across transects (Temperature 0 – 20 °C; Chlorophyll 0 – 7 µg/L; BAT 0 – 0.45). Contour lines on all plots show isotherms for visualization of the thermocline. Note different color scale and x-axis ranges.

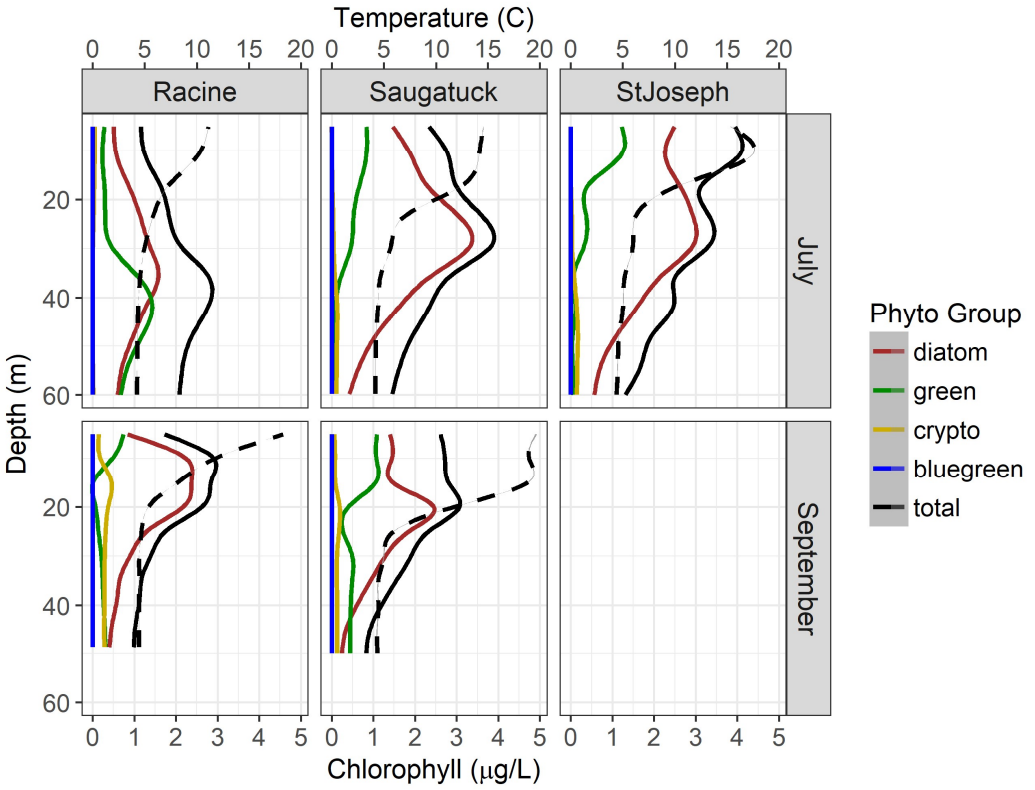

Figure 9. Fluoroprobe profiles showing the concentration of diatoms (red), green algae (green), cryptophytes (gold), and bluegreen (blue) algae with depth at offshore transects in southern Lake Michigan (Fig. 1) during July 2015. The dashed line is temperature (°C).

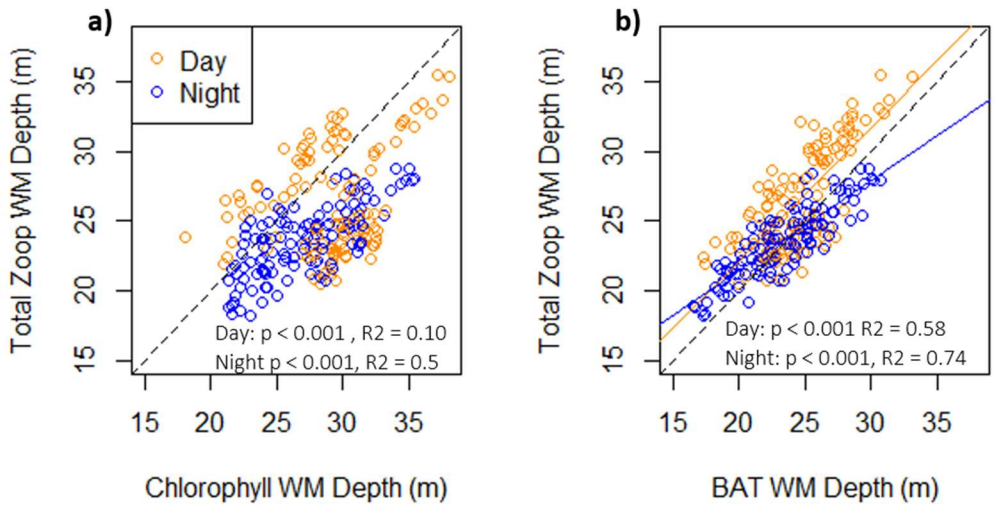

Figure 10. Weighted mean depth (WMD) of total zooplankton biomass from laser optical plankton counter (LOPC) data versus the WMD of total a) chlorophyll and b) beam attenuation (BAT) coefficients, split by time of day.

Supplemental Materials

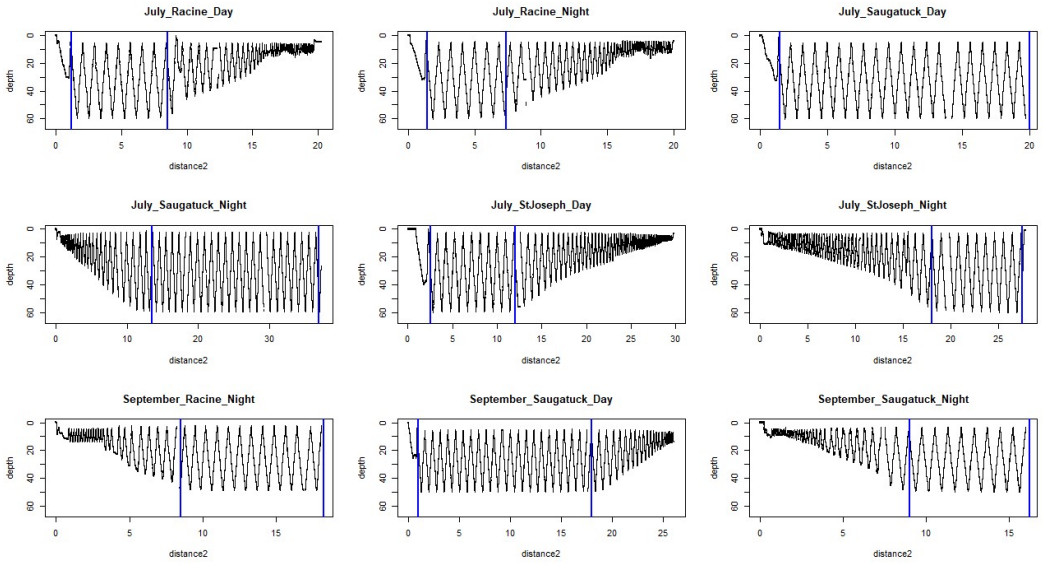

Figure S1. Tow paths for all transects showing the cut-off range included in the offshore dataset presented herein.

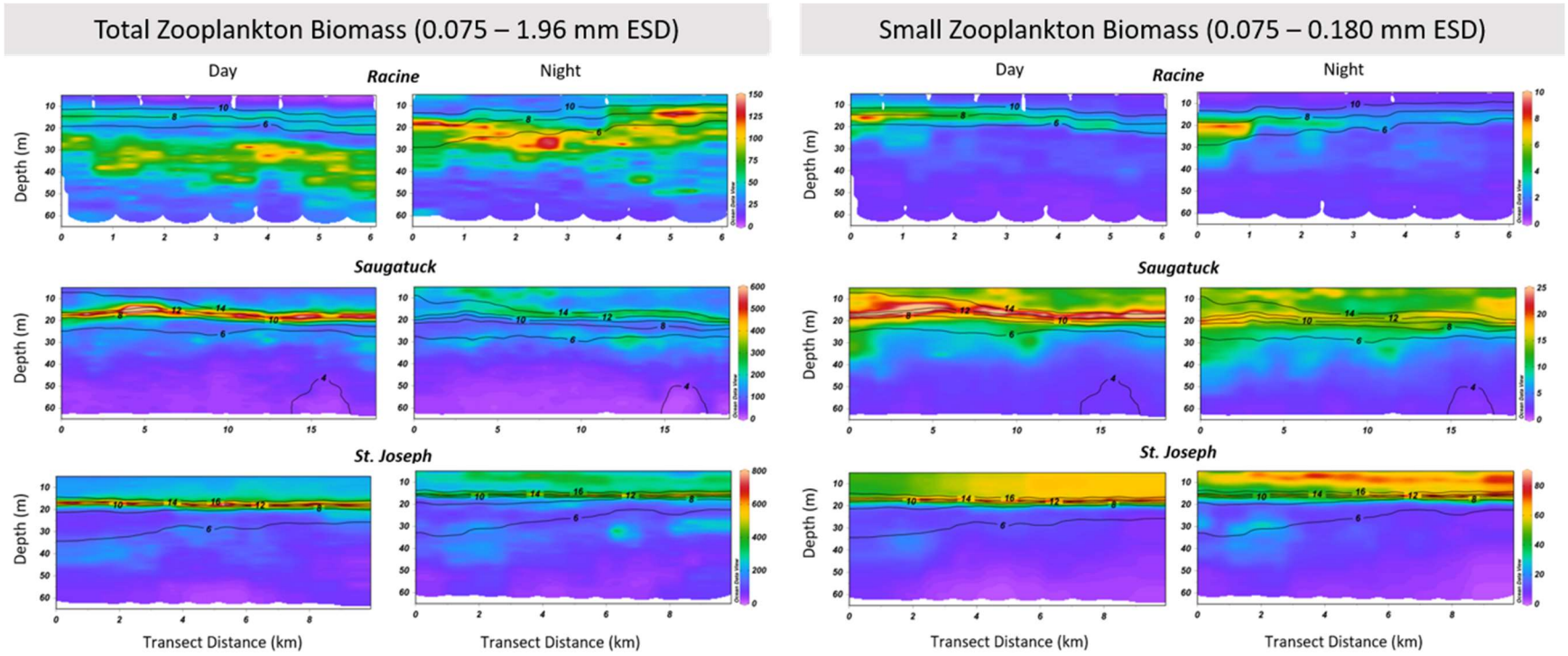

Figure S2. Depth distributions of total zooplankton biomass (left) and nauplius-sized biomass (0.075-0.180 mm ESD, right) from laser optical plankton counter (LOPC) data during the day and night transects for the Racine, Saugatuck, and St. Joseph transects in offshore southern Lake Michigan during July 2015. The transect distance is from nearshore to offshore (Fig 1). The color scale indicates zooplankton biomass in µg wet wt biomass/m^3 (note the different scales). The contour lines with labels show isotherms to visualize the thermocline. Note different color scale and x-axis ranges.

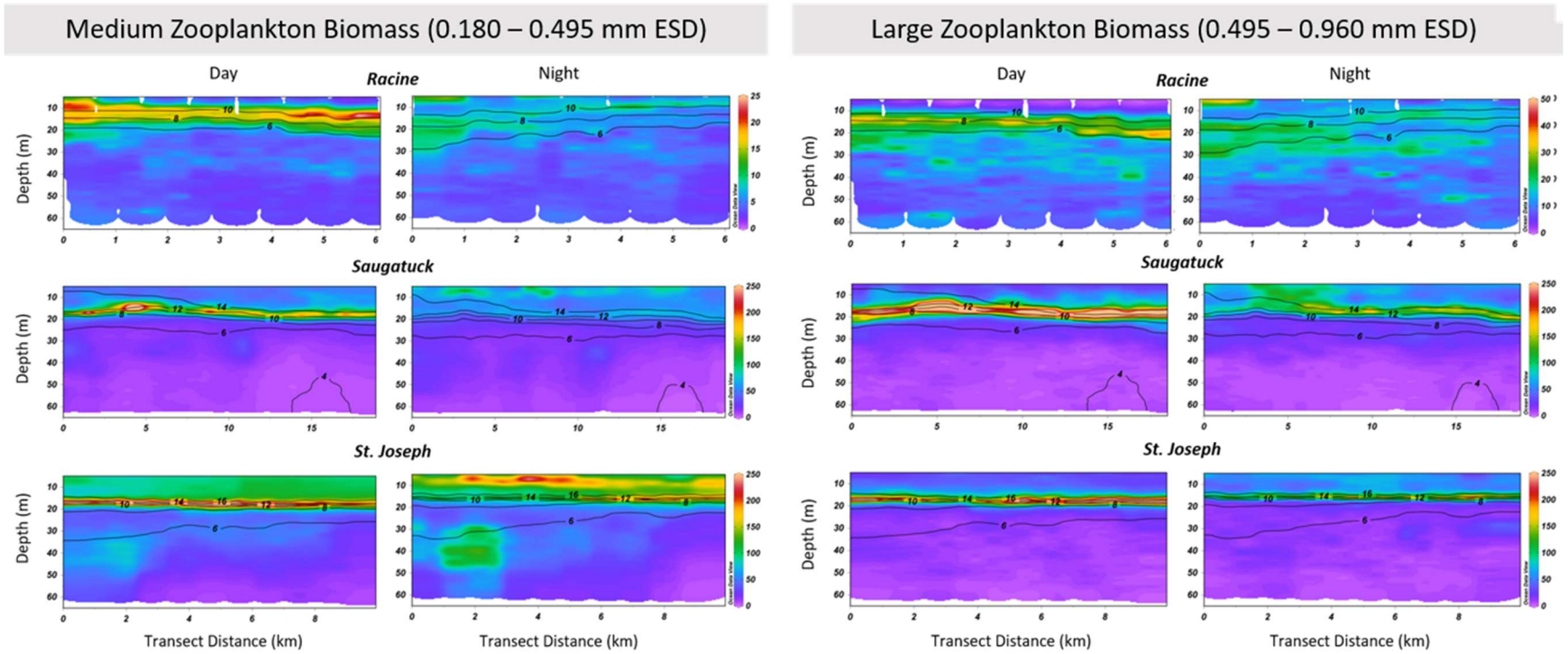

Figure S3. Depth distributions of copepodite-sized biomass (0.180 – 0.495 mm ESD, left) and calanoid-sized biomass (0.495-0.960 mm ESD, right) from laser optical plankton counter (LOPC) data during the day and night transects for the Racine, Saugatuck, and St. Joseph transects in offshore southern Lake Michigan during July 2015. The transect distance is from nearshore to offshore (Fig 1). The color scale indicates zooplankton biomass in µg wet wt biomass/m^3 (note the different scales). The contour lines with labels show isotherms to visualize the thermocline. Note different color scale and x-axis ranges.

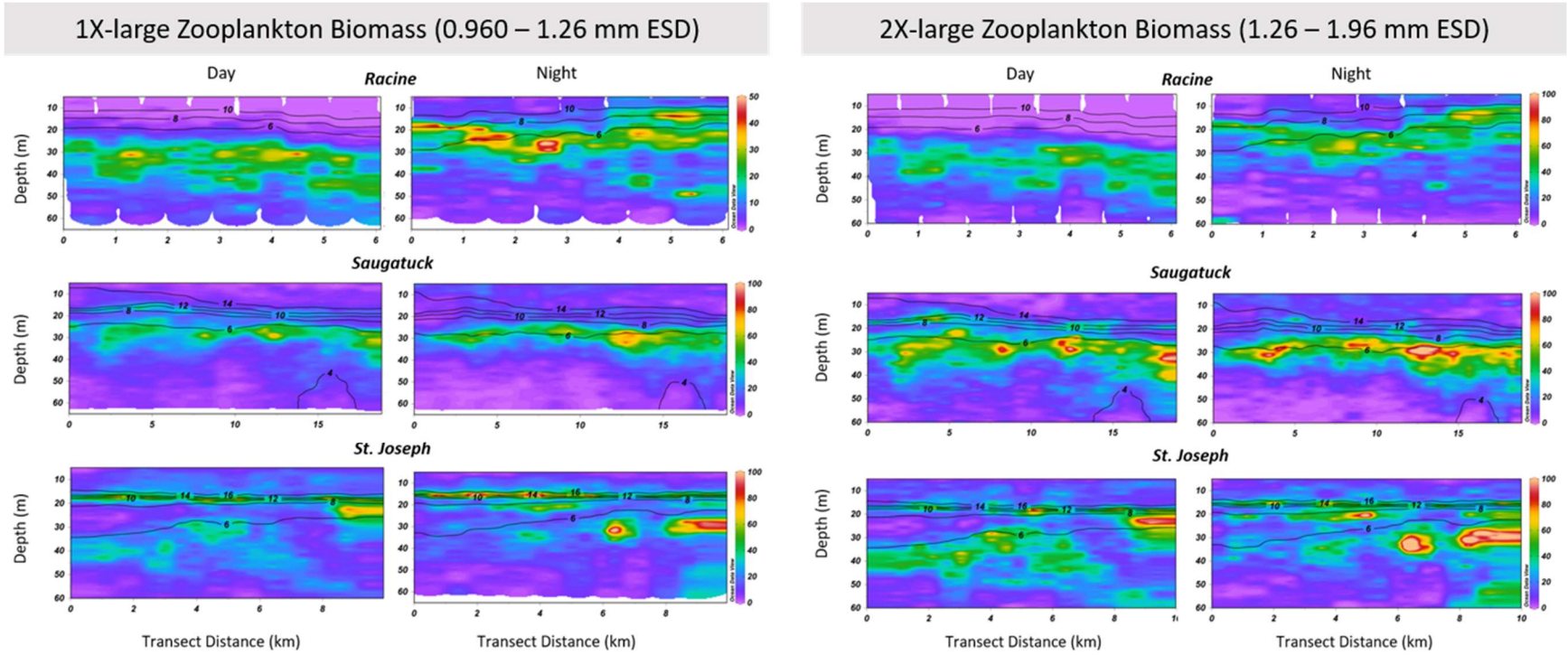

Figure S4. Depth distributions of *Limnocalanus*-sized biomass (split into smaller subset on left: 0.96 – 1.26 mm ESD and larger subset on right: 1.26 – 1.92 mm ESD) from laser optical plankton counter (LOPC) data during the day and night transects for the Racine, Saugatuck, and St. Joseph transects in offshore southern Lake Michigan during July 2015. The transect distance is from nearshore to offshore (Fig 1). The color scale indicates zooplankton biomass in µg wet wt biomass/m^3 (note the different scales). The contour lines with labels show isotherms to visualize the thermocline. Note different color scale and x-axis ranges.

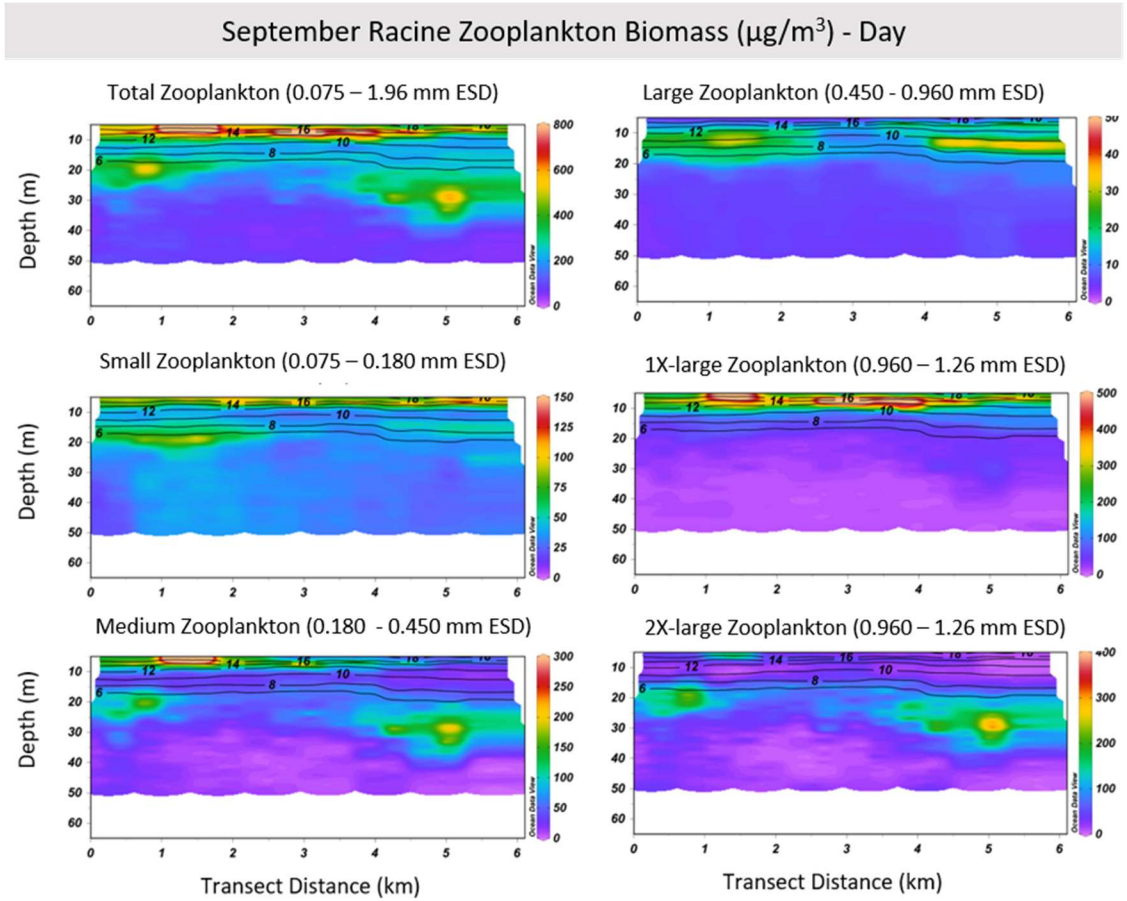

Figure S5. Depth distributions zooplankton biomass by size group for the Racine transect at night during September 2015. Note that data were not collected during the day due to bad weather. The transect distance is from nearshore to offshore (Fig 1). The color scale indicates zooplankton biomass in µg wet wt biomass/m^3 (note the different scales). The contour lines with labels show isotherms to visualize the thermocline. Note different color scale and x-axis ranges.

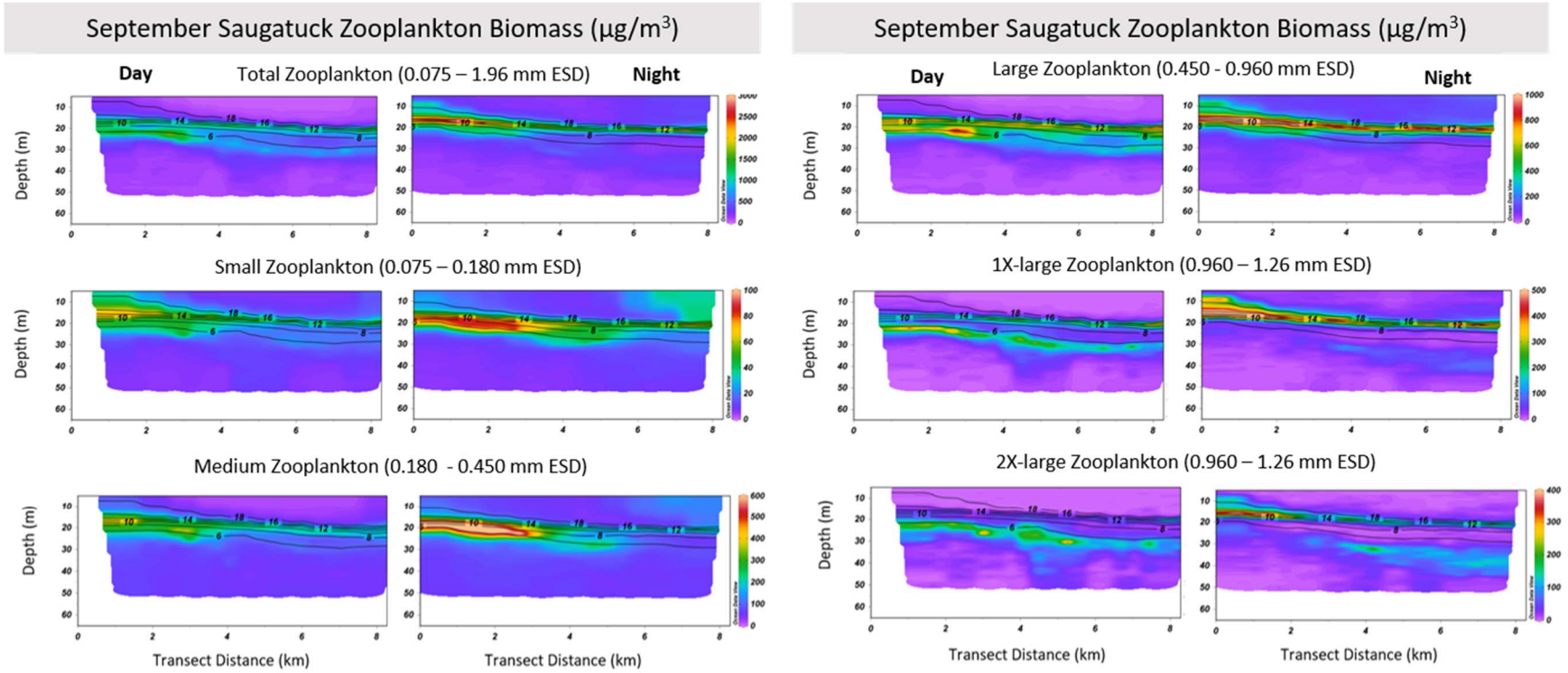

Figure S6. Depth distributions zooplankton biomass by size group for the Saugatuck transect during day and night during September 2015. The transect distance is from nearshore to offshore (Fig 1). The color scale indicates zooplankton biomass in µg wet wt biomass/m^3 (note the different scales). The contour lines with labels show isotherms to visualize the thermocline.